Propositions

1. Through participating in DR program, end-users can provide valuable flexibility to system operators, and therefore can contribute effectively in the energy delivery process, at the expense of little sacrifice to their comfort.
   (this thesis)

2. Local sensitivity analysis techniques are indispensable tools for the system operators to identify the relative importance of uncertainty and imperfection of input data in their decision making processes.
   (this thesis)

3. When decisions are made ignoring least probable outcomes, extremely rare events with catastrophic results might be overlooked.

4. The demand for more sustainable products and services will convert deniers of climate change into important contributors to a sustainable economy.

5. Academic institutions becoming fully part of the economic engine tend to sacrifice their primary objective.

6. Working towards a PhD degree is similar to creating artwork; it's a creative process that starts with intuition, and is completed by learning and implementing useful skills.

Propositions belonging to the thesis, entitled

Future Urban Energy Systems: Harnessing Demand Side Flexibility and Managing Data Uncertainty

Delaram Azari
Wageningen, 3 July 2020

Future Urban Energy Systems

Harnessing Demand Side Flexibility and Managing Data Uncertainty

Delaram Azari

Thesis committee

Promotor
Prof. Dr H.H.M. Rijnaarts
Professor of Environmental Technology
Wageningen University & Research

Co-promotors
Prof. Dr K.J. Keesman
Personal chair, Mathematical and Statistical Methods - Biometrics
Wageningen University & Research

Dr H.J. Cappon
Research Scientist, Environmental Technology
Wageningen University & Research
Associate Professor of Water Technology
HZ University of Applied Sciences, Vlissingen

Other members
Prof. Dr Gert Jan Hofstede, Wageningen University & Research
Prof. Dr Carolien Kroeze, Wageningen University & Research
Dr Emilia Motoasca, KU Leuven, Belgium
Dr Maarten van Blijderveen, Qirion Energy Consulting, Duiven

This research was conducted under the auspices of the Graduate School Socio-Economic and Natural Sciences of the Environment (SENSE).

Future Urban Energy Systems

Harnessing Demand Side Flexibility and Managing Data Uncertainty

Delaram Azari

Thesis
submitted in fulfilment of the requirements for the degree of doctor at
Wageningen University
by the authority of the Rector Magnificus
Prof. Dr A.P.J. Mol,
in the presence of the
Thesis Committee appointed by the Academic Board
to be defended in public
on Friday 3 July 2020
at 11:00 a.m. in the Aula.

Delaram Azari
Future urban energy systems
Harnessing demand side flexibility and managing data uncertainty
154 pages.

PhD thesis, Wageningen University, Wageningen, the Netherlands (2020)
With references, with summary in English

ISBN: 978-94-6395-404-4
DOI: https://doi.org/10.18174/521586

Contents

Chapter 1

Introduction

1.1 Motivation

The earth's average temperature has increased by 0.87 °over the past decade. There is a strong scientific consensus that human activities and greenhouse gas emissions are the dominant cause of global warming [1]. Sea level rise, heat waves, and changes in precipitation are examples of changes in climate which occur due to global warming. Reducing the net global greenhouse gas emissions, and subsequently, sustaining net zero emission for decades, may stop global warming [2]. Hence, it is of utmost urgency to take action and use low-carbon alternatives to fossil fuels and to transform accordingly the current energy provision systems.

Today, countries are enforcing legislation to increase energy efficiency and reduce emissions. As an example, Europe aims at reducing the greenhouse gas emissions by 40% compared to 1990 levels, increasing the share of renewable energy sources to at least 32%, and increasing the energy efficiency by 32.5% by 2030 [3]. Decarbonizing the power sector is an important step within the transition to a cleaner and more efficient energy system, and towards reaching such ambitious target.

Electric power systems around the world are responsible for a reliable electricity delivery to billions of consumers. Traditional power systems are characterized by a few large scale centralized power generation plants, which were mainly fossil fuel based. Recent transitions in the power sector towards low-carbon smart grids, have changed the structure of power systems to decentralized and renewable-based systems. Renewable energy sources (RES)[1], such as wind and solar energy, are an essential part of the smart grids, in which Large part of the RES are installed close to load centers. Decentralized RES have intermittent and variable power output and are non-dispatchable[2]. As a result, large scale integration of RES increases the uncertainty in planning and operation of power systems.

To maintain the security of supply in a system with a large share of RES, system operators need to increase the flexibility of the system. In this context, flexibility is defined as the ability of the system to cope with changes in the generation and demand in a cost effective way, to maintain a reliable power supply. A number of approaches have been proposed to increase the flexibility of the system [5, 6]. There is a significant interest in investing in energy storage infrastructure at the distribution level in order to store the excess energy when the energy demand and/or energy price is low, and inject it back when the energy demand is high [7, 8, 9]. Since the flexibility at the supply side with high contributions of decentralized RES components may be limited, it is of interest to also consider flexibility at the demand side. Another cost-effective, and potentially more efficient, alternative to energy storage at the distribution level, is to harness the flexibility that is available at the demand side through implementing demand side management (DSM) and demand response program (DR) [10, 11].

[1] Renewable energy sources refer to clean energy sources which are naturally replenished [4].

[2] Non-dispatchable refers to energy sources of which the power output cannot be changed according to the changes in demand and should be taken completely by the grid.

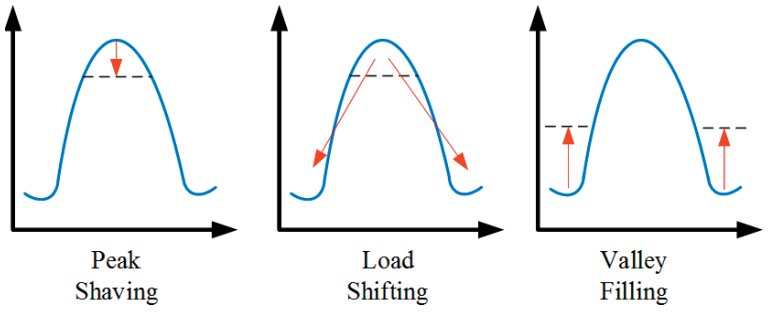

Figure 1.1: DSM techniques for load shaping. Horizontal axis indicates time (e.g., a day), and the vertical axis indicates energy consumption. Red arrows indicate reallocation of energy consumption in time.

DSM consists of any process or end-user activities which changes the magnitude or pattern of the electricity consumption [12]. Such changes include, but are not limited to, lowering the peak load during high demand periods (i.e., peak shaving), increasing the load during the low demand periods (i.e., valley filling), and shifting the load that can be shifted from high demand to low demand periods (i.e., load shifting) (Figure 1.1).

The DR program is one of the DSM categories, which seeks to motivate the consumers to adapt a change in their consumption or local production profile in response to a command signal (in a non-market based mechanism) or price signal (in a market based mechanism) [13]. A success of a DR program requires active engagement of end-users [14, 15].

The power system was traditionally designed as a load following system, with dispatchable resources (e.g., fuels as coal, oil and gas) and an inelastic demand [16]. In such system, consumers were passive users of the provided services. The emergence of domestic low and zero carbon technologies and strategies, and their inclusion in distributed energy resources (DER) and DR programs, change the nature of consumers to active participants in the energy systems [17]. Such structure of energy systems with DER and DR programs, enables new actors, with new roles and functionalities, to participate in a secure network management [18]. In this thesis, we focus on three main actors participating in a DR program, as presented in Figure 1.2 and explained in further detail below.

1. The distribution system operator (DSO) coordinates the energy transfer between the generators and the consumers in a market environment, and is responsible for maintaining the security of supply in the distribution grid.

2. Proactive consumers, who actively participate in network management by offering flexibility. The amount of flexibility proactive consumers can provide is constrained and reflected by their preferences.

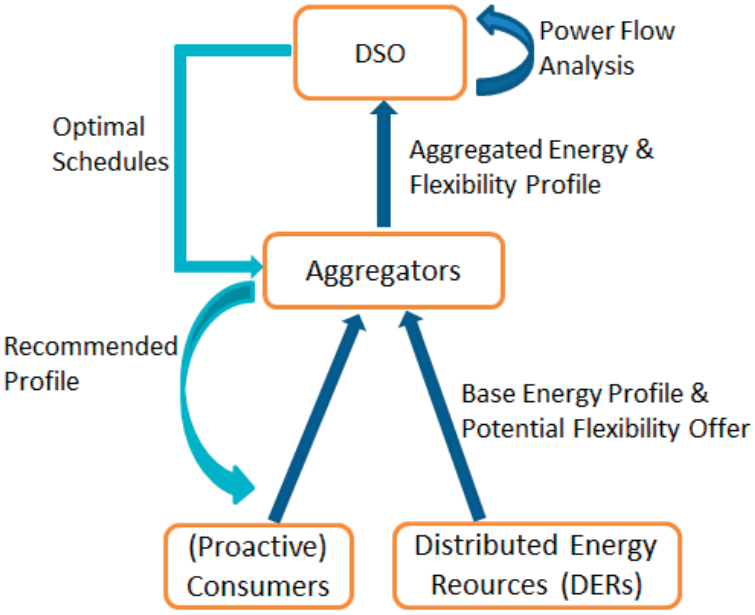

Figure 1.2: The DSO, aggregator, and active consumers, and interactions

3. Aggregators that can function as balance responsible parties (BRPs), to facilitate flexibility trades between the system operator and proactive consumers.

The above mentioned actors, need to make decisions before engaging in contractual agreements. Such decisions include a wide range of problems, from short-term operation (e.g., day-ahead scheduling) to long-term planning. A common way to study the energy systems of the future and make operational and planning decisions is to develop mathematical (optimization) models [19, 20]. Mathematical models are simplifications of current and/or future system, and simulate physical characteristics of the system, the behavior of different actors and their objectives, as well as their interactions.

Mathematical models are fed by empirical data. When such data is not available, forecasts based on historical data are generally used. The problem is, however, that forecasts are imperfect and subject to errors. Moreover, in new situations with no past track record available, the predictions suffer inherently from imperfect information. As the output of a mathematical model depends on the quality of the data that is fed into it, data inaccuracy is directly reflected on the performance of the mathematical models.

Models developed to simulate the energy systems of future also encounter data inaccuracy [21]. Inadequate consideration of uncertainties in operation of the DOS, aggregators, and proactive consumers, can result in impractical decisions. There is a need to investigate the impact of data

uncertainty on the performance of mathematical models developed to simulate the distribution system and electricity market of the future, with specific focus on the roles and objectives of the main actors in a DR program [21]. Such uncertainties, and their consequences, should be understood adequately, otherwise the implementation of a DR program may be sub-optimal, not cost-efficient, or might even be prevented from coming into existence. The complexity of such decisions in the presence of data uncertainty motivates and defines the goals and boundaries of this thesis.

1.2 State of the Art

Exploring the impact of data uncertainty on the decisions of different actors in a distribution system with DR resources is a multidisciplinary challenge. It includes mathematical (optimization) models which reflect the financial objectives of various actors, their behavioral constraints, as well as technical system constraint. In addition, such process requires thorough understanding of the uncertainties in the data.

Mathematical models consist of a set of equations, (dependent and independent) variables, model parameters, and input data. Each of these components are prone to uncertainty. Such uncertainties are modeled with probabilistic, possibilistic, or deterministic methods [22]. Probabilistic methods, model uncertainty as a probability distribution. Possibilistic methods represent the possibility or membership degree of a parameter value by a fuzzy set or a membership function. Deterministic methods define the domain within which the input parameter can vary.

Several approaches have been suggested in the literature for investigating the impact of such uncertainties on the planning and operational decisions in smart power grids [23, 24]. Robust optimization is a common approach used to find a feasible solution which satisfies the ‘worst-case’ scenario [25]. In such problems, uncertainty in input parameters is described as a probability distribution [26]. Robust solutions are less sensitive to uncertainty, and therefore are accountable for severely uncertain situations. However, results of a robust optimization problem are regarded as too conservative, and possibly sub-optimal [27]. Stochastic programming aims to find a solution that satisfies all scenarios. Similar to robust optimization, the uncertainties are dealt with probabilistically. One of the main challenges of stochastic programming is the size of the problem. In such problems the number of variables grows exponentially with increasing number of scenarios. As a result, stochastic models are characterized by having high computational burden. Moreover, it is challenging to estimate the probability distributions of input data and parameters.

Deterministic models, on the other hand, assume perfect knowledge of the input parameters and use nominal values for the input parameters. In deterministic models, the range of the parameter values are known and uncertainties in input parameters are reflected as deviations from the nominal value [28]. The impact of data uncertainty on the solution of deterministic

models can be quantified using uncertainty and sensitivity analysis [29]. Such methods are especially useful for problems with a large number of uncertain input parameters, or when the distributions of the input parameters are not known.

Uncertainty analysis is used to study how robust the output of a model is to uncertain inputs. In other words, uncertainty analysis aims to quantify the variability of the solution given uncertainty in the input parameters. It is commonly performed through Monte Carlo simulation, where the deterministic model is repeatedly evaluated for different values of the input parameter. Sensitivity analysis, on the other hand, is used to study 'how the variation in the output of a model can be apportioned, qualitatively or quantitatively, to different sources of variation' [28]. In addition, sensitivity analysis is used to investigate the dependency of a model to the data fed into it [30].

Sensitivity analysis can be performed locally or globally. Local sensitivity analysis focuses on small changes in the input parameters (i.e., perturbations or errors) in the vicinity of their nominal values. Global sensitivity analysis, on the other hand, looks into changes in the entire range of the input parameters [31]. Either of the two approaches can be used to identify the input parameters to which the model results are more sensitive, and therefore, the decision makers should give special care to their predicted values.

Commonly used data in power systems studies include technical and market data. Technical data include physical and topological parameters of the system, as well as operational data (e.g., generation, load and available flexibility). Market data include quantity and price of the commodity which is traded in the market (e.g., electricity price), as well as parameters which affect economic indices (e.g., investment costs) [32].

Data uncertainty in distribution energy systems arises due to various reasons [33]. In this thesis we identified four main sources of data uncertainty, categorized in two categories of model input and model parameters, as described below:

- Model input:

    1. Forecast errors: Forecasts on generation, load, and market prices are commonly used in operational decisions. Such forecasts are subject to error [34, 35, 36]. Specifically, load forecast at low aggregation levels (e.g., households or building level) strongly dependent on volatile factors, such as demographic, social and behavioral characteristics of the consumers [37]. Such dependencies make it difficult to obtain an accurate forecast for electric load, specially at low aggregation level [38, 39, 40].

    2. Data manipulation and cyber-attacks: One key component in modern power systems is information and communication technologies (ICT). While the ICT infrastructure provides numerous potentials for complex control of the system, it introduces a new source of security threat [41, 42]. In recent years there has been a growing attention towards cybersecurity of smart grids, considering manipulation in smart meter data

on appliance energy consumption and consumers' preferences[43, 44]. In addition, there are concerns about consumer manipulation of their baseline load profile, such that they gain larger benefit from the market [45].

- Model parameters:

  3. Behavior of (emerging) actors in future systems (e.g., DR providers): In an energy system with DR resources, DR operators engage in contracts with the DSO based on the flexibility they can acquire from proactive (flexible) consumers and offer to the DSO. In that regard, DR operators need to estimate the amount of flexibility consumers can potentially provide [46, 47]. There is lack of data on, and substantial uncertainty about involvement of proactive consumers in a DR program, the potential flexibility they can offer, and their compliance with the scheduled flexibility offers [48, 49]. Lack of information, about and full control over the proactive consumers, when it comes down to harnessing the available flexibility, creates uncertainty to the operation of a DR program.

  4. Uncertainties in building energy system's design variables: Available tools for simulating building energy consumption after technology implementation [50, 51], require knowledge of building parameters, which vary per building and are often difficult to obtain. Moreover, the energy system's design parameters, including the technologies used to improve the energy efficiency of the buildings such as capacity and efficiency of the energy storage technology, are prone to uncertainty [28].

In the absence of historical data, as well as inaccuracy of the available data and forecasts, decision makers need new means of assessing their decisions and investigate the possible impact of data uncertainty on their decisions for future systems. Such analysis provides foresight to all parties involved and is needed to ensure economic efficiency. In practice, the decision makers could reason as follows: 'Assume that next year we will be making an important decision, and when it is being made all parameters will be known with certainty. Now, however, that the parameters are unknown, but even so we need numbers for our budget for the next year. If we now solve the expected value problem, and based on sensitivity analysis and it is very stable, we can be quite confident that the numbers we put into the budget are good. Note the setting here. We are not making any decisions in face of uncertainty; we are simply predicting what will happen next year when we make a decision under certainty.' [52]

The uncertainty in flexibility potential of proactive consumers has been investigated in the literature using bottom-up or top-down models. A number of studies [53, 54] propose bottom-up models for simulating the energy demand of the residential consumers based on the appliances used and the time of use of the appliances. Then by defining flexible appliances, quantify the potential flexibility of the individual consumers. Such models use detailed information and physical characteristics of the buildings to generate activity profiles of the consumers and investigate their flexibility potential [47, 55]. However, when used for large scale systems, the large number of input data and the computational burden for such simulations is

prohibitive. Kara et al. [56] propose a data-driven approach to predict the flexibility potential of thermostatically controlled load. Top-down models, based on energy disaggregation methods, are used to identify the contribution of energy appliances, and further, quantify the potential flexibility of a residential building [57, 58, 59]. The proposed data-driven approaches require smart meter's data for different types of consumers, which is not accessible to the DR operator due to privacy protection [60].

Deciding about optimal operation of a distribution grid with flexibility resources in face of input uncertainty is an important issue, which has been addressed in the literature. At distribution network level, Zhao et al. [61] propose a robust optimization framework for optimal scheduling of distribution network with flexible resources (e.g., DR and energy storage) under input data (e.g., wind and DER generation) uncertainty. Mazidi et al. [27] propose a robust day-ahead energy and reserve scheduling, considering load and wind power output uncertainty in distribution networks with DR resources. Their optimal schedule hedges the system operator against the operation uncertainties. Nguyen et al. [62] suggest a scenario-based stochastic programming framework to maximize the profit of aggregators, considering data uncertainties.

Several methods are reported in the literature to address a robust operation of a future distribution grid. Such analyses are significant once the system is in place and the system operators need to observe the operation of the system under different uncertainty scenarios, or hedge against the operational uncertainties. Now, however, if the behavior and preferences of the consumers are unknown, different actors need to evaluate the stability of their decisions under short-run and long-run uncertainty, before engaging in contractual agreements. Questions such as 'what will happen in future when an aggregator makes a decision under input data uncertainty' remains unanswered and needs further research.

In general the goal of a DR program is to motivate end-users to make a change in their local production/consumption profile in response to a price (i.e., through a market-based mechanism) or a command (i.e., originated by a non-market-based mechanism) signal. Regardless of the mechanism considered in place, the DSO needs to become active in network management by taking a coordinating role through implementing a proper policy that provides an adequate price or command signal. This would enable the DSO to harness the flexibility from DR providers and maintain a secure and reliable operation of the distribution network. To do so, the DSO needs to determine the amount of flexibility it needs, and the associated prices, to procure from the flexibility resources.

Most works on harnessing flexibility from the distribution network, firstly, consider energy instead of flexibility as the commodity to trade. Secondly, the existing works either follow a purely economic approach neglecting technical constraints (including power flow constraints), or vice versa. And thirdly, even if optimal power flow (OPF) -based models are used (through which technical constraints are accounted for), they are computationally costly due to non-linearity of the AC power flow for large scale problems, or yield solutions for which the

exactness of the results cannot be guaranteed due to the error inherent to approximation and/or relaxation techniques applied. Fourthly, none of the available studies account for the impact of inaccurate input data on the optimal flexibility schedule and flexibility prices.

The impact of input data uncertainty on building energy system with DR resources is studied in the literature. At building level, optimal energy system design and operation under input data uncertainty is investigated using robust optimization approaches [63, 25]. Ashouri et al. [64] propose an optimization framework for selection, sizing and control of a building's energy system. They consider uncertainties in weather condition, energy demand, and energy costs in a building energy system, and compare the results of stochastic optimization to the results of deterministic optimization with sensitivity analysis for different level of uncertainties. Their conclusions show that a computationally efficient deterministic optimization yields a performance similar to that of the robust one. A visual representation of the sensitivity analysis assists in choosing a proper range of boundary conditions, especially when more than one of them is subject to uncertainties.

More research is required to assess the impact of model input variability and model parameter uncertainty on the decision making process of system operator and aggregators in a distribution electrical system. Hence, to summarize, the following knowledge gaps need to be revealed for scientific and practical reasons, to be able to deal with data uncertainty on the techno-economic decisions that existing and emerging actors need to make for the energy systems:

- A comprehensive framework to evaluate the performance of a potential DR program considering model input uncertainty (e.g., load and price forecast error) and model parameters uncertainty (e.g., flexibility potential of the consumers, and grid data unavailability) in a DR program
- A comprehensive framework, from a system operator's perspective, to determine the amount of flexibility and its associated price, and impact of input data uncertainty on such decisions
- A framework to investigate the impact of technological modifications and demand side management measures on building's energy consumption, and assess the sensitivity of such desicions on model parameter uncertainty (e.g., technical design parameters)

This leads to the research questions, as presented in Section 1.4.

1.3 Mathematical Background

This section provides an overview of the mathematical background that one would need to comprehend the research work that is presented in this thesis.

The mathematical models that are developed in this context of this thesis, are employed to study the decision making of various stakeholders that are involved in electrical energy value

chain. Such problems are generally formalized as optimization programs. In this regards, first, a brief introduction to analytical optimization theory is provided (section 1.3.1). Then, the structure of bi-level optimization problems and the analytical techniques that are used to solve such problems is discussed (section 1.3.2). Such structure is then used in 4. Finally, the mathematical framework used for conducting local sensitivity analysis for an optimization problem is discussed (in section 1.3.3).

1.3.1 Optimization Theory Principles

General formulation

Generally speaking, a decision making problem can be formalized an optimization framework. An optimization framework corresponds to a mathematical problem formulation that aims to determine the 'optimal way' things can be done. Optimization based decision making toolboxes are widely used in different disciplines including economics, engineering, and finance [65].

A mathematical optimization problem in general takes on the following form:

$$\min_{x} f^{obj}(x) \tag{1.1a}$$

subject to

$$f^{eq}(x) = 0 \quad , \lambda^{eq} \tag{1.1b}$$

$$f^{ineq}(x) \leq 0 \quad , \lambda^{ineq} \tag{1.1c}$$

where $x \in \mathbb{R}^n := (x_1, x_2, ..., x_n)$ is the vector of primal, independent optimization (decision) variables. The objective function $f^{obj}(x) : \mathbb{R}^n \to \mathbb{R}$ measures the desirability of any given set of solution variables. Functions $f^{eq}(x) : \mathbb{R}^n \to \mathbb{R}^{m_{eq}}$ and $f^{ineq}(x) : \mathbb{R}^n \to \mathbb{R}^{m_{ineq}}$ define the equality and inequality constraints, respectively. The Greek letter next to each constraint denotes the vector of Lagrangian dual variables for the corresponding constraint(s) [65].

Problem (1.1a)-(1.1c) is a mathematical programming that seeks to minimize the objective function (1.1a) subject to limits that are set by constraints (1.1b)-(1.1c) [65].

Any vector x that satisfies both the equality and inequality constraints is a feasible solution to the problem. A set of all possible feasible solutions is called the feasible set Ω_x. A feasible solution x^* that minimizes the objective function (1.1a) (i.e., gives the smallest value of the objective function) is called the optimal primal solution.[3] That is, for a feasible solution $\hat{x} \neq x^*$, with $f^{eq}(\hat{x}) \leq 0$, $f^{ineq}(\hat{x}) \leq 0$ we have $f^{obj}(\hat{x}) \geq f^{obj}(x^*)$ [65].

[3]Note that minimizing $f^{obj}(x)$ is equivalent to maximizing $-f^{obj}(x)$.

Types of optimization problems

Continuous vs. Mixed-Integer: If f^{obj}, f^{eq}, f^{ineq}, as well as the decision variables x are continuous, then problem is denominated as 'continues programming problem'. If any of the variables involved is integer, the problem is denominated 'mixed-integer programming problem'. As a special case, if vector x includes binary variables, then the problem is referred to as binary-problem.

Linear vs. Nonlinear: If f^{obj}, f^{eq}, f^{ineq} are linear functions in vector x, then the optimization problem is linear. Such problems can be efficiently solved using commercial and non-commercial solvers [66]. In contrast, if either the objective function and/or constraint functions are nonlinear in vector x, then the problem becomes nonlinear. Although there is no standard analytic method to solve these problems, several numerical techniques have been developed that enable one to determine a local optima of such problems [67].

Convexity: An optimization problem is called convex if the objective and constraint functions are convex.

Definition 1 (Convex Function) *A function is convex if for any $\epsilon \in [0,1]$ and for any $x, y \in \mathbb{R}^n$ satisfying the following inequality :*

$$f_i(\epsilon x + (1-\epsilon)y) \leq \epsilon f_i(x) + (1-\epsilon) f_i(y). \tag{1.2}$$

Equation (1.2) *implies that any point on the line segment joining any two points of a convex function curve lies entirely inside the curvature of the function curve.*

Definition 2 (Local vs. Global Optima) *Consider a feasible solution $x^* \in Omega_x$. x^* is a local optima of function f^{obj} if for all points x in the neighbourhood $\mathcal{N}_{x^*} \subset \Omega_x$ the following holds:*

$$f(x) \geq f(x^*), \forall x \in \mathcal{N}_{x^*}. \tag{1.3}$$

The solution x^* is a global optima of the problem if the neighbourhood $\mathcal{N}_{x^*}$ encompasses the whole feasible set Ω_x. That is:

$$f(x) \geq f(x^*), \forall x \in \Omega_x. \tag{1.4}$$

For a convex function, all local minima are also the global minimum. That is, for a feasible solution $\hat{x} \in \Omega_x$ and local optimam $x_1^*, x_2^* \in \Omega_x$, we have:

$$f(x_1^*) = f(x_2^*) \leq f(\hat{x}), \forall \hat{x} \tag{1.5}$$

If f is strictly convex, then there exists only one global minimum.

Optimality Conditions

Karush – Kuhn – Tucker (KKT) Optimality Conditions: In what follows, we first establish the Lagrangian dual problem and then, derive the Karush – Kuhn – Tucker (KKT) optimality condition. The idea here is to reformulate the optimization problem by relaxing the equality and inequality constraints and including them in the objective function, with a penalty factor called the Lagrangian dual variables [see the dual vectors presented with the Greek letters next to the constraints in problem (1.1a)-(1.1c)].

The Lagrangian $\mathcal{L} : \mathbb{R}^n \times \mathbb{R}^{m_{eq}} \times \mathbb{R}^{m_{ineq}}$ associated with the problem (1.1a)-(1.1c) is defined as:

$$\mathcal{L}(x, \lambda^{eq}, \lambda^{ineq}) = f^{obj}(x) + \sum_{i=1}^{m_{eq}} \lambda_i^{eq} f_i^{eq}(x) + \sum_{i=1}^{m_{ineq}} \lambda_i^{ineq} f_i^{ineq}(x) \tag{1.6}$$

Assume that $f^{obj}(x), f^{eq}(x), f^{ineq}(x)$ are differentiable. Suppose that x^* and $(\lambda^{eq*}, \lambda^{ineq*})$ are any primal and dual optimal solution to the problem. The KKT conditions for problem (1.1a)-(1.1c) are:

$$f^{ineq}(x^*) \leq 0 \tag{1.7a}$$

$$f^{eq}(x^*) = 0 \tag{1.7b}$$

$$\lambda^{ineq} \geq 0 \tag{1.7c}$$

$$\lambda^{ineq} f^{ineq}(x^*) = 0 \tag{1.7d}$$

$$\nabla_x f(x^*) + \sum_{i=1}^{m_{eq}} \lambda_i^{eq*} \nabla_x f_i^{eq}(x^*) + \sum_{i=1}^{m_{ineq}} \lambda_i^{ineq*} \nabla_x f_i^{ineq}(x^*) = 0. \tag{1.7e}$$

Conditions (1.7a) and (1.7b) enforce the inequality and equality constraints. Condition (1.7c) enforces that the Lagrangian multiplier are always non-negative. Condition (1.7d) states that the Lagrangian multiplier associated with inequality constraints is nonzero, only if the inequality constraint is binding. Condition (1.7e) states that for an optimal solution the gradient of the Lagrangian is zero.

Necessary and Sufficient Optimality Conditions: The linear independence constraint qualification (LICQ) is a common constraint qualification which states that if the gradient of all constraints are lineally independent, then the KKT conditions are the necessary conditions for optimality. The term 'necessary' implies that any optimal solution of the problem, satisfies the KKT conditions. Note that the vice versa is not true; that is, not every feasible point satisfying the KKT conditions is an optimal solution to the problem.

For a convex problem, the KKT conditions provides the necessary and sufficient optimality conditions. Thus, every point in the feasible domain that satisfies the KKT conditions is

the global solution to the convex optimization problem. On the contrary, if the problem is non-convex, then any solution that satisfies the KKT conditions is a local minimum of the problem.

The KKT conditions are most widely used to solve optimization problem analytically. As an example, the analytical discussion presented in Section 1.3.2 and Section 1.3.3, is mainly derived based on KKT optimality conditions.

1.3.2 Bi-level Optimization

General formulation

Bi-level optimization is a branch of mathematical programming with wide range of theoretical and practical applications. It belongs to a specific class of hierarchical [66] optimization problem which is structured such that an (upper) optimization problem is constrained by another (lower) optimization problem [68]. A general formulation for a bi-level optimization problem is as follows:

$$\min_{(x,y)} f_u^{obj}(x,y) \tag{1.8a}$$

subject to

$$f_u^{ineq}(x,y) \leq 0 \quad , \ \lambda_u^{ineq} \tag{1.8b}$$

$$f_u^{eq}(x,y) = 0 \quad , \ \lambda_u^{eq} \tag{1.8c}$$

$$\min_{y} f_l^{obj}(x,y) \tag{1.8d}$$

subject to

$$f_l^{ineq}(x,y) \leq 0, \quad , \ \lambda_l^{ineq} \tag{1.8e}$$

$$f_l^{eq}(x,y) = 0 \quad , \ \lambda_l^{eq} \tag{1.8f}$$

where $x \in \mathbb{R}^{n_u}$ and $y \in \mathbb{R}^{n_l}$ are the primal decision variables of the upper and lower problems, respectively. Likewise, functions $f_u^{obj} : \mathbb{R}^{n_u} \times \mathbb{R}^{n_l} \to \mathbb{R}$ and $f_l^{obj} : \mathbb{R}^{n_u} \times \mathbb{R}^{n_l} \to \mathbb{R}$ are the objective of the upper- and lower-level problems. respectively. Similarly, $f_u^{ineq} : \mathbb{R}^{n_u} \times \mathbb{R}^{n_l} \to \mathbb{R}^{m_u^{ineq}}$ ($f_u^{eq} : \mathbb{R}^{n_u} \times \mathbb{R}^{n_l} \to \mathbb{R}^{m_u^{eq}}$) and $f_l^{ineq} : \mathbb{R}^{n_u} \times \mathbb{R}^{n_l} \to \mathbb{R}^{m_l^{ineq}}$ ($f_u^{eq} : \mathbb{R}^{n_u} \times \mathbb{R}^{n_l} \to \mathbb{R}^{m_l^{eq}}$) denote the vector-valued function of inequality (equality) constraints of the upper- and lower-level problems, respectively. One can see that the constraints of the upper-level problem include variables of both levels. Now consider the dual variables associated with equality and inequality constraints that are indicated in parenthesis to the right of the respective constraint. One can see that the dual variables pertaining to the equality and inequality constraints of the lower-level problem are also variables of the upper-level problem and affect this problem. In contrast, the dual variables of the upper-level problem do not directly affect the lower-level problem.

A key feature of the bi-level formulation is that there is a hierarchical relationship between the two problems. That is, the objectives of the upper and lower level problems should be conflicting. Otherwise, one could easily reduce the bi-level problem to a single level problem by shifting the constraints of the lower-level problem to the upper-level problem and adding the upper- and lower-level objectives together. The bi-level optimization structure is closely related to Stackelberg gaming in economics. This issue is not discussed further here. An interested reader is invited to refer to [69] and [70] for further details.

Properties of bi-level programs have been investigated thoroughly in the literature [71, 72]. In its simplest setting where all functions are continuous and bounded, a bi-level program is non-convex, non-differentiable, and is shown to be NP-hard [68]. As a result, finding the optimal solution of a bi-level program is not guaranteed.

Analytical derivation of a bi-level problem

Consider a bi-level optimization problem which upper and lower level are convex and regular. One way to solve such bi-level problem is to reduce the bi-level structure to a single-level formulation by replacing the lower-level problem by its KKT conditions. The single-level formulation of problem (1.8a)-(1.8f) reads as:

$$\min_{(x,y)} f_u^{obj}(x,y) \tag{1.9a}$$

subject to

$$f_u^{ineq}(x,y) \leq 0, \quad ,\lambda_u^{ineq} \tag{1.9b}$$

$$f_u^{eq}(x,y) = 0, \quad , \lambda_u^{eq} \tag{1.9c}$$

$$f_l^{ineq}(x,y^*) \leq 0 \quad ,\lambda_l^{ineq} \tag{1.9d}$$

$$f_l^{eq}(x,y^*) = 0 \quad ,\lambda_l^{eq} \tag{1.9e}$$

$$\lambda_l^{ineq^*} \geq 0 \tag{1.9f}$$

$$\lambda_l^{ineq^*} f_l^{ineq}(x,y^*) = 0 \tag{1.9g}$$

$$\nabla_y f_l^{obj}(x,y^*) + \sum_{i=1}^{m_{eq}} \lambda_{l,i}^{eq^*} \nabla_y f_l^{eq}(x,y^*) + \sum_{i=1}^{m_{ineq}} \lambda_{l,i}^{ineq^*} \nabla_y f_l^{ineq}(x,y^*) = 0. \tag{1.9h}$$

As outlined above, under the convexity assumption of objective and constraints functions of the lower (and upper) level problem in decision variables y, solving the single-level formulation of the problem is difficult. It is mainly due to non-convexities resulted from the KKT complementarity conditions [4], which is combinatorial problem and can best be solved by enumeration algorithms, such as branch-and-bound, among other solvers [68]. However, state-of-the-art commercial software packages, such as CPLEX [73] are available to solve such problems. See chapter 4 where this issue is further addressed.

[4] A problem is complementarity problem when exists $x \in \mathbb{R}^n$ and $f(x)$ such that: $x \geq 0$, $f(x) \geq 0$ and $x.f(x) = 0$. The last condition implies that the the set of indices corresponding to nonzero components have an empty intersection. Thus no x exists such that $x.f(x) \neq 0$ [65, 66].

1.3.3 Local Sensitivity Analysis in Optimization Problems

Optimization models, used for decision making, are simplifications of the reality. However, the inputs to the optimization models and the parameters, are subject to error or they lack precision. Consequently, it is beneficial to assess the impact of such errors on the results of the optimization model. Moreover, one can benefit from identifying the variable to which the model outcome are the most sensitive. In this regard, sensitivity analysis is used to identify how the variations in the output of a model are related to different sources of data uncertainty. This subsection provides an analytical expression for the sensitivity of the objective function, the primal, and the dual variables of the optimization problem, with respect to data.

Consider the optimization problem of the form:

$$\min_{x} \{^{obj}(x, a) \tag{1.10a}$$

subject to

$$f^{eq}(x, a) = a \qquad , \lambda^{eq} \tag{1.10b}$$

$$f^{ineq}(x, a) \leq a \qquad , \lambda^{ineq} \tag{1.10c}$$

where $x \in \mathbb{R}^n := (x_1, x_2, ..., x_n)$ is the vector of primal, independent primal variables, and a is the vector of input parameters. $f^{obj}(x, a) : \mathbb{R}^n \to \mathbb{R}$, is the objective function, $f^{eq}(x, a) : \mathbb{R}^n \to \mathbb{R}^{m_{eq}}$ and $f^{ineq}(x, a) : \mathbb{R}^n \to \mathbb{R}^{m_{ineq}}$ are the equality and inequality constraints, respectively. The Greek letter next to each constraint denotes the vector of Lagrangian dual variables for the corresponding constraint(s) [65]. Note that in this formulation, to obtain the sensitivities to the optimization parameters, the parameter vector a is specifically indicated.

The KKT conditions for problem (1.10a)-(1.10c) reads as

$$\nabla_x \mathcal{L}(x^*, a) = 0 \tag{1.11a}$$

$$f^{eq}(x^*, a) = a \tag{1.11b}$$

$$f^{ineq}(x^*, a) \leq a \tag{1.11c}$$

$$\lambda^{ineq} f^{ineq}(x^*, a) = 0 \tag{1.11d}$$

$$\lambda^{ineq} \geq 0 \tag{1.11e}$$

where $\mathcal{L}$ indicates the Lagrangian associated with the opimitzation problem, and can be derived from (1.6).

One can obtain all the sensitivities of the optimal solutions (i.e., $x^*, \lambda^{eq*}, \lambda^{ineq*}$, and $f^{obj*}(x, a)$) to local changes in the parameters a, using the following set of equations [74]:

$$\nabla_x f^{obj}(x^*,a)dx + \nabla_a f^{obj}(x^*,a)da - f^{obj}(x^*,a) = 0 \tag{1.12a}$$

$$\nabla_{xx}\mathcal{L}(x^*,a)dx + \nabla_{xa}\mathcal{L}(x^*,a)da - \nabla_x f^{eq}(x^*,a)d\lambda^{eq} - \nabla_x f^{ineq}(x^*,a)d\lambda^{ineq} = 0 \tag{1.12b}$$

$$\nabla_x f^{eq}(x^*,a)dx + \nabla_a f^{eq}(x^*,a)da = 0 \tag{1.12c}$$

$$\nabla_x f^{ineq}(x^*,a)dx + \nabla_a f^{ineq}(x^*,a)da = 0\ ; \qquad \text{if } \lambda^{ineq*} \neq 0 \tag{1.12d}$$

$$\nabla_x f^{ineq}(x^*,a)dx + \nabla_a f^{ineq}(x^*,a)da \leq 0\ ; \qquad \text{if } \lambda^{ineq*} = 0 \tag{1.12e}$$

$$-d\lambda^{ineq} \leq 0\ ; \qquad \text{if } \lambda^{ineq*} = 0 \tag{1.12f}$$

$$d\lambda^{ineq}\left[\nabla_x f^{ineq}(x^*,a)dx + \nabla_a f^{ineq}(x^*,a)da\right] = 0\ ; \qquad \text{if } \lambda^{ineq*} = 0 \tag{1.12g}$$

Note that constraints (1.12d)- (1.12g) are derived from differentiating the complementarity constraint (1.11d). As mentioned in section 1.3.2, the complementarity constraint enforces the inequality constraint, or the associated dual variable to equal zero. Therefore, for each inequality constraint, either equality (1.12d) or the set of inequalities (1.12e)-(1.12g) should be considered.

When the inequality constraints are binding and the optimal values of the associated dual variables are non-zero, all perturbed equations are written in a linear matrix form as:

$$\begin{bmatrix} F_x & 0 & 0 & -1 \\ F_{xx} & H_x^T & G_x^T & 0 \\ H_x & 0 & 0 & 0 \\ G_x & 0 & 0 & 0 \end{bmatrix} \begin{bmatrix} dx \\ d\lambda^{eq} \\ d\lambda^{ineq} \\ df^{obj} \end{bmatrix} = - \begin{bmatrix} F_a \\ F_{xa} \\ H_a \\ G_a \end{bmatrix} da \tag{1.13}$$

The submatrices in (1.13) are obtained from:

$$F_x = \nabla_x(f^{obj}(x^*,a)) \tag{1.14a}$$

$$F_a = \nabla_a(f^{obj}(x^*,a)) \tag{1.14b}$$

$$F_{xx} = \nabla_{xx}(f^{obj}(x^*,a)) + \sum_k \lambda_k^{eq*}\nabla_{xx}(f_k^{eq}(x^*,a)) + \sum_j \lambda_j^{ineq*}\nabla_{xx}(f_j^{ineq}(x^*,a)) \tag{1.14c}$$

$$F_{xa} = \nabla_{xa}(f^{obj}(x^*,a)) + \sum_k \lambda_k^{eq*}\nabla_{xa}(f_k^{eq}(x^*,a)) + \sum_j \lambda_j^{ineq*}\nabla_{xa}(f_j^{ineq}(x^*,a)) \tag{1.14d}$$

$$H_x = \nabla_x(f^{eq}(x^*,a)) \tag{1.14e}$$

$$G_x = \nabla_x(f^{ineq}(x^*,a)) \tag{1.14f}$$

$$H_a = \nabla_a(f^{eq}(x^*,a)) \tag{1.14g}$$

$$G_a = \nabla_a(f^{ineq}(x^*,a)) \tag{1.14h}$$

Note that the set $dp = (dx, da, d\lambda^{eq}, d\lambda^{ineq}, df^{obj})$ includes the set of all feasible perturbations for moving from one solution which satisfies the KKT conditions to another.

1.4 Research Objective and Research Questions

As stated above in section 1.2, assessing the performance of a potential energy system with flexible resources is subject to data uncertainty. This thesis aims to investigate the impact of data uncertainty on the techno-economic decisions that existing and emerging actors need to make for the energy systems of future. Therefore, the main research question is formulated as follows:

How can different actors in future distribution energy systems with various flexibility resources, account for data uncertainty when making techno-economic decisions?

This question not only defines the core objective of this thesis, but also four sub-questions described bellow.

At distribution level evaluating the real potential of the DR at the system level requires data and information about emerging actors. However, widely available historical data lack information on the new actors with new roles, functionalities and financial objectives. Moreover, DR operators (e.g., aggregator companies), who facilitate the flexibility trades, might have limited access to future grid data due to security reasons. In the absence of historical data regarding preferences of DR providers (e.g., proactive consumers), and limited availability of the grid data, DR operators need new means of assessing the performance of a future DR program, and its possible impacts on an existing grid, if such DR program would be implemented in the future. Such framework provides foresight to all parties involved and is needed to ensure economic efficiency.

In this regard, the first research question this thesis attempts to address is:

1. *What is a suitable framework to assist a DR operator (e.g., aggregator) to assess the performance of a hypothetical DR program, in the absence of historical data regarding the flexibility potential of the DR providers?*

Another source of uncertainty in a DR program is load and price forecast errors [75, 76]. Considerable forecast errors can affect the operation and performance of a DR program [77]. Deciding about optimal operation of a distribution grid with flexibility resources in face of short-run uncertainty is an important issue, which has been addressed in [27, 61, 62]. Available literature considers technical characteristics of the DR implemented in the distribution grid, as well as specific contractual agreements between the DR operator and the flexibility providers. Such analyses are significant once the DR program is in place and the DR operators need to observe the operation of the system under different uncertainty scenarios, or hedge against the operational uncertainties. Now, however, before engaging in contractual agreements, behavior and preferences of the flexibility providers are unknown, and the DR operators need to evaluate

the stability of their decisions under short-run uncertainty. The questions of what will happen in the future when DR operators, with limited access to grid information, make a decision under model input uncertainty (e.g., load and price) remains unanswered and needs further research.

Therefore, the second research question of this thesis is:

2. *What is a suitable framework to assist a DR operator (e.g., aggregator) to assess the impact of load and price forecast errors on the performance of a hypothetical DR program?*

In general the goal of a DR program is to motivate end-users to change in their local production/consumption profile in response to a price (i.e., through a market-based mechanism) or a command (i.e., originated by a non-market-based mechanism) signal. Regardless of the mechanism considered in place, the DSO needs to become active in network management by taking a coordinating role through implementing a proper policy that provides an adequate price or command signal. This would enable the DSO to harness the flexibility from DR providers and maintain a secure and reliable operation of the distribution network. To do so, the DSO needs to determine the amount of flexibility it needs, and the associated prices, to procure from the flexibility resources. Moreover, there is a need for investigating the impact of inaccurate input data on the optimal flexibility schedule and flexibility prices.

In this regard, the third research question of this thesis is:

3. *What is the impact of input data uncertainty on the optimal flexibility that the DSO needs to procure from the flexible resources and its associated prices?*

In recent years, there has been a significant interest in increasing the self-sufficiency of the buildings, through various measures, including but not limited to, energy storage and DSM. Extensive research has focused on reducing net electricity demand via implementation of building-scale technologies, such as solar photovoltaics (PV) coupled with electrical energy storage, as well as DSM strategies [78, 79, 80]. Authors in [81] additionally looked into measures affecting net thermal energy demand of a building from the demand side such as improving building insulation, as well as from the supply side, such as introducing combined heat and power, collecting solar thermal energy and installing heat pumps. However, more research is required to investigate the combined effect of these measures on net energy demand reduction, in order to assess the overall efficiency improvement in a building.

This brings us to the last research question of this thesis as follows:

4. *What is the impact of technological (e.g., storage) or demand side measures (e.g., DR program) on reducing net energy consumption of a residential building, considering model parameter uncertainty?*

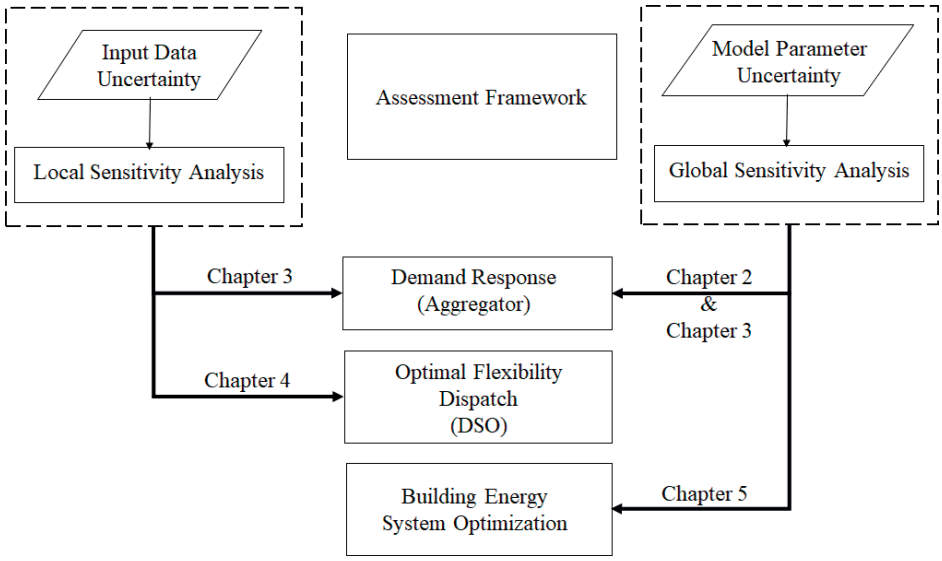

Figure 1.3: Overview of the content of Chapters 2, 3, 4, and 5.

1.5 Outline of this Thesis

Figure 6.1 gives an overview of the five content chapters in this thesis. A data-driven flexibility assessment framework is introduced in **Chapter 2**, to assess the sensitivity of performance of a hypothetical DR program to flexibility preference of proactive consumers. The proposed framework contains a data analytics and a DR module. The data analytics module processes the historical energy consumption and electricity market price data, to select informative subsets and define simulation scenarios. The DR module is an optimization problem which seeks to flatten the daily load profile. The optimization problem reflects the preferences of the DR providers. This chapter addresses the first research question of this thesis.

In **Chapter 3**, we investigate the impact of uncertainties in load and price data on the performance of a DR program, by improving the flexibility assessment framework introduced in Chapter 2. In the improved version of the flexibility assessment framework, a data post-processing sub-module is added that allows local and global sensitivity analysis on the performance of the DR program to uncertain and inaccurate data. The uncertainty in preferences of the DR providers is investigated through global (scenario-based) sensitivity analysis. The impact of load and price forecasts uncertainty on the performance of the DR is analyzed by performing local (perturbation-based) sensitivity analysis. This chapter addresses the second research question introduced in this thesis.

In **Chapter 4** the optimal flexibility that the DSO needs to procure from the flexible resources, and its associated price is determined using a bi-level optimization problem. The proposed

problem considers a local flexibility market framework and accounts for distribution network constraints. We then perform local sensitivity analysis to investigate the sensitivity of the optimal flexibility dispatch solution (i.e., amount of flexibility and its associated price) to forecast errors. This chapter addresses the third research question introduced in this thesis.

Chapter 5 presents a framework for assessing the impact of technical and DSM measures on energy system of a residential building. The proposed framework uses response surface methodology to investigate the combined effect and interaction of the proposed measures on reducing the non-renewable primary energy consumption of a residential household. This chapter addresses the last research question introduced in this thesis.

Finally, in **Chapter 6** findings and outcomes of the presented work in this dissertation are synthesized and reflected.

Chapter 2

Assessing the flexibility potential of the residential load in smart electricity grids – A data-driven approach

This chapter has been published as:

D. Azari, S.S. Torbaghan, H. Cappon, M. Gibescu, K. Keesman, and H. Rijnaarts, "Assessing the flexibility potential of the residential load in smart electricity grids-A data-driven approach," *2017 14th International Conference on the European Energy Market (EEM)*, pp. 1-6, IEEE, 2017

Abstract

This paper proposes a framework for assessing the sensitivity of the performance of a hypothetical demand response (DR) program to consumers' preferences, should they enable DR and become prosumers. The proposed framework contains a data analytics module and a DR simulation module. The data analytics module, processes the historical data to select informative subsets and define simulation scenarios to investigate the performance of the DR module. The DR module is, in essence, an optimization problem that seeks to meet the objective of the distribution system operator (DSO); it minimizes active power losses, by utilizing the potential flexibility prosumers can provide. The optimization problem is solved subject to physical and economic constraints. It considers the fact that cost of energy for the prosumers, after implementing DR, remains less than or equal to its value before that. We defined six scenarios to investigate the sensitivity of the performance of DR on prosumers preferences, in four representative days (so called case studies). Our results demonstrate the effectiveness of the proposed framework in helping the DSO assessing the potential flexibility of various users, and from there, improving the success rate of implementing DR in energy systems of the future.

Keyworkds: Demand Response (DR), Data-driven framework, Prosumers' preferences, Sensitivity analysis.

2.1 Introduction

Large scale integration of distributed energy resources (DERs), with variable, intermittent, and partially dispatchable power output, increases the uncertainty of power systems. The increased uncertainty, in the distribution network imposes new technical challenges to the distribution system operators (DSOs) to operate the grid.

To ensure a reliable electricity supply in a grid with a large share of DER, system operators need to increase the flexibility of the power system[18]. At grid level, this can be done by reinforcing the transmission and distribution grids and/or investing in new energy storage infrastructures [12]. However, such developments involve long development delays (due to various regulatory and economic barriers) and are capital intensive [6, 82, 83, 84]. A more viable and cost effective solution is to utilize the flexibility that exists at the distribution level using demand response (DR) programs[14]. DR enables larger involvement of proactive consumers (i.e., prosumers) in operating the grid[13].

The DSO makes planning and operational decisions based on historical data. This is done by processing the data, extracting useful information and conducting simulations to investigate the possible outcomes in the future [85]. However, the emergence of the new actors in energy systems with new functionalities and financial objectives [86], pose doubt on the validity of the (widely available) historical data. Such data might lack information about the new actors (e.g., factors that influences the potential flexibility prosumers can provide). Such information is needed for the DSO to make valid and credible decisions.

Quantifying the potential flexibility of prosumers is investigated in literature using bottom-up models. These models use detailed information (e.g., physical characteristic of buildings, electricity consumption, consumers' behavior) to study the impact of implementing various DR strategies on flexibility enhancement [87, 53]. The problem is, such approaches are mostly suitable for studying small systems with few number of consumers (e.g., households). The reason is, such approaches include a large number of parameters, which increases exponentially as the size of the system grows. As a result, the computational time for such simulations becomes prohibitive when used for studying medium- and large-scale systems.

Another approach, is to use disaggregation methods[57] to determine the appliance contribution in the total electricity consumption of the households, and further, identify the flexible load of the consumers [58, 88]. Such data-driven models require smart meter data at appliance level for different types of consumers. The problem is, firstly that such data is not always accessible, due to legal (i.e., data privacy) and economic (i.e., smart meters and the ICT infrastructure are costly to install) reasons. Secondly, before installing smart meter infrastructure, it is almost impossible to approximate the potential flexibility that is available to different prosumers. One solution to this problem is for different actors interested in harnessing flexibility to analyze the sensitivity of performance of a DR program to the potential of various prosumers to scale and/or shift their consumption [11].

In this work we propose a data-driven framework to assess the sensitivity of a future DR program to the potential flexibility prosumers can provide. Our proposed framework contains a data analytics module, which processes the historical energy consumption and electricity market price data to select informative subsets and define simulation scenarios. These are further investigated into the DR module, which is built as an optimization problem, utilizing the viewpoint of the DSO. Our proposed framework provides insight to the DSO on the sensitivity of the DR program to preferences of various users on the potential flexibility they can provide, and from there, it helps the DSO improve the success rate of implementing DR in the energy systems of the future.

2.2 Framework

Our proposed framework contains a data analytics and a DR module. The data analytics module contains data pre- and post-processing. The data pre-processing component selects informative subsets, and defines simulation scenarios from the historical data. The data post-processing is used to investigate the sensitivity of the performance of the DR program (optimization module) to prosumers' preferences (i.e., scenarios). The DR module is an optimization problem that seeks to minimize the active power losses for the DSO, and thus, results in more efficient utilization of the distribution network assets. In what follows, the objective of the DR module is discussed, and the parameters of the optimization problem (i.e., prosumers' preferences) are explained.

2.2.1 DR objective

In the context of this paper, the objective of DR is to minimize the operation cost of the DSO, without enforcing excessive costs to prosumers.

We assume that operational cost of the DSO comprises of congestion costs and cost of losses. One way to reduce the power losses in the distribution systems is through peak shaving [89]. Here we show that, under the assumption of equal program time units (PTUs), for a radial distribution system, the active power loss minimization problem is equivalent to standard deviation minimization of the daily net energy consumption of prosumers.

Literature shows that 10-13% of the power losses in the distribution system is through RI^2 losses[90]. The power losses of each line are defined as follows:

$$P_{l,t} = Re\left\{\mathcal{Z} \times I_t^2\right\} = R \times I_t^2 \tag{2.1}$$

$$I_t = \bar{I} + \epsilon_{I_t} \tag{2.2}$$

where $\mathcal{Z}$ is the impedance of the line, $\bar{I}$ is the average line current, and ϵ_{I_t} is the deviation of instantaneous current at PTU t from the average line current. Substituting equation (2.2) into (2.1), the average power losses for one operating day (where $t = 1 : T$, with $T = 96$) is:

$$\begin{aligned}\bar{P}_l &= 1/T \cdot [\sum_{t=1}^{T} P_{l,t}] = 1/T \cdot R[\sum_{t=1}^{T} (\bar{I} + \epsilon_{I_t})^2] \\ &= 1/T \cdot R[\bar{I}^2 \cdot T + \sum_{t=1}^{T} (\epsilon_{I_t})^2 + 2\bar{I} \cdot \sum_{t=1}^{T} (\epsilon_{I_t})] \end{aligned} \tag{2.3}$$

Considering $\sum_{t=1}^{T} (\epsilon_{I_t}) = 0$, one can rewrite (2.3) as:

$$\bar{P}_l = 1/T \cdot R[\bar{I}^2 \cdot T + \sum_{t=1}^{T} (\epsilon_{I_t})^2] \tag{2.4}$$

Under the assumption of constant R and $\bar{I}$, minimizing $\bar{P}_l$ in equation (2.4) is equivalent to minimizing the variance of line current (σ_I^2):

$$\min\left\{\bar{P}_l\right\} = \min\left\{1/T \cdot \sum_{t=1}^{T} (\epsilon_{I_t})^2\right\} = \min\left\{\sigma_I^2\right\}$$

Now assuming that the voltage at the customer connection point is kept almost constant, one can derive the variance of active power consumption of a given building as follows:

$$\begin{aligned} &P_t = V \cdot I_t \\ &\Rightarrow \sigma_P^2 = V^2 \cdot \sigma_I^2 \end{aligned} \tag{2.5}$$

where V^2 is constant. Equation (2.5) expresses the variance of current as a ratio to the variance of the active power consumption of a corresponding household. Therefore, under the assumption of constant voltage at the point of connection, minimizing power losses corresponds to minimizing the variance of daily active power consumption of the household under study, which means flattening the daily power consumption profile:

$$\min\left\{\bar{P}_l\right\} \propto \min\left\{\sigma_P^2\right\} \tag{2.6}$$

where σ_P^2 is the variance of daily active power consumption.

2.2.2 Prosumers' preferences

In the context of this work we consider pro-active consumers that can provide flexibility as prosumers. The amount of flexibility that prosumers can provide is constrained by prosumers' preferences. We define two parameters to reflect prosumers' preferences:

1. Downward (α^d) and Upward (α^u) flexibility: Maximum percentage of load that prosumers afford to reduce or increase at every PTU (t_m).
2. Load-shifting time window (ω^{tt}): Length of time window that a prosumer allows DR to shift its load.

The parameters outlined above are used to restrict the potential flexibility prosumers offer to the DSO.

2.3 Problem Formulation

This section first reviews the assumptions and then presents the formulation of the optimization problem that represents the operation of DR program.

2.3.1 Assumptions

1. Prosumers are exposed to the (hourly-varying) wholesale day-ahead (DA) market prices;
2. Energy conservation: the total energy consumption of each operating period (e.g., one operational day) does not change after DR implementation. Therefore, there is no conversion of electricity to other, storable forms of energy;
3. Load shifting can be implemented in both directions: scheduling to the succeeding PTUs (delay), or scheduling to the preceding PTUs (advance scheduling).

2.3.2 Optimization framework

The optimization problem which simulates the DR process take on the form:

$$\min_{(\Delta \mathcal{P}_{t_m t_n})} \{\sigma_{\mathcal{P}_t}\} \tag{2.7}$$

subject to

$$\sigma_{\mathcal{P}_t} = \sqrt{1/T \cdot \sum_{m \in \Omega_t} \left\{\mathcal{P}_{t_m} - \bar{\mathcal{P}}_{t_m}\right\}^2} \tag{2.8}$$

$$\mathcal{P}_{t_m} = \mathcal{P}^0_{t_m} + \sum_{n \in \Omega_t} \Delta \mathcal{P}_{t_m t_n},\ \forall m \in \Omega_t \tag{2.9}$$

$$\sum_{m \in \Omega_t} \sum_{n \in \Omega_t} \Delta \mathcal{P}_{t_m t_n} = 0 \tag{2.10}$$

$$\sum_{n\in\Omega_t} \Delta\mathcal{P}_{t_m t_n} \geq -\alpha^d \times \mathcal{P}^0_{t_m},\ \forall m \in \Omega_t \tag{2.11}$$

$$\Delta\mathcal{P}_{t_m t_n} = 0,\ \forall \left\{|t_m - t_n| \geq \omega^{tt}\right\}, m, n \in \Omega_t \tag{2.12}$$

$$\sum_{m\in\Omega_t} \mathcal{P}_{t_m} \cdot \rho_{t_m} \leq \sum_{m\in\Omega_t} \mathcal{P}^0_{t_m} \cdot \rho_{t_m} \tag{2.13}$$

The decision variable of the optimization problem is $\Delta\mathcal{P}_{t_m t_n} \in \mathbb{R}$, which denotes the amount of load (in kWh) shifted from t_m to t_n. $\Delta\mathcal{P}_{t_m t_n}$ is a continuous variable and can get a positive or negative value. The objective of the optimization problem (2.7) is to minimize the standard deviation (SD) of daily electricity consumption after implementing DR ($\mathcal{P}_t$), and is calculated from (2.8). Ω_t is the set of the time intervals. Equation (2.9) defines the electricity consumption after implementing DR ($\mathcal{P}_{t_m}$), as the sum of the initial load before implementing DR ($\mathcal{P}^0_{t_m}$) and the total load shifted from other PTUs to the PTU t_m ($\Delta\mathcal{P}_{t_m} = \sum_{n\in\Omega_t} \Delta\mathcal{P}_{t_m t_n}$). We refer to $\Delta\mathcal{P}_{t_m}$ as 'executed flexibility' during PTU t_m. Constraint (2.10) enforces energy conservation. In constraint (2.11) the lower band of the 'executed' flexibility (i.e., negative values of $\Delta\mathcal{P}_{t_m t_n}$) is limited to the maximum amount of load prosumers can afford to reduce. α^d is the maximum percentage of load that can be reduced during PTU t_m. Constraint (2.12) limits the load to shift within the time window of $t_m \pm \omega^{tt}$, imposed by prosumers preferences. Constraint (2.13) enforces $EC = \sum_{m\in\Omega_t} \mathcal{P}_{t_m} \cdot \rho_{t_m}$ after implementing DR to be less than or equal to the electricity cost before implementing DR. Note that constraint (2.13) implicitly limits the execution of flexibility in upward direction. Therefore, no hard constraint is imposed on flexibility in upward direction (α^u). Finally, ρ_{t_m} denotes the day-ahead spot market price of electricity during PTU t_m. The proposed framework can be formulated for different levels of aggregation of prosumers (i.e., a single prosumer or a set of prosumers), provided the data is available.

2.4 Numerical Results

This section presents the results of the data analysis and the DR simulation, for the selected case studies under various hypothetical scenarios of prosumers' preferences.

2.4.1 Case Study

To test the effectiveness of the proposed framework, we perform simulations on a data set of electricity consumption, obtained from a student housing complex in Wageningen, the Netherlands. The measurements were made per house, with 15-minute resolution. In this work, we use the aggregated data for 44 houses in the data set. We combine the consumption data with historical day-ahead (DA) market price data of the Scandinavian electricity market (Nord-Pool spot market) [91], with 1 hour resolution, from 1 January 2014 to 31 December 2014. The simulations are performed per one operating day (i.e., 24 hours) with 15 minutes resolution (i.e., from 00:15 hr to 24:00 hr).

2.4.2 Data Selection

Due to the dimensionality of the search space and the computational intensity of the optimization problem, it is not feasible to solve optimization problem (2.7) - (2.13) for one complete year (i.e., 365 simulations, each having 4560 variables). To illustrate the potential of our method, we solve the problem for four representative days. Each day represents a case study. The cases are selected based on the standard deviation of daily electricity consumption and the DA market price, as follows:

1. Case 1: Day with the highest standard deviation of daily consumption (Monday, 1 December 2014)
2. Case 2: Day with the lowest standard deviation of daily consumption (Saturday, 5 July 2014)
3. Case 3: Day with the largest average DA price (Monday, 29 December 2014)
4. Case 4: Day with the smallest average DA price (Monday, 27 October 2014)

2.4.3 Model Parameters

As outlined above, prior to implementing DR programs, there is an uncertainty associated with the prosumers' preferences. To investigate the sensitivity of the performance of DR to prosumers' preferences, we define six scenarios. Each scenario contains different values for the parameters that reflect prosumers' preferences (i.e., the scaling and shifting factors α^d, and ω^{tt}), as follows:

1. Scenario (S1): $\alpha^d = 10\%, \omega^{tt} = 3hr$
2. Scenario (S2): $\alpha^d = 10\%, \omega^{tt} = 8hr$
3. Scenario (S3): $\alpha^d = 10\%, \omega^{tt} = 23hr$
4. Scenario (S4): $\alpha^d = 20\%, \omega^{tt} = 3hr$
5. Scenario (S5): $\alpha^d = 20\%, \omega^{tt} = 8hr$
6. Scenario (S6): $\alpha^d = 20\%, \omega^{tt} = 23hr$

It can be seen that scenario S1, with the maximum load reduction at each PTU of 10% and the maximum load shifting time window of 3 hours (i.e., 12 PTU), is the most restrictive scenario and offers the lowest potential flexibility. Conversely, scenario S6 with 20% load reduction allowed at each PTU, and no time limit enforced on load shifting, offers the highest potential flexibility. Finally, as no hard constraint is imposed on α^u, this parameters is not included in defining scenarios.

Table 2.1: Standard deviation of daily electricity consumption ($\mathcal{SD}$) before (Ex-Ante) and after DR implementation, for six scenarios on prosumers' preferences (S1 to S6), and 4 cases of representative days (Case1 to Case4).

	Case1	Case2	Case3	Case4
Ex-Ante	2.333	0.301	0.878	1.590
S1	2.196	0.192	0.775	1.368
S2	1.913	0.155	0.671	1.195
S3	1.696	0.143	0.556	1.025
S4	2.200	0.190	0.751	1.304
S5	1.675	0.139	0.642	1.076
S6	1.086	0.075	0.348	0.045

Table 2.2: Daily energy cost (EC[€]), before (Ex-Ante) and after DR implementation, for six scenarios on prosumers' preferences (S1 to S6), and 4 cases of representative days (Case1 to Case4).

	Case1	Case2	Case3	Case4
Ex-Ante	18.15	7.43	15.18	11.62
S1	18.14	7.43	15.18	11.59
S2	18.15	7.43	15.18	11.52
S3	18.09	7.42	15.05	11.21
S4	18.13	7.43	15.18	11.58
S5	18.13	7.42	15.15	11.46
S6	18.02	7.42	14.92	10.97

2.4.4 DR Results

The optimization problem was implemented in MATLAB R2015b optimization toolbox, using fmincon interior-point algorithm. The computational time to solve each daily optimization problem on an Intel Xeon CPU E-1650 3.2GHz and 24GB RAM computer varies between 45 and 75 minutes, depending on the case study and the scenario. It is important to mention that solving the optimization does not necessarily lead to a global optimum since we are dealing with a non-linear non-convex problem. We run the simulations from several initial points for each case and under each scenario, and here we have reported the best results. This is sufficient as a starting point for analyzing the potential for DR of residential consumers.

Figures 2.1 show electricity consumption under Case 1, before implementing DR (ex-ante) and after that (ex-post), under scenarios with $\alpha^d = 10\%$ (S1 to S3) and $\alpha^d = 20\%$ (S4 to S6). One can see that the DR module shifts the load from PTUs with load above the average value to PTUs with load below the average value. For scenarios with $\omega^{tt} = 3hr$, load is shifted mainly to the afternoon hours ($\sim$ 14:00 to 16:00). For scenarios with $\omega^{tt} = 8hr$, the load is shifted to afternoon and morning hours ($\sim$ 9:00 to 12:00). And, for the scenarios with $\omega^{tt} = 23hr$ (i.e.,

when there is no limit on the time window), load is mainly shifted to the midnight and early morning hours ($\sim$ 00:00 to 8:00).

Table 2.1 shows the standard deviation ($\mathcal{SD}$) for all cases and under all scenarios. For each case, comparing $\mathcal{SD}$ ex-ante under S1 to S6, one observes that implementing DR results in $\mathcal{SD}$ reduction. For each case, moving from S1 to S3, and from S4 to S6 (i.e., scenarios with a similar α^d) larger ω^{tt} results in smaller $\mathcal{SD}$. Consequently, the lowest $\mathcal{SD}$, which is close to zero, is achieved when there is no limit on the time shift window (i.e., S6).

Table 2.2 shows the total daily electricity cost (EC) for all cases and under all scenarios. For each case, the ex-post value of EC is less than or equal to its ex-ante value. For each case, under all scenarios with constant α^d, EC has the lowest value when there is no limit on the time window (i.e., S3 and S6). EC has the largest decrease after DR implementation (5.6%) under S6 in Case 4 (i.e., the representative day with minimum DA price), and has the smallest decreases (0.1%) under S6 in Case 2 (i.e., the representative day with minimum $\mathcal{SD}$), i.e. least variable consumption profile.

In order to illustrate the sensitivity of DR to prosumers' preferences (α^d and ω^{tt}), we investigated an extra set of scenarios for $\alpha^d = 30\%$, with $\omega^{tt} = 3hr, 8hr, 23hr$, only for Case 1. Figures 2.2- 2.3 show the results of this analysis. Figure 2.2 shows the changes in $\mathcal{SD}$ for different values of α^d. One can see that when $\omega^{tt} = 23hr$ (the black line), changes in $\mathcal{SD}$ has a near to linear relation with α^d. For small time window (i.e., $\omega^{tt} = 3hr$), changes in $\mathcal{SD}$ are not sensitive to downward flexibility (α^d). For $\omega^{tt} = 8hr$, changes in $\mathcal{SD}$ reaches a saturation point after $\alpha^d = 20\%$.

Figure 2.3 shows the changes in $\mathcal{SD}$ for different values of ω^{tt}. For large value of $\alpha^d = 30\%$, the changes in $\mathcal{SD}$ has a nearly linear relation with ω^{tt}. For $\alpha^d = 10\%$ the slope of changes in $\mathcal{SD}$ becomes smaller for ω^{tt} larger than 8hr.

2.5 Conclusions

In this work, we proposed a data-driven framework which helps the DSO (and other interested actors) to assess the sensitivity of a DR program to prosumers' preferences, and from there, to improve the success rate of implementing DR. Implementing DR, for any level of prosumers' preferences, results in a lower standard deviation of the daily energy consumption profile, and thus a reduction in active power losses for the DSO, meaning more efficient transport of electricity.

Our analysis shows that the success rate of the DSO in minimizing the active power losses (i.e., minimizing the variance and thus the standard deviation of the daily electricity consumption), is positively correlated with the flexibility potential imposed by prosumers' preferences. The results show that a minimum standard deviation can be achieved when prosumers allow maximum load shifting time window ($\omega^{tt} = 23hr$). Under such scenarios, the DSO can achieve

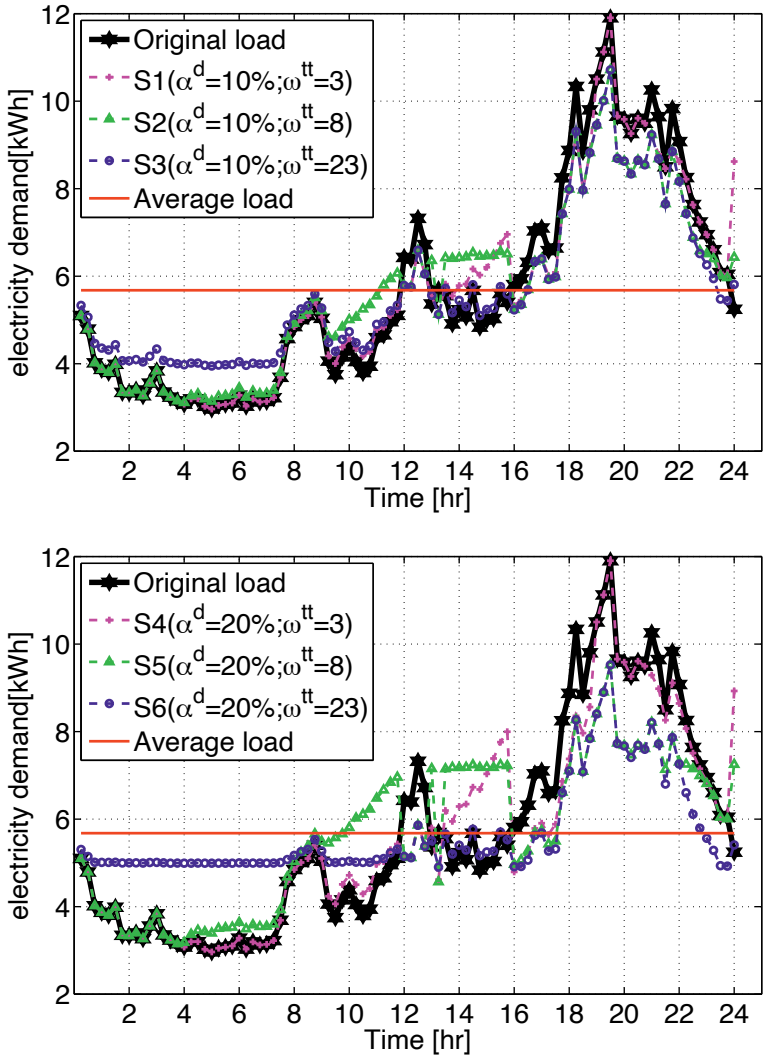

Figure 2.1: Electricity consumption for Case1, before (black line) and after implementing DR, under scenarios with $\alpha^d = 10\%$ (S1 to S3 in the upper figure) and under scenarios with $\alpha^d = 20\%$ (S4 to S6 in the lower figure), for ω^{tt} 3hr, 8hr, and 23hr (the magenta, green, and blue lines, respectively). The red line is the average daily demand.

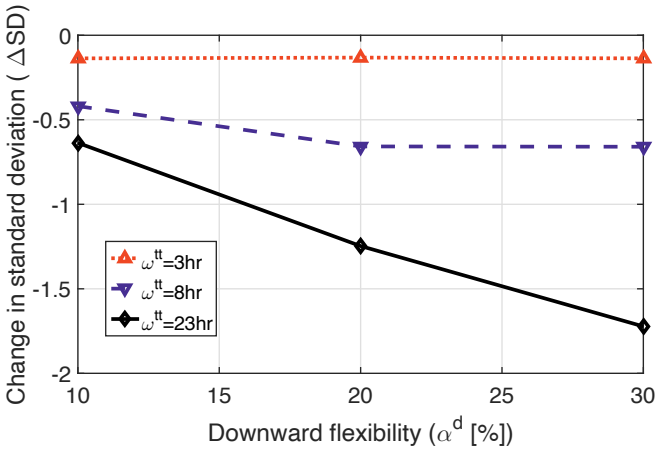

Figure 2.2: Changes in standard deviation of daily electricity consumption $\Delta\mathcal{SD}$ for different values of α^d, under scenarios with constant ω^{tt}; the dotted line for $\omega^{tt} = 3hr$, dashed line for $\omega^{tt} = 8hr$ and solid line for $\omega^{tt} = 23hr$.

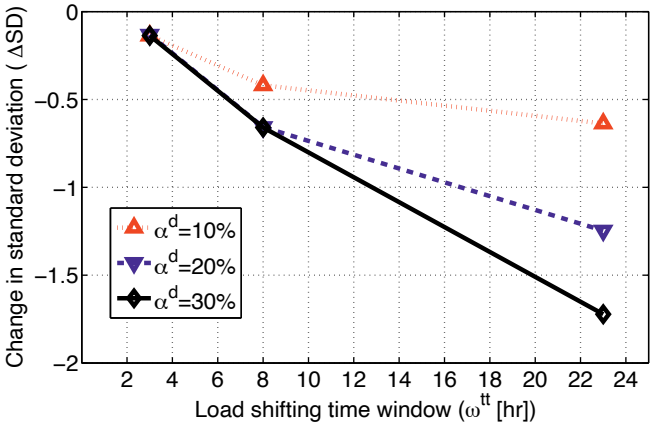

Figure 2.3: Changes in standard deviation of daily electricity consumption $\Delta\mathcal{SD}$ for different values of ω^{tt}, under scenarios with constant α^d; the dotted line for $\alpha^d = 10\%$, dashed line for $\alpha^d = 20\%$ and solid line for $\alpha^d = 30\%$.

lower standard deviation (and thus, lower power losses) when prosumers allow a larger value for load reduction (i.e., downward flexibility α^d).

We also observe that, for a given load shifting time window (i.e., $\omega^{tt} = 3hr$, and $8hr$), there is a saturation point for standard deviation reduction; under such scenarios, increasing the downward flexibility (α^d) above 10% has no impact on power losses.

Finally, when no limit is imposed on the load shifting time window, implementing DR results in shifts from evening peak to midnight valley, when the electricity price is at its lowest. Thus, an unconstrained time shifting window results in a lower electricity bill for prosumers.

One possible extension of this work, can be to assess the sensitivity of the DR program to prosumers preferences, when local PV generation is integrated into the system. Other work could be to modify the optimization problem to meet the objective of the other actors (e.g., maximizing the profit of aggregators).

Chapter 3

Exploring the impact of data uncertainty on the performance of a demand response program

This chapter has been published as:

D. Azari, S.S. Torbaghan, H. Cappon, K.J. Keesman, H. Rijnaarts, and M. Gibescu,"Exploring the impact of data uncertainty on the performance of a demand response program," *Sustainable Energy, Grids and Networks*, 2019

Abstract

There is a significant interest in utilizing demand response (DR) programs to increase the flexibility of sustainable power systems. The DR operators (e.g., aggregator companies) need a robust means to assess the performance of a potential DR program that will be employed in the future. Such assessments should be based on data, some of which are hardly available. Knowledge about the DR providers (e.g., the behavior of proactive consumers) is key to the success of a DR program. In this paper, we devise a data-driven framework to assess the impact of uncertainties associated with future DR programs. The proposed framework comprises two modules: the DR simulation module, and the data analytics module. The DR module solves an optimization problem which simulates the operation of a hypothetical DR program. The data analytics module, firstly, selects subsets from historical load and price data. Secondly, it performs sensitivity analysis on the optimal solution to capture the impact of uncertainties. We consider two sources of uncertainty. First, we consider lack of information about DR providers due to the absence of a DR program in the current system. Second, we consider errors in load and price forecasts, whose impacts are investigated by formulating a sensitivity matrix from the perturbed KKT equations of the optimization problem solved by the DR module. The proposed framework provides insights regarding the potential of a prospective DR program. Such information can be useful for DR operators as a starting point to decide their position in the contractual agreement they will engage in with the (distribution) system operator and/or DR providers in the future.

Keywords: Demand Response, Data uncertainty, Sensitivity analysis

3.1 Introduction

3.1.1 Motivation and Background

Distributed energy resources (DERs) are variable, partially unpredictable, and location-dependent. Large-scale integration of DERs into the power system introduces new challenges to the distribution system operators (DSOs), such as line losses, reverse flows, overloads and voltage deviations [92, 93]. One way DSOs can deal with the above-mentioned challenges in a cost-efficient manner is to utilize the flexibility that is available at the demand side.

The potential flexibility in electrical demand can be harnessed through Demand Response (DR) programs [14]. DR is defined as modifications pro-active consumers (i.e., DR providers) make in their electricity pattern in response to a command or price signal [87]. DR enables an active network management, through larger involvement of the regional DSOs and DR providers in solving system problems [94, 95, 96, 97]. The flexibility provided through a DR program to DSOs can facilitate the grid operation by contributing to several grid services, such as load smoothing and cost of loss minimization [89, 98].

This work focuses on DR services at the distribution level. We consider the following actors in a DR program:

1. The DSOs, which are responsible for maintaining the security of supply. As a regulated entity, the DSO seeks to minimize its total cost which consists of operational cost and investment cost. The operational cost of the DSO includes cost of congestion (including over voltage and line congestion), and cost of losses. The investment cost of the DSO is related to system expansion (e.g., installing new distribution lines).

2. DR providers, which can offer flexibility to address the system's needs. We assume that DR providers (e.g., pro-active consumers) seek to benefit from DR services they provide to the distribution system.

3. DR operators, which are entities facilitating flexibility trades between the DSO and the DR providers. DR operators (e.g., aggregators) seek to profit from flexibility trades. We assume DR operators have contractual agreements with the DSO and the DR providers. Upon a request from the DSO, DR operators procure flexibility services from the DR providers (while considering their preferences on providing flexibility) and provide it to the DSO.

In a future DR program, DR operators engage in contracts with the DSO based on the flexibility they can offer. Therefore, DR operators need to foresee the operation of the grid in the near future, and estimate the potential flexibility they can trade. Evaluating the real potential of the DR at the system level requires data and information about emerging actors, as well as future grid data (e.g., voltages, power flows). However, widely available historical data

lack information on the new actors with new roles, functionalities and financial objectives. Moreover, the availability of future grid data is limited due to security reasons [99]. In the absence of historical data regarding a DR program, and limited availability of the grid data, DR operators need new means to assess the operation of a DR program and its possible impacts on an existing grid, if such DR program would be implemented in the future. Such analysis provides foresight to all parties involved and is needed to ensure economic efficiency.

3.1.2 Literature Review

The behavior of DR providers is a major source of uncertainty to a DR program. There is lack of data on, and substantial uncertainty about, their involvement in a DR program, the potential flexibility they can offer, and their compliance with the scheduled flexibility offers [46, 47]. Lack of information, about and full control over DR providers, when it comes down to harnessing the available flexibility, creates uncertainty to the operation of a DR program [48, 49].

The amount of flexibility the DR providers can offer has been investigated in the literature. Authors in [53] and [54] simulate the energy demand of the residential consumers based on the appliances used and the time of use of the appliances, then quantify the potential flexibility of the individual consumers. Such models use detailed information and physical characteristics of the buildings, to generate activity profiles of the consumers and investigate their DR potential [47, 55]. However, when used for large scale systems, the large number of input data and the computational burden for such simulations is prohibitive. In [56] a data-driven approach is proposed to predict the flexibility potential of thermostatically controlled load. In [57, 58, 59] energy disaggregation methods are used to identify the contribution of energy appliances, and further, quantify the potential flexibility of a residential building. The proposed data-driven approaches require smart meter's data for different types of consumers, which is not accessible to the DR operator due to privacy protection [60].

There are also concerns about consumer manipulation of their baseline load profile, in a way to gain larger benefit from the flexibility market [45]. However, for a large number of flexible consumers, the liquidity of the flexibility market is high, and there is a competition amongst the flexible providers. Such situations would reduce the chance for manipulating the market by changing the load profile. In addition, recently there has been a growing attention to cybersecurity of smart grids, considering manipulation of smart meter data on appliance energy consumption and consumers' preferences [43, 44, 13]. Such manipulations imply that even scarce high resolution smart meter data are not entirely reliable to be used in data-driven approaches. In this situation, DR operators have limited capabilities to predict the flexibility potential of the DR providers.

Another source of uncertainty in a DR program is forecast errors [75, 76]. At low aggregation levels (e.g., small aggregation of households), the energy consumption is strongly dependent on volatile factors such as demographic, social and psychological characteristics of the DR

providers [37]. Such dependencies makes it is difficult to have accurate forecasts at low aggregation level [38, 39, 40]. Considerable forecast errors can affect the operation and performance of a DR program [77].

The impact of data uncertainty on optimal operation of a distribution network with DR resources is studied in the literature. In [27] authors consider load and wind power output uncertainty in distribution networks with DR resources. They determine a robust day-ahead energy and reserve schedule, which hedges the system operator against the operation uncertainties. Authors in [61] propose a framework for optimal unit commitment considering DR as well as wind power output uncertainty. In [62] authors suggest a scenario-based stochastic programming framework to maximize the profit of micro-grid aggregators, considering data uncertainties. In these studies, it is assumed that the DR is implemented in the system, and there is a specific contractual agreement between the DR operator and the DR providers. The result of such studies is an optimal schedule for the DSO. However, to the best of our knowledge no work has been done on assessing the impact of data uncertainty on the decision making process of DR operators, considering data scarcity and limitation on grid information accessibility.

3.1.3 Paper Objective and Contributions

The objective of this paper is to develop a framework to evaluate the performance of a DR program, and assess its sensitivity to uncertain sources, considering limited data that is available. Two main sources of uncertainty are considered: 1) the flexibility potential of the DR providers, and 2) load and price forecast. We introduce a data-driven flexibility assessment framework, to evaluate the potential flexibility DR providers can provide, and analyze the sensitivity of the performance of the DR to two sources of uncertainty mentioned above. The proposed framework enables DR operators to evaluate the performance of a future DR program under uncertainty, and sheds lights on the potential value of the DR in future systems.

The main contributions of this paper can be summarized as follows:

1. We formulate a continuous optimization problem to simulate the load re-scheduling in a DR program. The optimization problem reflects the preferences of the DR providers and serves the DSO's needs to manage network congestion by reducing the peak load, and therefore, postpone capital intensive grid investments in the network infrastructure. Our proposed formulation assures that, under certain assumptions, the objective of the DSO can be reached without modelling the distribution grid.

2. We investigate the performance of a DR program subject to small perturbations in load and price data (e.g., forecast errors). The continuity of the proposed optimization problem enables us to provide an analytical sensitivity analysis framework from the perturbed Karush–Kuhn–Tucker (KKT) equations of the proposed optimization problem, and formulate a sensitivity matrix [74].

3. We employ scenario-based sensitivity analysis to evaluate and compare the performance

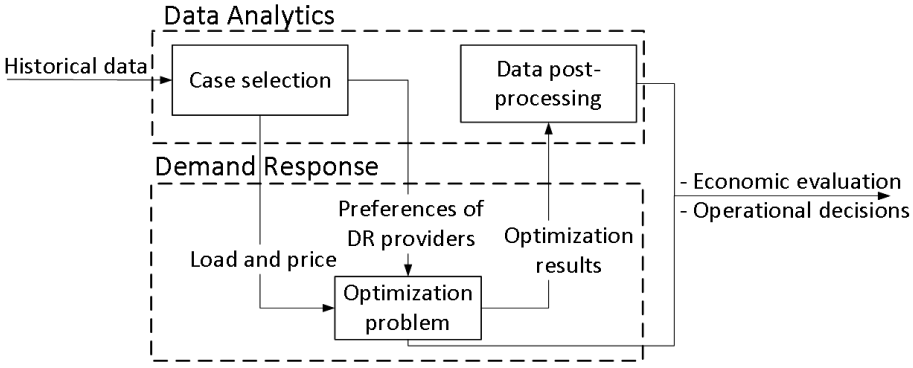

Figure 3.1: Flexibility Assessment Framework

of a DR program under various preferences of the DR providers.

3.2 Flexibility Assessment Framework

The data-driven Flexibility Assessment Framework is a tool to evaluate the performance of a DR program, and assess its sensitivity to data uncertainty. Figure 3.1 shows that the proposed framework consists of two processing modules: Demand Response (DR) and Data Analytics.

The DR module allows us to simulate the operation of a hypothetical DR program, if it would be put in place, by solving a constrained optimization problem. The optimization problem reflects the objective of the DSO that is to minimize the variation of daily load, and as a result to reduce network losses.

The data analytics module contains two sub-modules: i) case selection and ii) data post-processing. The case selection sub-module prepares the data required to feed into the optimization problem (i.e., DR module); Preferences of the DR providers, which reflect possible flexibility ranges of future DR providers, are defined under various scenarios. In addition, informative subsets (Cases) from historical load and price data are selected. The load and price profile of the selected days define the baseline setting of the optimization problem [1]. In the data post-processing sub-module, sensitivity of the performance of the DR program to uncertain and inaccurate data is investigated. The uncertainty in preferences of the DR providers is investigated through scenario-based sensitivity analysis. The impact of load and price forecasts uncertainty on the performance of the DR is analyzed by performing a local sensitivity analysis based on perturbed KKT equations [74].

[1]The case selection can include processes more than what we have suggested in this work, such as load and price forecasting, and clustering (for consumer segmentation).

In what follows, we firstly present the underlying assumptions and the formulation of the optimization problem that reflects the operation of a DR program (Section 3.2.1). Secondly, we dive into the data analytics module and explain the mechanisms within the case selection and data post-processing sub-modules (Section 3.2.2).

3.2.1 Demand Response (DR) module

Assumptions

The DR operator is assumed to harness the flexibility from DR providers through load shifting, during each DR operation horizon (in our case 24hr). We consider that load shifting comprises two actions; a load increase at one programmable time unit (PTU) and a corresponding complementary action (i.e., load decrease) at another. Such load shift can occur from one PTU to multiple other PTUs. Although shift in load can naturally modify the need of total electricity consumption, here we assume that the total energy consumption remains unchanged after implementing the DR.

The DR module allows us to simulate the operation of a demand response program through solving a constrained optimization problem. We assume that the DR pursues the objective of the DSO to level the load throughout the day, so that costly investments in network infrastructure can be delayed, without enforcing excessive costs to the DR providers. We assume that DR providers are not rewarded monetarily for providing flexibility. However, we consider that the their electricity cost shall not exceed its value after implementing the DR program. Therefore, in the context of this work, we assume that the DR operator seeks to minimize the variance of the daily load profile.

The proposed objective function contributes to reducing both operational and investment cost. The operation cost of the DSO comprises of cost of congestion and cost of losses. The investment cost of the DSO corresponds to cost of grid expansion and/or reinforcement. In our previous work [100] we show that, under certain assumptions, minimizing the cost of losses is proportional to minimizing the variance of daily load profile. Moreover, one can see that minimizing the variance of daily load (while keeping the daily average constant) implies a more flat load profile with lower and less frequent peaks, and therefore, reduces the stressful utilization of the network. Consequently, in addition to reducing network losses, minimizing the variance of daily load can postpone investments in network reinforcement.

The amount of flexibility DR providers are willing to provide is constrained by their preferences. Preferences of DR providers in a future DR program are reflected in this framework using the following two control variables:

- Downward flexibility (α^d), which denotes the percentage of instantaneous load DR providers are willing to put available, and allow the DR operator to reduce at every PTU.
- Load shifting time window (ω^{tt}), which denotes the time interval within which DR providers allow the DR operator to shift their flexible load.

We assume that α^d and ω^{tt} are input parameters to the optimization problem, and therefore, are constant at all PTUs. Moreover, flexible load can be shifted to the succeeding PTUs (delay), or scheduling to the preceding PTUs (advance scheduling) within one operating horizon.

Further, we assume that DR providers are exposed to the wholesale day-ahead (DA) market prices with hourly resolution. Finally, small errors in load and price forecast are accounted for as local perturbations in the data .

Problem formulation

Consider a DR program which operates over one operating horizon of one day. The operating horizon is divided into T PTUs of equal length, indexed by $m, n \in \{1, \cdots, T\}$. Ω_t is the set of PTUs analyzed.

Variable $\Delta\mathcal{P}_{t_m t_n}$ denotes the amount of flexible load (in kWh) reduced at t_m and shifted to t_n. $\Delta\mathcal{P}_{t_m t_n}$ is a continuous variable and is positive when load is shifted from t_n to t_m (i.e., DR providers increase their consumption at the t_m), and negative otherwise. To ensure energy conservation we define $\Delta\mathcal{P}_{t_n t_m} = -\Delta\mathcal{P}_{t_m t_n}$. The amount of load at t_m after implementing the DR reads as:

$$\mathcal{P}_{t_m} = \mathcal{P}^0_{t_m} + \sum_{n \in \Omega_t} \Delta\mathcal{P}_{t_m t_n} \tag{3.1}$$

where $\mathcal{P}^0_{t_m}$ denotes the initial load at t_m.

The flexibility at each PTU can be positive, zero, or negative. That is reflected in the model via:

$$\Delta\mathcal{P}_{t_m t_n} W_{t_m t_n} \leq 0, \ \forall m, n \in \Omega_t, \tag{3.2}$$

where,

$$W_{t_m t_n} = \begin{cases} 1, & \forall \left\{\mathcal{P}^0_{t_m} \geq \bar{\mathcal{P}}\right\}, m, n \in \Omega_t \\ -1, & \text{otherwise.} \end{cases} \tag{3.3}$$

Parameter $W_{t_m t_n}$ is defined in (3.3) to enforce the appropriate direction of flexibility which minimizes the variance of daily load profile. That is, if the initial load at PTU t_m is above the daily average load, $W_{t_m t_n}$ is positive and constraint (3.2) enforces the model to utilizes the flexibility in negative direction to reduce the load at the PTU, and vice versa.

The load shifting should be restricted to stay within the allowed flexibility time window ($t_m \pm \omega^{tt}$) which is determined by the DR providers. That is:

$$-M_{t_m t_n} \leq \Delta\mathcal{P}_{t_m t_n} \leq M_{t_m t_n},\ \forall m, n \in \Omega_t. \tag{3.4}$$

Note that parameter $M_{t_m t_n}$ is defined in (3.5) in such a way that the load shifting stays within the allowed time window by imposing $\Delta\mathcal{P}_{t_m t_n}$ to be zero for $t_m - t_n$ exceeding the allowed time window.

$$M_{t_m t_n} = \begin{cases} 0, & \forall \left\{|t_m - t_n| \geq \omega^{tt}\right\}, m, n \in \Omega_t \\ \infty, & \text{otherwise} \end{cases} \tag{3.5}$$

The amount of load that the DR providers are willing to reduce during each PTU to put available to the DR operator should be restricted by their preferences on α^d. We define the maximum allowed load reduction at each PTU as $\alpha^d \mathcal{P}^0_{t_m}$. Therefore, the total load reduction (i.e., negative flexibility) during each PTU is limited as:

$$-\sum_{n \in \Omega_t} \Delta\mathcal{P}_{t_m t_n} \leq \alpha^d \mathcal{P}^0_{t_m},\ \forall m \in \Omega_t \tag{3.6}$$

A key point to encourage DR providers to participate in the program is to ensure that they avoid opportunity loss due to providing DR services. That is, the total electricity cost of the DR providers after implementing the DR program falls short of its value before implementing it. This fact is reflected in the model via:

$$\sum_{m \in \Omega_t} \mathcal{P}_{t_m} \rho_{t_m} \leq \sum_{m \in \Omega_t} \mathcal{P}^0_{t_m} \rho_{t_m} \tag{3.7}$$

in which ρ_{t_m} denotes the day-ahead electricity price. This constraint can be reformulated as:

$$\sum_{m \in \Omega_t} \sum_{n \in \Omega_t} \Delta\mathcal{P}_{t_m t_n} \rho_{t_m} \leq 0 \tag{3.8}$$

where the left hand side of the inequality represents the change in the total daily electricity cost of the DR providers after implementing the DR program (ΔC). A negative ΔC indicates that the DR providers are gaining money by engaging in the DR program.

Following the objective of the DSO, we assume that the DR operator seeks to minimize the variance of the daily load of aggregated DR providers. Thus, the objective function of the DR optimizer (Ψ) reads as:

$$\Psi = \sigma_{\mathcal{P}}^2 = 1/T \cdot \sum_{m \in \Omega_t} \left(\mathcal{P}_{t_m} - \bar{\mathcal{P}}\right)^2 \tag{3.9}$$

where $\bar{\mathcal{P}}$ denotes the daily average load. The optimization problem takes on the following form:

$$\min_{\Delta \mathcal{P}_{t_m t_n}} \ \Psi = \sigma_{\mathcal{P}}^2 \tag{3.10}$$

subject to

$$(\nu_{t_m t_n}, \zeta_{t_m t_n}) : -M_{t_m t_n} \leq \Delta \mathcal{P}_{t_m t_n} \leq M_{t_m t_n}, \ \forall m, n \in \Omega_t \tag{3.11}$$

$$(\mu_{t_m t_n}) : \quad \Delta \mathcal{P}_{t_m t_n} W_{t_m t_n} \leq 0, \ \forall m, n \in \Omega_t \tag{3.12}$$

$$(\eta_{t_m}) : \quad -\sum_{n \in \Omega_t} \Delta \mathcal{P}_{t_m t_n} \leq \alpha^d \mathcal{P}^0_{t_m}, \ \forall m \in \Omega_t \tag{3.13}$$

$$(\xi) : \quad \sum_{m \in \Omega_t} \mathcal{P}_{t_m} \rho_{t_m} \leq \sum_{m \in \Omega_t} \mathcal{P}^0_{t_m} \rho_{t_m} \tag{3.14}$$

where $M_{t_m t_n}$ and $W_{t_m t_n}$ are defined in (3.5),(3.3) respectively. Note that the dual multipliers are indicated with Greek letters at the left side of the constraints (3.11)-(3.14).

Analytical solution

The problem (3.10)-(3.14) is a non-linear, convex optimization problem, which is solved by forming the Lagrangian function $\mathcal{L}$. The KKT optimality conditions for problem (3.10)-(3.14) are summarized as:

$$(\nu_{t_m t_n}, \zeta_{t_m t_n}) : -M_{t_m t_n} \leq \Delta \mathcal{P}_{t_m t_n} \leq M_{t_m t_n}, \ \forall m, n \in \Omega_t \tag{3.15}$$

$$(\mu_{t_m t_n}) : \quad \Delta \mathcal{P}_{t_m t_n} W_{t_m t_n} \leq 0, \ \forall m, n \in \Omega_t \tag{3.16}$$

$$(\eta_{t_m}) : \quad -\sum_{n \in \Omega_t} \Delta \mathcal{P}_{t_m t_n} \leq \alpha^d \mathcal{P}^0_{t_m}, \ \forall m \in \Omega_t \tag{3.17}$$

$$(\xi) : \quad \sum_{m \in \Omega_t} \mathcal{P}_{t_m} \rho_{t_m} \leq \sum_{m \in \Omega_t} \mathcal{P}^0_{t_m} \rho_{t_m} \tag{3.18}$$

$$\begin{aligned} &\frac{\partial \mathcal{L}}{\partial \Delta \mathcal{P}_{t_m t_n}} = \\ &2/T \left(\mathcal{P}^*_{t_m} - \mathcal{P}^*_{t_n}\right) + \left(\nu^*_{t_m t_n} - \nu^*_{t_n t_m}\right) + \left(\zeta^*_{t_m t_n} - \zeta^*_{t_n t_m}\right) \\ &+ \left(W_{t_m t_n} \mu^*_{t_m t_n} - W_{t_n t_m} \mu^*_{t_n t_m}\right) - \left(\eta^*_{t_m} - \eta^*_{t_n}\right) \\ &+ \xi^* \left(\rho_{t_m} - \rho_{t_n}\right) = 0 \ , \ \forall m, n \in \Omega_t \end{aligned} \tag{3.19}$$

$$\sum_{m\in\Omega_t}\sum_{n\in\Omega_t}\Big(\nu^*_{t_mt_n}(\Delta\mathcal{P}^*_{t_mt_n}-M_{t_mt_n}) + \zeta^*_{t_mt_n}(-\Delta\mathcal{P}^*_{t_mt_n}-M_{t_mt_n})\Big)=0 \tag{3.20}$$

$$\sum_{m\in\Omega_t}\sum_{n\in\Omega_t}\big(\mu^*_{t_mt_n}(\Delta\mathcal{P}^*_{t_mt_n}\cdot W_{t_mt_n})\big)=0 \tag{3.21}$$

$$\sum_{m\in\Omega_t}\eta^*_{t_m}\cdot(-\alpha^d\cdot\mathcal{P}^0_{t_m}-\sum_{j\in\Omega_t}\Delta\mathcal{P}^*_{t_mt_n})=0\ ,\ \forall n\in\Omega_t \tag{3.22}$$

$$\xi^*\cdot\left(\sum_{m\in\Omega_t}(\mathcal{P}^*_{t_m}\cdot\rho_{t_m})-\sum_{m\in\Omega_t}\mathcal{P}^0_{t_m}\cdot\rho_{t_m}\right)=0. \tag{3.23}$$

$$\nu^*_{t_mt_n}\geq 0\ ,\ \forall m,n\in\Omega_t \tag{3.24}$$

$$\zeta^*_{t_mt_n}\geq 0\ ,\ \forall m,n\in\Omega_t \tag{3.25}$$

$$\gamma^*_{t_mt_n}\geq 0\ ,\ \forall m,n\in\Omega_t \tag{3.26}$$

$$\mu^*_{t_mt_n}\geq 0\ ,\ \forall m,n\in\Omega_t \tag{3.27}$$

$$\eta^*_{t_m}\geq 0\ ,\ \forall m\in\Omega_t \tag{3.28}$$

$$\xi^*\geq 0. \tag{3.29}$$

where $\Delta\mathcal{P}^*_{t_mt_n}$ and ($\nu^*_{t_mt_n}$, $\zeta^*_{t_mt_n}$, $\gamma^*_{t_mt_n}$, $\mu^*_{t_mt_n}$, $\eta^*_{t_m}$, ξ^*) denote the optimal value of the primal and dual optimization variables.

3.2.2 Data Analytics Module

The DR module, formulated in section 3.2.1, uses electric load and market price data, as well as information about preferences of DR providers on providing flexibility. There is uncertainty associated with these type of data. The reason is that, as elaborated above, these data are hardly available or they are subject to error due to poor forecasting or data manipulation. The data analytics module delivers two services: data extraction (in the case selection), and sensitivity analysis (in data post-processing).

Case selection

The case selection sub-module determines the input set of a future DR program (here formulated as an optimization problem) from existing data. This input set contains i) load and price data, and ii) preferences of the DR providers.

The DR module runs load shifting simulations on load and price profiles for each operating period (i.e., 24 hours). Due to the dimensionality of the optimization problem (3.10)-(3.14) and its computational intensity, the size of the input set should be restricted to a limited number of

operating periods. This step allows to identify and select informative subsets from the available historical load and price data to perform the DR optimization.

Another input to the DR module is preferences of DR providers in terms of variables α^d and ω^{tt} (see sub-section 3.2.1). The values of these variables are not known prior to implementing DR. In order to assess the performance of a future DR under different preferences of DR providers, we introduce scenarios on the values of the control variable. The proposed scenarios cover a feasible range for these variables (e.g., 5% to 20% for α^d, and 4hr to 23hr for ω^{tt}).

Data post-processing and sensitivity matrix

In the data post-processing sub-module, performance of the proposed DR program is evaluated and compared under various scenarios of preferences of DR providers. Moreover, sensitivity of the DR program to load and price data is determined by formulating the sensitivity matrix from the perturbed KKT equations of problem (3.10)-(3.14). The remainder of this section presents the procedure to derive an analytical expression of the sensitivity matrix.

The objective function (3.10) and all KKT equations (3.19)-(3.23) are perturbed with respect to the inputs (matrix $\boldsymbol{a}$ in (3.30)), Lagrange multipliers (matrix $\boldsymbol{\kappa}$ in (3.30)), and the decision variables of the optimization problem (matrix x^* in (3.31)), in the vicinity of the optimal point. That is, a set of feasible perturbations includes moving from one KKT solution to another KKT solution.

$$\boldsymbol{a}_{(P\times 1)} = \begin{bmatrix} \left[\mathcal{P}^0_{t_i}\right]_{(T\times 1)} \\ \left[\alpha^d\right]_{(1\times 1)} \\ \left[\rho_{t_i}\right]_{(T\times 1)} \\ \left[M_{t_i t_j}\right]_{(N\times 1)} \\ \left[W_{t_i t_j}\right]_{(N\times 1)} \end{bmatrix}, \quad \boldsymbol{\kappa}_{(m_J\times 1)} = \begin{bmatrix} \left[\gamma_{t_i t_j}\right]_{(N\times 1)} \\ \left[\mu_{t_i t_j}\right]_{(N\times 1)} \\ \left[\eta_{t_i}\right]_{(T\times 1)} \\ \left[\xi\right]_{(1\times 1)} \end{bmatrix} \tag{3.30}$$

$$x^* = \left[\Delta\mathcal{P}_{t_i t_j}\right]_{(N\times 1)} \tag{3.31}$$

Note that in this work $T = 24hr$, and $N = T(T-1)/2$.

Under the condition that active constraints remain active after the perturbation, all perturbed equations can be written in a matrix form as follows:

$$\underbrace{\begin{bmatrix} \boldsymbol{F_x} & \mathbf{0} & \mathbf{0} & -1 \\ \boldsymbol{F_{xx}} & \boldsymbol{H_x^T} & \boldsymbol{G_x^T} & 0 \\ \boldsymbol{H_x} & \mathbf{0} & \mathbf{0} & 0 \\ \boldsymbol{G_x} & \mathbf{0} & \mathbf{0} & 0 \end{bmatrix}}_{\boldsymbol{U}} \underbrace{\begin{bmatrix} d\boldsymbol{x} \\ d\boldsymbol{\upsilon} \\ d\boldsymbol{\kappa} \\ d\Psi \end{bmatrix}}_{d\boldsymbol{X}} = -\underbrace{\begin{bmatrix} \boldsymbol{F_a} \\ \boldsymbol{F_{xa}} \\ \boldsymbol{H_a} \\ \boldsymbol{G_a} \end{bmatrix}}_{\boldsymbol{V}} d\boldsymbol{a} \tag{3.32}$$

where $\boldsymbol{G}$ and $\boldsymbol{H}$ represent the equality and inequality constraints, respectively. $\boldsymbol{\upsilon}$ and $\boldsymbol{\kappa}$ are the matrices of Lagrangian multipliers associated with the equality and inequality constraints, respectively. The corresponding sub-matrices in (3.32) are presented in 3.2.3.

We define the matrix of sensitivities $\boldsymbol{S_M} = d\boldsymbol{X}/d\boldsymbol{a}$ which includes all the sensitivities with respect to components of the parameter $\boldsymbol{a}$. In order to determine the matrix of sensitivities from the system of equations (3.32), we first need to know the characteristic of the optimal point. An optimal point can be characterized as a 'regular point' when the gradient vector of the active constraints are linearly independent. In that case, matrix $\boldsymbol{U}$ is invertible, and therefore the matrix of sensitivities can be determined as $\boldsymbol{S_M} = \boldsymbol{U}^{-1}\boldsymbol{V}$ [74].

Consider the case when the optimal point is a 'non-regular point'; that occurs when the gradient vector of active inequality constraints are linearly dependent. In this case, matrix $\boldsymbol{U}$ is not invertible (so-called 'ill-posed' problem). Ill-posed problems can be solved using regularization. Regularization provides accurate approximate solutions by introducing prior information [101]. Using the Tikhonov regularization method, the sensitivity matrix can be determined as

$$\boldsymbol{S_M} = (\boldsymbol{U} + \delta I)^{-1}(\boldsymbol{V}) \tag{3.33}$$

where δ is the regularization parameter and is introduced to prevent singularities in the matrix. Parameter δ is a scalar with a positive value. In this work, the optimal point is non-regular, thus the value of δ is determined in an iterative process.

3.2.3 Perturbation Matrices

This subsection presents the corresponding sub-matrices in (3.32). It should be noted that there are no equality constraints in the proposed optimization problem. Therefore, vector ν containing the Lagrange multipliers associated with the equality constraints, and matrices $\boldsymbol{H_x}$ and $\boldsymbol{H_a}$ in (3.32) are null.

$$\boldsymbol{F_x}_{(1\times N)} = \left[2/T\left(\mathcal{P}^*_{t_i} - \mathcal{P}^*_{t_j}\right)\right]_{(1\times N)} \tag{3.34}$$

$$\boldsymbol{F_a}_{(1\times P)} = \left[\boldsymbol{F^1_a}_{(1\times T)} \quad 0 \quad \boldsymbol{0}_{(1\times T)} \quad \boldsymbol{0}_{(1\times N)} \quad \boldsymbol{0}_{(1\times N)}\right] \tag{3.35}$$

$$\boldsymbol{F^1_a}_{(1\times T)} = \left[2/T\cdot\left(\mathcal{P}^*_{t_i} - \bar{\mathcal{P}}\right)\right]_{(1\times T)} \tag{3.36}$$

$$\boldsymbol{F_{xx}} = 2/T\left[\frac{\partial}{\partial\Delta\mathcal{P}_{t_i t_j}}\left(\sum_{m\in\Omega_t}\Delta\mathcal{P}_{t_r t_m} - \sum_{n\in\Omega_t}\Delta\mathcal{P}_{t_q t_n}\right)\right]_{(N\times N)} \tag{3.37}$$

$$\tag{3.38}$$

where

$$\frac{\partial}{\partial \Delta \mathcal{P}_{t_i t_j}} \left(\Delta \mathcal{P}_{t_m t_n} \right) = \begin{cases} 1, & \forall m = i, n = j \\ -1, & \forall m = j, n = i \\ 0, & else \end{cases} \tag{3.39}$$

$$\boldsymbol{F_{xa}}_{(N \times P)} = \begin{bmatrix} \boldsymbol{F^1_{xa}} & \boldsymbol{F^2_{xa}} & \boldsymbol{F^3_{xa}} & \boldsymbol{F^4_{xa}} & \boldsymbol{F^5_{xa}} \end{bmatrix} \tag{3.40}$$

$$\boldsymbol{F^1_{xa}}_{(N \times T)} = 2/T \left[\frac{\partial}{\partial \mathcal{P}^0_{t_i}} \left(\mathcal{P}^0_{t_m} - \mathcal{P}^0_{t_n} \right) \right]_{(N \times T)} \tag{3.41}$$

$$\boldsymbol{F^2_{xa}}_{(N \times 1)} = \mathbf{0} \tag{3.42}$$

$$\boldsymbol{F^3_{xa}}_{(N \times T)} = \xi^* \left[\frac{\partial}{\partial \rho_{t_i}} \left(\rho_{t_m} - \rho_{t_n} \right) \right]_{(N \times T)} \tag{3.43}$$

$$\boldsymbol{F^4_{xa}}_{(N \times N)} = \mathbf{0} \tag{3.44}$$

$$\boldsymbol{F^5_{xa}} = \left[\frac{\partial}{\partial W_{t_i t_j}} \left(W_{t_m t_n} \cdot \mu_{t_m t_n} - W_{t_n t_m} \cdot \mu_{t_n t_m} \right) \right]_{(N \times N)} \tag{3.45}$$

$$\boldsymbol{G_x}_{(M \times N)} = \begin{bmatrix} \boldsymbol{G^1_x} & \boldsymbol{G^2_x} & \boldsymbol{G^3_x} & \boldsymbol{G^4_x} & \boldsymbol{G^5_x} \end{bmatrix}^T \tag{3.46}$$

$$\boldsymbol{G^1_x}_{(N \times N)} = \left[\frac{\partial}{\partial \Delta \mathcal{P}_{t_i t_j}} (\Delta \mathcal{P}_{t_m t_n}) \right]_{(N \times N)} \tag{3.47}$$

$$\boldsymbol{G^2_x}_{(N \times N)} = \left[\frac{\partial}{\partial \Delta \mathcal{P}_{t_i t_j}} (\Delta \mathcal{P}_{t_m t_n}) \right]_{(N \times N)} \tag{3.48}$$

$$\boldsymbol{G^3_x}_{(N \times N)} = \left[\frac{\partial}{\partial \Delta \mathcal{P}_{t_i t_j}} (\Delta \mathcal{P}_{t_m t_n} \cdot W_{t_m t_n}) \right]_{(N \times N)} \tag{3.49}$$

$$\boldsymbol{G^4_x}_{(N \times T)} = \left[\frac{\partial}{\partial \Delta \mathcal{P}_{t_i t_j}} (- \sum_{r \in \Omega_t} \Delta \mathcal{P}_{t_m t_r}) \right]_{(N \times T)} \tag{3.50}$$

$$\boldsymbol{G^5_x}_{(N \times 1)} = \left[\rho_{t_i} - \rho_{t_j} \right]_{(N \times 1)} \tag{3.51}$$

$$\boldsymbol{G_a}_{(M \times P)} = \begin{bmatrix} \boldsymbol{G^1_a} & \boldsymbol{G^2_a} & \boldsymbol{G^3_a} & \boldsymbol{G^4_a} & \boldsymbol{G^5_a} \end{bmatrix}^T \tag{3.52}$$

$$\boldsymbol{G^1_{a(P\times N)}} = \boldsymbol{G^2_{a(P\times N)}} = \\ \begin{bmatrix} \mathbf{0}_{(T\times N)} & \mathbf{0}_{(1\times N)} & \mathbf{0}_{(T\times N)} & -I_N & \mathbf{0}_{(N\times N)} \end{bmatrix} \tag{3.53}$$

$$\boldsymbol{G^3_{a(P\times N)}} = \begin{bmatrix} \mathbf{0}_{(T\times N)} & \mathbf{0}_{(1\times N)} & \mathbf{0}_{(T\times N)} & \mathbf{0}_N & \boldsymbol{G^3_{a_5}} \end{bmatrix} \tag{3.54}$$

$$\boldsymbol{G^3_{a_5(N\times N)}} = \begin{cases} \left[\Delta \mathcal{P}^*_{t_i t_j}\right]_{(N\times N)} & , \forall m = i, n = j \\ [\mathbf{0}]_{(N\times N)} & , else \end{cases} \tag{3.55}$$

$$\tag{3.56}$$

$$\boldsymbol{G^4_{a(P\times T)}} = \begin{bmatrix} \boldsymbol{G^4_{a_1}} & \boldsymbol{G^4_{a_2}} & \mathbf{0}_{(T\times T)} & \mathbf{0}_{(N\times T)} & \mathbf{0}_{(N\times T)} \end{bmatrix} \tag{3.57}$$

$$\boldsymbol{G^4_{a_1}} = Diag\left(-\alpha^d\right)_{(T\times T)},\ \boldsymbol{G^4_{a_2}} = \left[-\mathcal{P}^0_{t_i}\right]_{(1\times T)} \tag{3.58}$$

$$\boldsymbol{G^5_{a(P\times 1)}} = \begin{bmatrix} \mathbf{0}_{(T\times 1)} & \mathbf{0}_{(T\times 1)} & \boldsymbol{G^5_{a_3}} & \mathbf{0}_{(N\times 1)} & \mathbf{0}_{(N\times 1)} \end{bmatrix} \tag{3.59}$$

$$\boldsymbol{G^5_{a_3(T\times 1)}} = \left[\sum_{j\in\Omega_t} \Delta \mathcal{P}_{t_i t_j}\right]_{(T\times 1)} \tag{3.60}$$

3.3 Results and Discussion

3.3.1 Input Data

In order to show the effectiveness of our framework, we tested our framework on a data set of electricity consumption from a student housing complex in Wageningen, the Netherlands. We used the aggregated data for 44 houses in the data set, with 15-minutes resolution, from 1 January 2014 to 31 December 2014. Historical day-ahead (DA) market price data was gathered from the Scandinavian electricity market (Noord-Pool spot market) with 1-hour resolution, for the same period. We ran the simulations for one DR operating period with 30-minutes resolution (i.e., from 00:30 to 24:00).

3.3.2 Case Selection

Due to high dimensionality of the search space of the DR optimization problem (i.e., $N = (48 \times 47)/2 = 1128$ decision variables, for an operating period of 24 hours with 30-minute time resolution), solving the problem for one complete year is not feasible. To investigate the performance of our framework, and compare the results under various load profiles, we selected informative subset from the available data set. As the objective of the DR is to minimize the variance of daily load, we considered that as the basis of our selection. Accordingly, we selected three representative days, as follows:

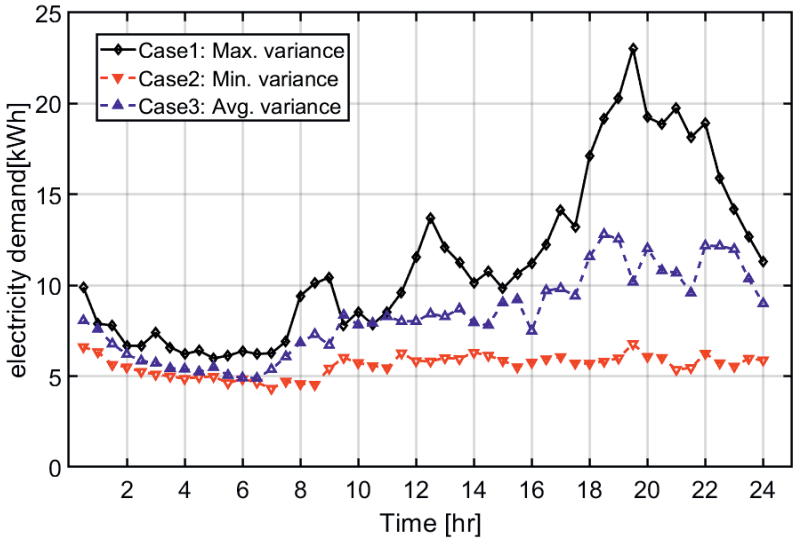

Figure 3.2: Load profile of Case1 (solid black line), the day with the maximum variance, Case2 (dashed red line), the day with the minimum variance, and Case3 (dashed blue line), with moderate variance of daily load.

- Case 1: the day with the largest variance of daily load (i.e., Monday, 1 December 2014), and therefore, the highest potential for load shifting.
- Case 2: the day with the smallest variance of daily load (i.e., Saturday, 19 July 2014).
- Case 3: the day with the average variance of daily load (i.e., Tuesday, 10 June 2014).

Figures 3.2 and 3.3 show the daily load profile and the daily price profile, respectively, for the three representative days. Case 1 is the day with the largest load volatility, and the highest potential for load shifting. Therefore, we use Case 1 as a benchmark to study the performance of the DR program (sections 3.3.3), and its sensitivity to preferences of DR providers (section 3.3.4). Further, we extensively elaborate on the sensitivity of DR to variations in load and price data for Case 1, and in the end make a comparison with Case 2 and Case 3 (section 3.3.5).

As outlined above, our goal is to study the performance of a future DR program, and investigate its sensitivity to various preferences of DR providers. However, the preferences of the DR providers (namely α^d and ω^{tt}), are not accessible to the DR operator, for a future DR program prior to its implementation. To investigate the impact of preferences of DR providers on the performance of the DR program, we introduce the following 20 scenarios:

- $S_{1,1}$ to $S_{1,4}$: $\omega^{tt} = 23hr,\ \alpha^d = 20\%, 15\%, 10\%, 5\%,$

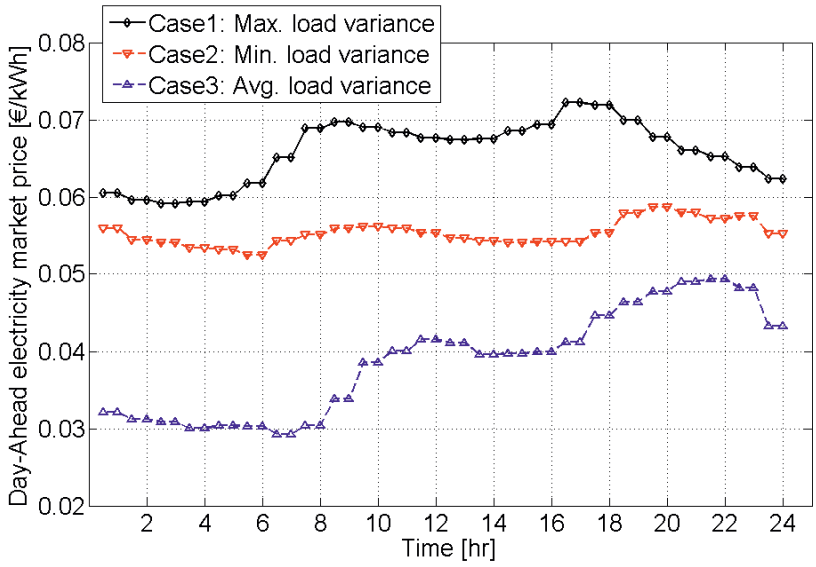

Figure 3.3: Price profile of Case1 (solid black line), the day with the maximum variance, Case2 (dashed red line), the day with the minimum variance, and Case3 (dashed blue line), with moderate variance of daily load.

- $S_{2,1}$ to $S_{2,4}$: $\omega^{tt} = 16hr$, $\alpha^d = 20\%, 15\%, 10\%, 5\%$,
- $S_{3,1}$ to $S_{3,4}$: $\omega^{tt} = 12hr$, $\alpha^d = 20\%, 15\%, 10\%, 5\%$,
- $S_{4,1}$ to $S_{4,4}$: $\omega^{tt} = 8hr$, $\alpha^d = 20\%, 15\%, 10\%, 5\%$,
- $S_{5,1}$ to $S_{5,4}$: $\omega^{tt} = 4hr$, $\alpha^d = 20\%, 15\%, 10\%, 5\%$.

Among all scenarios, Scenario $S_{1,1}$, with $\omega^{tt} = 23hr$ which puts no limit on the load shifting time window, and $\alpha^d = 20\%$, potentially offers the largest flexibility to the DR operator. On the other hand, Scenario $S_{5,4}$ with a tight load shifting time window of $\omega^{tt} = 4hr$ and $\alpha^d = 5\%$, offers the lowest flexibility to the DR operator.

Note that, α^d and ω^{tt} can be load-type dependent, and therefore take different values to represent different types of DR providers. In this work, for the sake of simplicity and also to make the results easily interpretable, in each scenario we assume a constant value for α^d and ω^{tt}.

3.3.3 DR Simulation Results for Case 1

In this subsection we present the DR simulations results for the day with maximum variance of daily load (Case 1). The optimization problem (3.10)-(3.14) is implemented in the MATLAB function 'fmincon', using an interior-point algorithm.

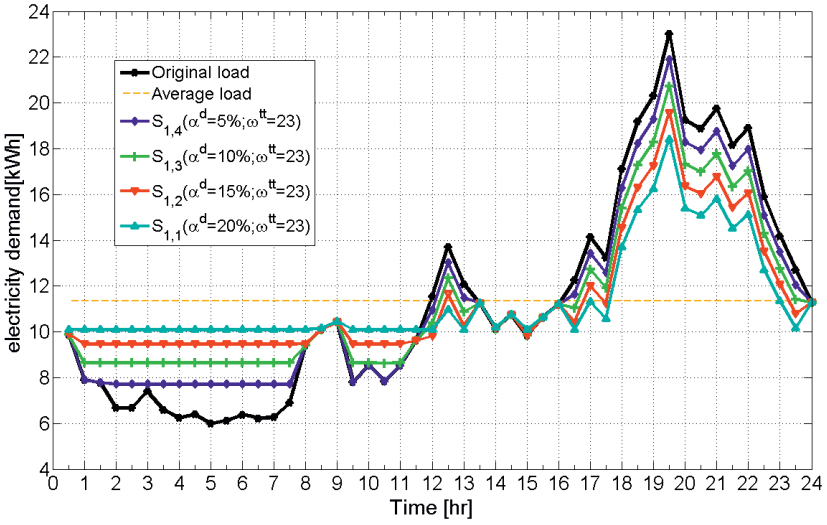

Figure 3.4: Original load profile (black line), average load (dashed orange line), and the load profile after implementing DR under scenarios $S_{1,1}$ to $S_{1,4}$ with $\omega^{tt} = 23hr$ and $\alpha^d = 20\%$ (solid cyan), $\alpha^d = 15\%$ (solid red), $\alpha^d = 10\%$ (solid green) , $\alpha^d = 5\%$ (solid blue).

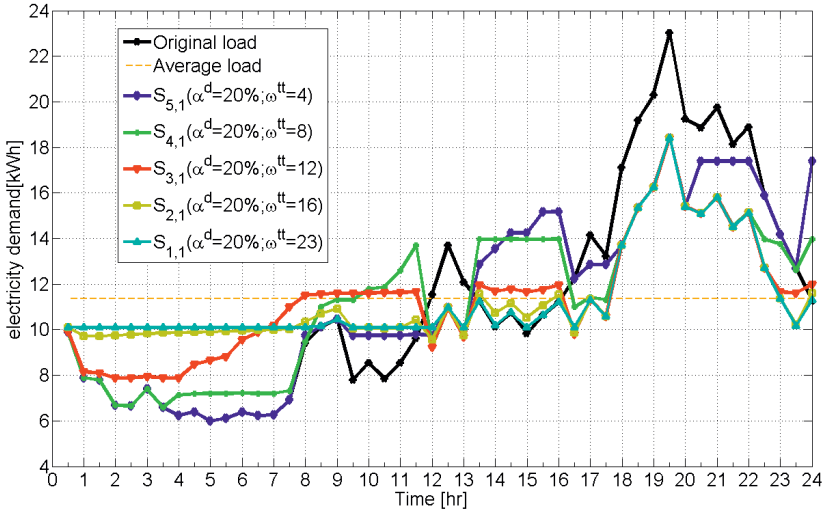

Figure 3.5: Original load profile (black line), average load (dashed orange line), and the load profile after implementing DR under scenarios $S_{1,1}$ to $S_{5,1}$ with $\alpha^d = 20\%$ and $\omega^{tt} = 23hr$ (solid cyan), $\omega^{tt} = 16hr$ (solid yellow), $\omega^{tt} = 12hr$ (solid red), $\omega^{tt} = 8hr$ (solid green), $\omega^{tt} = 4hr$ (solid blue).

Figure 3.4 shows the daily average load (dashed orange line), the original load profile (solid black line). The figure also shows the load profile after implementing the DR program, for scenarios $S_{1,1}$ to $S_{1,4}$ (i.e., $\omega^{tt} = 23hr$ and $\alpha^d \in \{20\%, 15\%, 10\%, 5\%\}$). Under all scenarios, the DR program shifts the load from the PTUs with load above the daily average (i.e., PTUs corresponding to 12:00 hr to 13:30 hr and 16:00 hr to 24:00 hr) to the ones with load below the average (i.e., PTUs corresponding to 00:00 hr to 12:00 hr and 13:30 hr to 16:00 hr), to reduce the variance of the daily load profile. Comparing the load profile under scenarios $S_{1,1}$ to $S_{1,4}$, one observes that larger values of α^d resulted in larger peak load reduction, a larger increase in the load of the PTUs corresponding to 00:00 hr to 12:00 hr, and therefore, a more flat load profile. This implies that the DSO benefits more from the DR for larger levels of downward flexibility α^d when the DR providers have no limit on the load shifting time window ω^{tt}.

Figure 3.5 shows the original load profile (solid black line), daily average load (dashed orange line), and the load profile after implementing DR for scenarios $S_{1,1}$ to $S_{5,1}$ (i.e., $\alpha^d = 20\%$ and $\omega^{tt} \in \{23hr, 16hr, 8hr, 4hr\}$). As the objective of the DR is to minimize the variance of the daily load profile, one can observe here too, that implementing the DR program results in shifting the load from the PTUs with load above the average load to the ones with load below the average.

Comparing the load profiles resulted under the scenarios $S_{1,1}$ to $S_{5,1}$ (see Figure 3.5), one can observe that a larger ω^{tt} results in a larger load shift from different hours to 00:00-12:00 hr intervals (i.e., midnight/early-morning hours). Under scenarios $S_{1,1}$ and $S_{2,1}$ (with $\omega^{tt} = 23, 16hr$, respectively), the load shift pattern is mostly from evening peak hours (i.e., 16:00-24:00 hr interval) which contain the night peak, to the midnight/early morning hours which is off-peak hours. Under scenarios $S_{4,1}$ and $S_{5,1}$ (i.e., $\omega^{tt} = 8, 4hr$), the midnight/early-morning hours are not available to host the flexible load of the evening peak hours. Under such scenarios, the evening peak load is shifted mainly to 13:30-16:00 hr intervals, which results in load values larger than the average load, and steep changes in the load profile. Yet, the variance of the load profile, and thus the power losses, decreases under these scenarios. Under the scenario $S_{3,1}$ with $\omega^{tt} = 12hr$ one can observe that during PTUs corresponding to 08:00-11:30hr, and 13:30-16:00hr the load values are very close to the daily average load. This observation confirms the fact that α^d works as a 'scaling' factor, and ω^{tt} as a 'shaping' factor in load profile after implementing the DR program. A similar trend exists in the load profiles associated with other Scenarios that are not presented here.

Figure 3.6 demonstrates the reduction in the total daily electricity cost of DR providers, as a percentage of their cost before implementing DR program (i.e., ΔC). Each line represents the scenarios with a constant ω^{tt}. One can observe that ΔC has a negative value after implementing the DR program (i.e., $\alpha^d \geq 5\%$). That is, the daily electricity cost of the DR providers decreases under all scenarios. Moreover, for a constant ω^{tt} the daily electricity cost of the DR providers decreases for larger values of α^d.

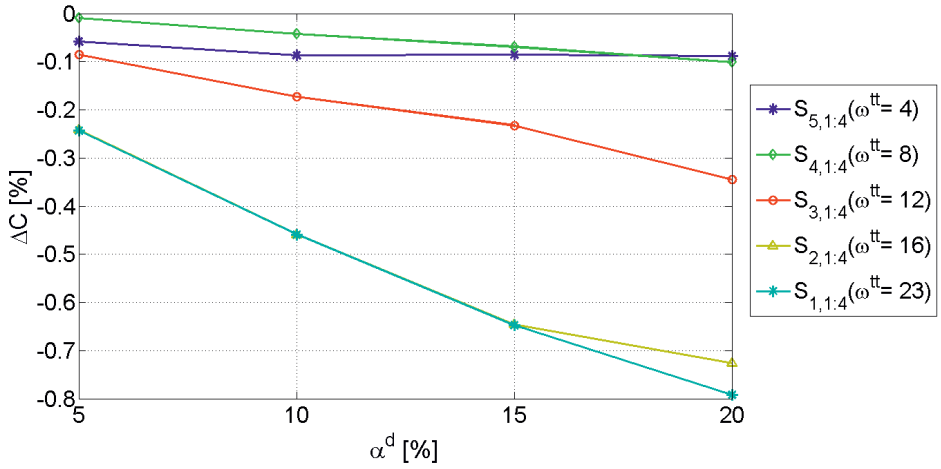

Figure 3.6: Total daily electricity cost reduction of the DR providers (% ΔC), under scenarios $S_{5,1:4}$ with $\omega^{tt} = 4hr$ (blue line), $S_{4,1:4}$ with $\omega^{tt} = 8hr$ (green line), $S_{3,1:4}$ with $\omega^{tt} = 12hr$ (red line), $S_{2,1:4}$ with $\omega^{tt} = 16hr$ (yellow line), $S_{1,1:4}$ with $\omega^{tt} = 23hr$ (cyan line).

3.3.4 Sensitivity of Performance of DR to the Preferences of the DR Providers

Figure 3.7 shows the contour plot of the optimal value of the objective function Ψ in Equation 3.10 (i.e., the variance of the daily load profile), versus the preferences of the DR providers ω^{tt} and α^d. The contour lines show the values of Ψ, and the color intensity shows the value of Ψ, which increases moving from dark brown to yellow.

One can observe that the objective function Ψ has the largest value when $\omega^{tt} = 0hr$ and $\alpha^d = 0\%$ (i.e., before implementing the DR). By increasing ω^{tt} and α^d, the value of Ψ decreases. Ψ reaches its lowest value for $\omega^{tt} = 23hr$ and $\alpha^d = 20\%$ (i.e., $S_{1,1}$ with largest flexibility). Therefore, implementing DR program in future energy systems can reduce the variance of daily load. Moreover, the contour lines show that a certain value of the objective function Ψ can be reached with different combinations of ω^{tt} and α^d.

An important observation from Figure 3.7 is about the individual impact of each variable ω^{tt} and α^d on the objective function Ψ. For a certain α^d moving along the horizontal-axis from left to right (larger values of ω^{tt}) one can see that the contour intervals, which show changes in the optimal value of the objective function Ψ, increase and eventually the objective function reaches a horizontal asymptote. For a small α^d (e.g., 5%) the objective function reaches the horizontal asymptote at lower values of ω^{tt}. This observation implies that, firstly, for a certain downward flexibility (α^d), the performance of the DR program improves by allowing a larger load shifting time window (ω^{tt}). However, this improvement has a limit and it reaches a saturation point, that depends on the available shiftable load. Secondly, the performance of the DR is highly sensitive

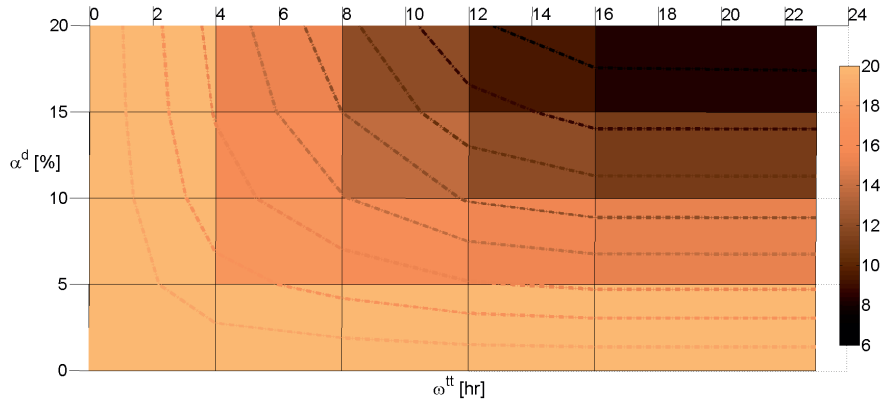

Figure 3.7: Contour plot of variance of daily load profile (Ψ) for Case1, before implementing the DR and after that, under scenarios $S_{1,1}$ to $S_{5,4}$. The contours show constant values of Ψ.

to load shifting time window only when sufficient amount of load is available to shift. When the flexible load is scarce, the load shifting time window has low impact on the performance of the DR program.

In a similar fashion, from Figure 3.7 one can observe the impact of α^d on performance of the DR program. For a certain ω^{tt}, moving along the vertical-axis from bottom to top (i.e., from small to large values of α^d), the contour intervals increase. For ω^{tt}s smaller than $4hrs$, the figure shows vertical asymptotes, which represent the lowest value Ψ can reach for that ω^{tt}. For $\omega^{tt} = 4hr$, a change in the value of α^d has less impact on Ψ compared to $\omega^{tt} = 16hr$ and $\omega^{tt} = 23hr$. This observation shows that, performance of the DR program for a certain load shifting time window improves by allowing larger downward flexibility. However, there is a limit to this improvement, and the limit depends on the allowed time window.

The result presented above can give practical insight to DR operators. Before engaging in contracts with the DR providers, the DR operator would opt for DR providers (i.e., flexible consumers) that are more likely to allow higher percentage of load reduction (more than 10%) and larger load shifting time window (more than 4 hours). Moreover, the DR operator can give DR providers the freedom to choose from possible combinations of load reduction and load shifting time window (ω^{tt} and α^d), which guarantee the same load profile for the DSO. As a result, the DR operator has more degrees of freedom in its contracts with the DR providers.

3.3.5 Sensitivity of Performance of DR to Input Data

This sub-section presents the numerical results concerning the impact of uncertainties in load and price data forecasts, on the performance of the proposed DR program. We used the

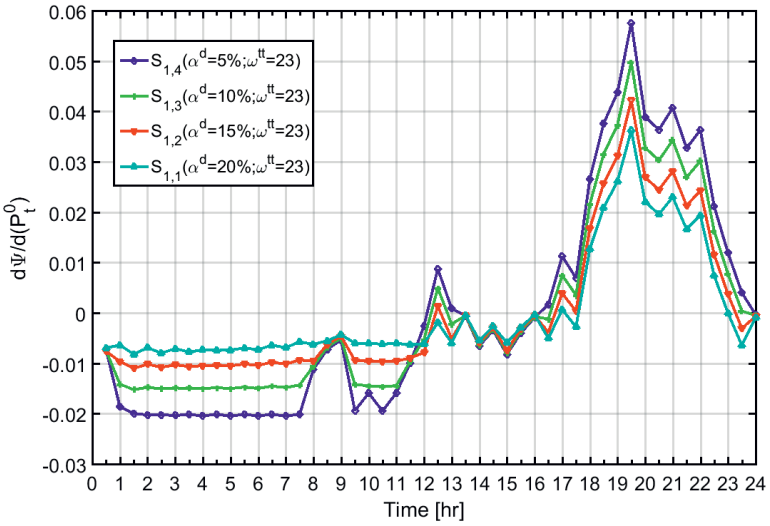

Figure 3.8: Sensitivity of the objective function at the optimal point with respect to perturbations in load ($\frac{d\Psi}{d\mathcal{P}_t^0}|_{\omega^{tt}=23hr}$), for scenarios $S_{1,1}$ to $S_{1,4}$ with $\omega^{tt} = 23hr$ and $\alpha^d = 20\%$ (cyan line), $\alpha^d = 15\%$ (red line), $\alpha^d = 10\%$ (green line), and $\alpha^d = 5\%$ (blue line).

sensitivity matrix S_M in (3.33) to compute the local sensitivity of the optimal objective function value with respect to perturbations in load and price (i.e., $\frac{d\Psi}{d\mathcal{P}_t^0}$ and $\frac{d\Psi}{d\rho_t}$, respectively).

It should be noted that the proposed DR framework is based on the assumption of taking the aggregated load of the DR providers. It is established that for such arrangement the unintentional deviations are canceled out [38, 102, 103]. Therefore, we can assume that load and price forecast errors are small enough to fall within the set of feasible perturbations for the local sensitivity analysis.

The sensitivities are evaluated and compared under different scenarios of preferences of the DR providers. In what follows, we first provide an elaborated analysis and discussion on the results for Case 1. Then, we compare the results for all three representative Cases.

Figure 3.8 shows the sensitivity of the objective function of the DR optimization problem (Ψ) to perturbations in load, for scenarios $S_{1,1}$ to $S_{1,4}$ with $\omega^{tt} = 23hr$, (i.e., $\frac{d\Psi}{d\mathcal{P}_t^0}|_{\omega^{tt}=23hr}$). For a certain α^d, the performance of the DR in reducing the variance of daily load is most sensitive to forecast accuracy of $\mathcal{P}_t^0$ during the evening peak hours (i.e., PTUs corresponding to 16:00-22:00 hr). For this period, moving from $\alpha^d = 20\%$ to $\alpha^d = 5\%$, one can see that for a smaller α^d the objective function (Ψ) is more sensitive to load forecast error. This behavior is expected, because at each PTU the executed (negative) flexibility is limited by $\mathcal{P}_t^0\alpha^d$ (see constraint (3.13)). A small α^d means a tighter constraint, and implies that less flexibility is available to be utilized during the

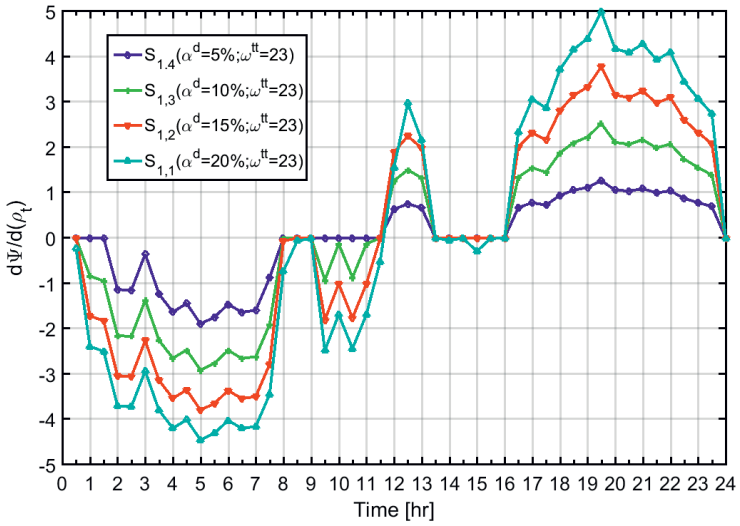

Figure 3.9: Sensitivity of the objective function at the optimal point with respect to perturbations in price ($\frac{d\Psi}{d\rho_t}|_{\omega^{tt}=23hr}$) data, for scenarios $S_{1,1}$ to $S_{1,4}$ with $\omega^{tt} = 23hr$ and $\alpha^d = 20\%$ (cyan line), $\alpha^d = 15\%$ (red line), $\alpha^d = 10\%$ (green line), and $\alpha^d = 5\%$ (blue line).

evening peak hours. One can conclude that $\mathcal{P}_t^0$ plays a more significant role on the performance of the DR when α^d is small. In practice, the DR operator needs higher accuracy in load forecasts from the DR providers whose shiftable load is scarce (e.g., $\alpha^d = 5\%$).

Figure 3.9 shows the sensitivity of the objective function of the DR optimization problem (Ψ) to perturbations in price, for scenarios $S_{1,1}$ to $S_{1,4}$ with $\omega^{tt} = 23hr$ (i.e., $\frac{d\Psi}{d\rho_t}|_{\omega^{tt}=23hr}$). One can observe that for a constant α^d, the DR program is most sensitive to perturbations in price during the evening peak (i.e., 16:00-24:00 hr) and midnight/early morning hours (i.e., 00:00-8:00 hr). Moving from $S_{1,1}$ with $\alpha^d = 5\%$ to $S_{1,4}$ with $\alpha^d = 20\%$ in this period, one can observe that the sensitivity of the performance of the DR to price increases for larger α^d. This effect can be associated with constraint (3.14), which imposes a limit to the electricity cost after implementing the DR program to be lower than its value before implementing the DR. In practice, this result implies that the DR operator can afford larger deviations in price for DR providers with limited shiftable load. However, DR operators should provide more accurate price forecasts to DR providers who are willing to shift larger amount of their load.

Figure 3.10 and Figure 3.11 show the sensitivity of the performance of the DR to perturbations in load and price, respectively, for scenarios $S_{1,1}$ to $S_{5,1}$ with $\alpha^d = 20\%$ (i.e., $\frac{d\Psi}{d\mathcal{P}_t^0}|_{\alpha^d=20\%}$, and $\frac{d\Psi}{d\rho_t}|_{\alpha^d=20\%}$). One can observe that for a certain ω^{tt}, $\frac{d\Psi}{d\mathcal{P}_t^0}|_{\alpha^d=20\%}$ and $\frac{d\Psi}{d\rho_t}|_{\alpha^d=20\%}$ have the largest values during the evening peak (i.e., PTUs corresponding to 16:00 hr to 22:00 hr) compared to other PTUs. This behavior can be associated with constraint (3.11), which imposes the limit on

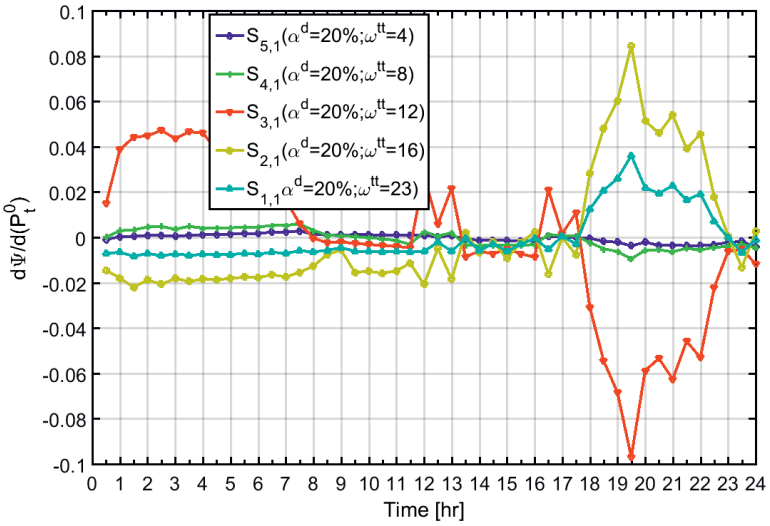

Figure 3.10: Sensitivity of the objective function at the optimal point with respect to perturbations in load ($\frac{d\Psi}{d\mathcal{P}_t^0}|_{\alpha^d=20\%}$), for scenarios $S_{1,1}$ to $S_{5,1}$ with $\alpha^d = 20\%$ and $\omega^{tt} = 23hr$ (cyan line), $\omega^{tt} = 16hr$ (yellow line) , $\omega^{tt} = 12hr$ (red line), $\omega^{tt} = 8hr$ (green line), and $\omega^{tt} = 4hr$ (blue line).

the load shifting time window.

For a given α^d, the maximum amount of flexible load that is available to the DR operator at every PTU is known. What imposes a limit to the performance of the DR, is the time at which that available flexibility can be utilized (i.e., ω^{tt}). Consider also the load profiles in Figure 3.5. The performance of the DR in reducing the variance of the daily load profile largely depends on the load which can be shifted from the evening peak (i.e., 16:00-24:00 hr) to the midnight/early-morning hours (i.e., 00:00-08:00 hr). Under the scenarios $S_{3,1}$ to $S_{5,1}$, one can see that during PTUs corresponding to 13:30-16:00 hr electricity demand surpasses the average load. This observation reflects the fact that there is not enough capacity available during the midnight hours (00:00-08:00hr) to 'host' the shiftable load from the evening peak hours.

Scenario $S_{3,1}$ in Figures 3.10 and 3.11, with $\alpha^d = 20\%$ and $\omega^{tt} = 12hr$ presents a specific case. Under this scenarios the so-called hosting capacity is saturated. As the values of α^d and ω^{tt} are fixed, the available flexibility at every PTU and the maximum possible shift from each PTU is fixed. In that situation, a slight perturbation in load ($\mathcal{P}_t^0$) results in extra available flexibility from the peak hours to shift to the off-peak hours (i.e., 00:00-08:00hr) which are already saturated. This can have a large effect on the optimal solution, as the system is already running at its edge. Therefore, under scenario $S_{3,1}$, a small deviation from the expected values of load and price largely affects the performance of the DR. The results show that the sensitivity of the performance of DR to perturbations in load, is almost negligible for DR providers who

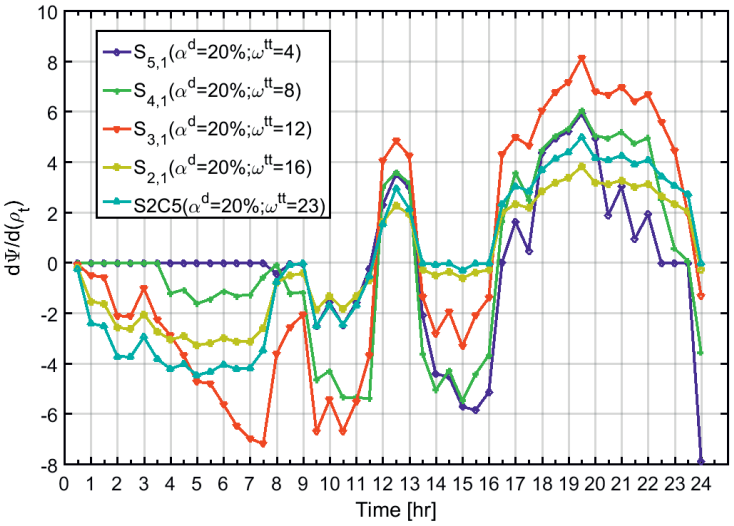

Figure 3.11: Sensitivity of the objective function at the optimal point with respect to perturbations in price ($\frac{d\Psi}{d\rho_t}|_{\alpha^d=20\%}$), for scenarios $S_{1,1}$ to $S_{5,1}$ with $\alpha^d = 20\%$ and $\omega^{tt} = 23hr$ (yellow line), $\omega^{tt} = 16hr$ (cyan line) , $\omega^{tt} = 12hr$ (red line), $\omega^{tt} = 8hr$ (green line), and $\omega^{tt} = 4hr$ (blue line).

offer small load shifting time window (i.e., $\omega^{tt} = 4, 8hr$). On the other hand, the performance of DR is largely sensitive to perturbations in load and price, for DR providers with 12 hours load shifting time window.

Figures 3.12 and 3.13 show the variation in the sensitivity of the objective function to perturbations in load and price, under the Scenario $S_{1,1}$ (i.e., $\frac{d\Psi}{d\mathrm{p}_t^0}|_{\alpha^d=20\%,\omega^{tt}=23hr}$ and $\frac{d\Psi}{d\rho_t}|_{\alpha^d=20\%,\omega^{tt}=23hr}$, respectively), under the three representative days (i.e., Case 1, Case 2, and Case 3). Figures 3.12 shows that the sensitivity of DR to perturbations in load under different Cases, has the largest variations during the evening peak hours, compared to other hours. This behavior can be associated to the difference in the amount of load that is available to the DR operator to reduce at every PTU (see Figure 3.2). From Figure 3.13 one can observe that the sensitivity of DR to perturbations in price varies largely over different days of the year. This variation is especially large during the evening peak and midnight hours. As we observed and discussed above, the sensitivity of DR to perturbations in price follows the load change (reduction or increase) at every PTU. For a fixed value of α^d and ω^{tt}, the variance of daily load indicates the potential to reduce the load, as well as the capacity to increase the load. The sensitivity of the performance of the DR program to load and price varies depending on the load profiles of various days.

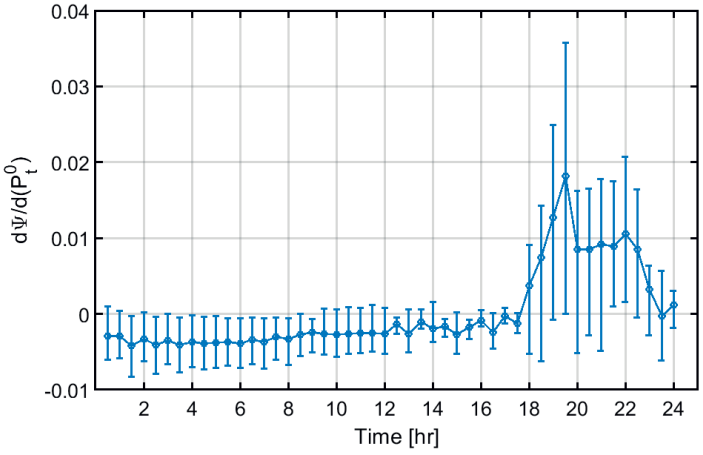

Figure 3.12: Variations in the sensitivity of the objective function at the optimal point with respect to perturbations in load ($\frac{d\Psi}{dP_t^0}|_{\alpha^d=20\%,\omega^{tt}=23hr}$), for the day with maximum (Case1), average (Case2), and minimum (Case3) variation in daily load.

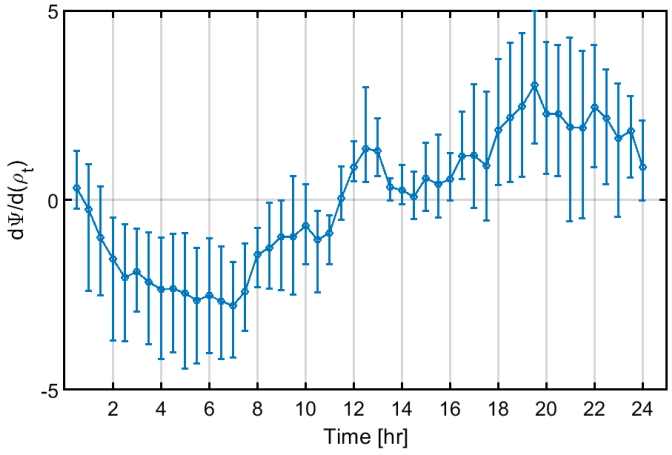

Figure 3.13: Variations in the sensitivity of the objective function at the optimal point with respect to perturbations in price ($\frac{d\Psi}{d\rho_t}|_{\alpha^d=20\%,\omega^{tt}=23hr}$), for the day with maximum (Case1), average (Case2), and minimum (Case3) variation in daily load.

3.3.6 Discussion

The results provided here correspond to a special case of load and price profile, which includes only the residential consumers as DR providers. However, the proposed framework is entirely general and can be employed for analyzing other consumer types (i.e., commercial and industrial [104]). When the proposed framework is intended to be used for other type of consumers, one needs to consider the following aspects:

1. The DR operating horizon (which is considered 24hr in this work): The DR operator utilizes the available flexibility through load shifting in one operating horizon, during which the total consumption is constant (see sub-section 3.2.1). However, commercial and industrial consumers might be able to reduce their load in one day and shift that load to the next day.
2. The assumption that the daily average load remains constant: This assumption is valid for residential loads, but not the industrial loads. Industrial loads can reduce their average load on a given day and increase their production the next day. Also note that, assuming that average load can change, may change the number of decision variables, because the equality $\Delta\mathcal{P}_{t_n t_m} = -\Delta\mathcal{P}_{t_m t_n}$ will not hold.
3. The difference in the range of flexibility the consumers can provide, which is reflected in our DR model with two parameters α^d and ω^{tt}: Commercial and industrial consumers might allow a different range of the flexibility than what is used in this study [53].
4. Electricity prices: Commercial and industrial consumers are exposed to different DA market prices. Therefore, when using this framework for various types of consumers, one might consider to include different price profiles.

3.4 Conclusions and Future Work

This work presented here proposes a data-driven Flexibility Assessment Framework to quantify the flexibility that DR providers could provide to the DSO, if a DR program (that does not exist yet) would be implemented. In addition, the proposed framework enables the future DR operators to quantify the sensitivity of performance of a DR program to data uncertainty.

The proposed framework entails a DR simulation and a data analytics module. The DR module encompasses an optimization problem that allows us to simulates the operation of a future DR program. The optimization problem seeks to minimize the variance in the daily load profile, which results in more efficient use of current infrastructure, and deferral of new investments.

The data analytics module, firstly, selects subsets from historical load and price data and composes scenarios on the preferences of the DR providers. Secondly, sensitivity analysis is performed, to determine how sensitive to uncertain and unknown data (load and price forecasts,

and preferences of the DR providers) the performance of the DR program will be.

The objective function assumed here allows for derivation of very useful results. Our analysis shows that the proposed DR framework enables the DR operator to provide flexibility services to the DSO by flattening the aggregated load profile of the DR providers. One major insight of the proposed DR framework is that the DR providers need to consider that if the peak load is high but the variance of the daily load profile is low, the DR program may not be able to reduce the peak demand effectively.

The success rate of the DR operator in reaching its goal of reducing load variability has a strong, and non-linear relationship with the amount of flexibility DR providers are willing to offer, which is captured in our framework by two variables (α^d and ω^{tt}). We observe that when DR providers have no limit on their load shifting time window (i.e., $\omega^{tt} = 23hr$), the performance of the DR program improves for larger values of downward flexibility. However, this improvement reaches a limit when the load shifting time window is bounded. In a similar way, when the flexible load is scarce (e.g., $\alpha^d = 5\%$), increasing the load shifting time window has low impact on the performance of a DR program. We observe that offering larger load reduction (α^d) or load shifting time window (ω^{tt}) does not necessarily lead to a lower variance. This observation can help the DR operators in making contractual agreements with the DR providers in the sense that, the DR providers who equally contribute to reduce the variance of daily load shall be reimbursed similarly (i.e., be paid the same amount of money), although they might be offering very large α^d or very large ω^{tt}. It also means that the DR providers might have the flexibility in their contracts for choosing to offer different combination of α^d and ω^{tt}.

Once the optimal solution for the DR is known, the sensitivity matrix can be analyzed. The numerical results of the local sensitivity analysis show that, in general, under all levels of preferences of the DR providers, the performance of the DR is more sensitive to perturbations in price than in the load. When narrowing the time window to 12 hours, small perturbations in load and price during the evening peak hours has a strong influence on the performance of the DR. Such analysis can help the DR operators, before engaging in contracts with the DSO, to identify the preferences of the DR providers that result in large deviations from the optimal performance of a DR program when there is data uncertainty.

The flexibility assessment framework proposed in this paper can benefit the DR operators. It can provide foresight on the operation of a DR program, before it is implemented in the system. A salient feature of this formulation is that, it enables the DR providers to gain adequate insight about the future grid without having access to any information regarding the grid. The results of such analysis can be used as the building block of the contractual agreements a DR operator would engage in with the DSO and/or DR providers. However, determining the flexibility prices in such contracts, and the way the DR providers will be paid for, is a crucial topic that needs further research.

The value of α^d and ω^{tt} is selected by the DR providers based on their convenience. One possible extension of the current work can be to investigate how different financial objectives,

in addition to their convenience, can steer the preferences of the DR providers in setting α^d and ω^{tt}, and therefore, influence the contractual agreement between the DR providers and the DR operator. Moreover, the DR providers might deviate from their scheduled flexibility profiles. Therefore, in our future work, we are going to investigate the impact of non-compliance or unexpected deviations from the scheduled flexibility program in real time DR operation. In addition, it would be interesting to investigate how input data uncertainty can affect the development and operation of a DR program that includes energy storage units in its portfolio.

Chapter 4

On the sensitivity of local flexibility markets to forecast error: A bi-level optimization approach

This chapter has been published as:

D. Azari, S.S. Torbaghan, H. Cappon, M. Gibescu, K.J. Keesman, and H. Rijnaarts, "On the sensitivity of local flexibility markets to forecast error: A bi-level optimization approach," *Energies*, 2020

4.1 Abstract

The large scale integration of intermittent distributed energy resources has led to increased uncertainty in the planning and operation of distribution networks. The optimal flexibility dispatch is a recently-introduced, power flow based method that a distribution system operator can use to effectively determine the amount of flexibility it needs to procure from the controllable resources available on the demand side. However, the drawback of this method is that the optimal flexibility dispatch is inexact due to the relaxation error inherent in the second-order cone formulation. In this paper we propose a novel bi-level optimization problem, where the upper level problem seeks to minimize the relaxation error and the lower level solves the earlier introduced convex second-order cone optimal flexibility dispatch (SOC-OFD) problem. To make the problem tractable, we introduce an innovative reformulation to recast the bi-level problem as a non-linear, single level optimization problem which results in no loss of accuracy. We subsequently investigate the sensitivity of the optimal flexibility schedules and the locational flexibility prices with respect to uncertainty in load forecast and flexibility ranges of the demand response providers which are input parameters to the problem. The sensitivity analysis is performed based on the perturbed Karush–Kuhn–Tucker (KKT) conditions. We investigate the feasibility and scalability of the proposed method in three case studies of standardized 9-bus, 30-bus, and 300-bus test systems. Simulation results in terms of local flexibility prices are interpreted in economic terms and show the effectiveness of the proposed approach.

Keywords: Optimal Flexibility Dispatch, Bi-level optimization, Sensitivity analysis

4.2 Introduction

The large scale integration of intermittent renewable energy resources (RES) and the change in the role of end-users from energy consumers to prosumers with new technologies (e.g., distributed energy resources (DERs) and storage facilities) have increased the uncertainty in the operation of the power systems at all levels. One way to overcome the uncertainty is to increase flexibility in the distribution system by harnessing the flexibility that is available to the end-users by implementing demand response (DR) programs.

In general the goal of a DR program is to motivate end-users to adapt changes in their local production/consumption profiles in response to a price (i.e., through a market based mechanism) or a command (i.e., originated by a non-market based mechanism) signal [13]. Regardless of the mechanism considered in place, the DSO needs to become active in network management by taking a coordinating role through implementing a proper policy that provides an adequate price or command signal. This for one, would enable the DSO to harness the flexibility from DR providers and overcome the uncertainty.

To do so, the DSO needs to determine the amount of flexibility it needs to procure to maintain

the secure and reliable operation of the network. The DSO also needs to determine a reliable projection (i.e., prediction) of the amount of flexibility that will potentially be available at its disposal, at different times and locations during the real-time operation. Once these infromation are available, the DSO can implement the mechanism to determine (i.e., estimate or calculate) a proper price (or command) signal such that it encourages DR providers to engage in network management by offering their flexibility in an efficient manner.

Harnessing the flexibility potential of the consumers has been investigated in the literature. In [100, 87, 105, 106] authors investigate mechanisms that can provide a price or command signal to DR providers to harness their flexibility and maintain power balance in power system, neglecting the network constraints. Subsequently, references [56, 58, 54] introduce new algorithms that enable an aggregator to estimate the flexibility that is potentially available to DR providers under certain assumptions. These works provide valuable insight into the existing network management potential through harnessing end-users' flexibility. What is missing in these studies is to account for the impact of including the topology and operational constraints of the distribution grid (e.g., voltage limits). The grid constraints play a crucial role in determining the accurate amount of flexibility that is required to maintain a secure and reliable operation of the network.

A common method to account for network constraints in the analysis of the operation of electricity network (including flexibility analysis) is to use Optimal Power Flow (OPF) based models [107, 108, 109, 110, 111, 112, 113]. In this regard, Capitanescu et al. [110] proposed an OPF model that seeks to minimize the curtailment of the distributed energy resources (DERs) while maintaining voltage constraints in a distribution grid. One can see that existing works are mostly concerned with the technical aspects of the grid. However, to ensure a successful network management, the economic aspects also need to be considered properly in the analysis [114].

References [115, 116, 117] introduce OPF based models to analyze the relation of power flows, network congestion and voltage constraints on the formation of distribution locational marginal energy prices (DLMP) in an stylized network. However, the nonlinearities of AC power flows introduce computational complexities. Li et al. [115] use DC-OPF which is a linear approximation of the full AC-OPF to investigate the day-ahead DLPMs. Likewise, Yuan et al. [116] propose a new model for pricing the electric power at the distribution level, considering voltage constraints, using linearized AC power flows. Papavasiliou [117] uses .second-order cone relaxation of AC power flows and proposes a novel framework to study the formation of DLMPs in distribution network, considering congestion, voltage constrains, real and reactive power limits and losses, as well as the non-linearities of the AC power flow at the distribution grid.

In recent years in parallel with higher penetration of DERs with their variable and unpredictable production, there has been a growing interest in flexibility (defined as in [118]) as the service to be traded, instead of absolute energy, in local energy communities [86, 92, 119,

120, 94]. To this end, authors in [121] introduce the optimal flexibility dispatch (OFD) as an optimization problem. The OFD is an auction-based platform for trading flexibility in distribution grids. The OFD seeks to minimize the costs of curtailing RES and, as a side product, determines the quantity and price of active and reactive power flexibility that the DSO needs to procure from different flexibility providers at different locations in the network. The proposed OFD framework considers network constraints, end-users' flexibility limits as well as the non-linearities of AC power flow. The problem is, considering non-linearities of AC power flows in OFD as such makes the problem non-convex and non-tractable for large-scale systems. To make the AC-OFD problem tractable, authors in [121] use second-order cone (SOC) relaxation of the AC power flow formulation. However, the exactness of the solution of the SOC-relaxed problem is a concerning issue and is guaranteed only under certain assumptions [122]. Inexact solutions lack a physical interpretation that coincides with Kirchhoff's law (i.e., are not AC feasible).

In summary, most works on harnessing flexibility from the distribution network firstly consider energy instead of flexibility as the commodity to trade. Secondly, the existing works either follow a purely economic approach neglecting technical constraints including power flow constraints, or vice versa. And thirdly, even if OPF-based models are used (through which technical constraints are accounted for), they are computationally costly due to non-linearites of the AC power flow for large scale problems, or yield solutions for which the exactness of the results cannot be guaranteed due to error inherent to approximation and/or relaxation techniques applied. Fourthly, none of the studies above account for the impact of inaccurate input data on the optimal energy or flexibility programs.

Note that the accuracy of the input data is an important factor because, in the real world application, the amount of flexibility that the DSO can have at its disposal in the real-time is uncertain and is not fully known before hand. As a result, an estimation of the available flexibility values shall be used in practice. This can affect the operational decisions. Therefore, it is important to study the impact of uncertainty in the potential flexibility that is available to the DSO on the flexibility schedule and flexibility prices.

In this work we propose a bi-level optimization model to minimize the relaxation error in the OFD problem. The lower level (i.e., inner) problem solves the second-order cone relaxed optimal flexibility dispatch (SOC-OFD) problem while the upper (i.e., outer) problem seeks to minimize the relaxation error of the SOC-OFD. As the lower level problem is SOC convex, using Karush-Kuhn-Tucker (KKT) conditions we recast the bi-level structure into a mathematical problem with complementarity constraints (MPCC) [66].To make the problem tractable, we apply an innovative relaxation method to relax the complementarity constraints and reformulate the problem as a non-linear problem (NLP), without losing accuracy. In this sese, the propose methodology establishes a good trade-off between accuracy and tractability. Finally, we use local sensitivity analysis technique to investigate the sensitivity of the optimal flexibility dispatch program to imperfect forecast and uncertain parameters.

The major contributions of this paper are as follows:

- proposes a new formulation for the SOC-OFD problem that seeks to find an optimal flexibility schedule (i.e., amount and price of flexibility to be dispatched at each bus) with zero relaxation error. This is done by formulating a bi-level optimization model that seeks to solve the SOC-OFD problem while minimizing the SOC relaxation error,
- introduces an effective reduction/relaxation technique that makes the bi-level problem tractable both analytically and numerically, and
- provides an analytical framework for performing local sensitivity analysis on the reduced OFD problem, which determines the robustness of the resulted optimal flexibility dispatch against imperfect forecasts of input data.

The bi-level OFD framework introduced here has two key characteristics. Firstly, it results in a solution with zero relaxation error. Secondly, it returns 'locational flexibility prices' (LFPs) as explicit optimisation variables that are otherwise only available as the dual of the power balance constraint at every bus, and thus only available through specific solvers.

The remainder of this paper is organized as follows. Section 4.3 firstly provides a brief overview of the SOC-OFD problem. It then dives into the mathematical formulation of the bi-level optimization model that seeks to minimize the relaxation error while solving the SOC-OFD problem. Section 4.4 presents the numerical results for the case studies. Section 4.6 concludes the paper and discusses directions for future research.

4.3 Problem Formulation

In the context of this work, we define the OFD framework as an optimization problem that seeks to minimize the curtailment of DERs while keeping the distribution grid congestion free. We use the SOC formulation of the AC power flow as a practical approach to model the network constraints while accounting for the non-linearities of AC power flow. To keep the SOC-relaxation error as small as possible, we propose a bi-level structure in which the UL problem seeks to minimize the SOC relaxation error, while the LL problem models the SOC-OFD problem. As the SOC-OFD is convex, the bi-level problem can be solved by replacing the LL by its KKT optimality condition. The resulted single-level problem is MPCC problem which usually very difficult to solve. Thus a novel methodology is discussed to transform the resulted MPCC problem into MINLP and subsequently a tractable NLP problem.

Solving the proposed bi-level optimization problem enables the DSO to determine the quantity of the active and reactive power flexibility, as well as the distribution locational marginal prices of flexibility, with minimum error. Note that the convexity of SOC-OFD it allows one to apply local sensitivity analysis to determine the sensitivity of the optimal flexibility dispatch program

with respect to perturbation in input data (e.g., available flexibility) which mimics imperfect forecast data [74].

4.3.1 Assumptions

Consider a distribution grid with N buses. We use indices i or j and $i, j \in \Omega_N$ to refer to buses where Ω_N is the set of buses. Assume that every bus can comprise of a number of households with flexible and non-flexible units. A flexible unit can be a generator (e.g., DERs) or a load (e.g., DR). For the sake of simplicity, we assume that all generators are flexible. Loads can be flexible or non-flexible. Suppose that each bus is operated by an aggregator. Each aggregator receives the "base-power program". It entails supply and demand forecast of the flexible and non-flexible units. The aggregator also receives the "available flexibility" forecast of the flexible units. The aggregator processes these information and provides them to the DSO. For every bus, the aggregator provides the base active and reactive program (i.e., p_u^0, q_u^0) where p and q denote respectively active and reactive power of unit $u \in \Omega_{k_i}$ in bus i. Index k determines whether unit u in bus i is a generator (i.e., $\{k = G | u \in \Omega_{G_i}\}$) or load (i.e., $\{k = D | u \in \Omega_{D_i}\}$). Ω_{G_i} and Ω_{D_i} denote respectively the set of generation or consumption units in bus i. The aggregator also provides the upper and lower bounds of active and reactive flexibility of the flexible units ($\overline{\Delta p_u}, \underline{\Delta p_u}, \overline{\Delta q_u}, \underline{\Delta q_u}$) where Δp_u and Δq_u denote respectively the active and reactive flexibility of unit $u \in \Omega_{k_i}$. Note that $\underline{x}, \overline{x}$ denote respectively the lower and upper bound values of an arbitrary variable x. The operational limits include power flow limits of the lines and bus voltage limits. The power flow limits are represented as $\underline{p_{i,j}}, \overline{p_{i,j}}$, $\underline{q_{i,j}}, \overline{q_{i,j}}$, where $p_{i,j}$ and $q_{i,j}$ denote the active and reactive power flow of the line $(i, j) \in \Omega_E$ connecting bus i to bus j. Ω_E is the set of power flows when power flows from the sending bus (i.e., bus i) to the receiving end (i.e., bus j). Note that Ω_{E^r} will be used to refer to the set of power flows in the reverse direction (i.e., for line i, j, and the convention of bus i being the send bus and j being the receiving bus, we have $p_{i,j} \in \Omega_E, p_{j,i} \in \Omega_{E^r}$). The bus voltage limits are $\underline{w_i}, \overline{w_i}$, $\underline{w_{i,j}^i}, \overline{w_{i,j}^i}$, $\underline{w_{i,j}^r}, \overline{w_{i,j}^r}$, where $w_i = (v_i)^2$ is the squared voltage magnitude of bus i in which we have $\overline{w_{i,j}^r} = |\overline{v_i}| \cdot |\overline{v_j}| \cdot cos(\underline{\theta_{i,j}})$, $\overline{w_{i,j}^i} = |\overline{v_i}| \cdot |\overline{v_j}| \cdot sin(\overline{\theta_{i,j}})$ $\underline{w_{i,j}^r} = |\underline{v_i}| \cdot |\overline{v_j}| \cdot cos(\overline{\theta_{i,j}})$ and $\underline{w_{i,j}^i} = |\underline{v_i}| \cdot |\overline{v_j}| \cdot sin(\underline{\theta_{i,j}})$. In this formulation $|\overline{v_i}|$ and $|\underline{v_i}|$ are the upper and lower bound of the bus voltage, and $\theta_{i,j}$ is the phase angle difference between buses i and j.

4.3.2 Second-Order Cone Relaxed OFD (SOC-OFD)

The SOC-OFD problem can be formulated as follows:

$$\min_{(\Xi^{LL})} \Psi^{LL} = \sum_{i \in \Omega_N} \sum_{u \in \Omega_{G_i}} (\overline{p_u} - (p_u^0 + \Delta p_u)) \tau^{DER} \tag{4.1a}$$

subject to

$$(\underline{\phi_i^w}, \overline{\phi_i^w}) : \ \underline{w_i} \leq w_i \leq \overline{w_i}, \quad \forall i \in \Omega_N \tag{4.1b}$$

$$(\underline{\phi^r_{i,j}}, \overline{\phi^r_{i,j}}): \ \underline{w^r_{i,j}} \leq w^r_{i,j} \leq \overline{w^r_{i,j}}, \quad \forall (i,j) \in \Omega_E \tag{4.1c}$$

$$(\underline{\phi^i_{i,j}}, \overline{\phi^i_{i,j}}): \ \underline{w^i_{i,j}} \leq w^i_{i,j} \leq \overline{w^i_{i,j}}, \quad \forall (i,j) \in \Omega_E \tag{4.1d}$$

$$(\eta_{i,j}): \ (w^i_{i,j})^2 + (w^r_{i,j})^2 \leq w_i w_j, \quad \forall (i,j) \in \Omega_E \tag{4.1e}$$

$$(\underline{\phi^{\Delta p}_u}, \overline{\phi^{\Delta p}_u}): \ \underline{\Delta p_u} \leq \Delta p_u \leq \overline{\Delta p_u}, \quad \forall u \in \Omega_{k_i}, i \in \Omega_N \tag{4.1f}$$

$$(\underline{\phi^{\Delta q}_u}, \overline{\phi^{\Delta q}_u}): \ \underline{\Delta q_u} \leq \Delta q_u \leq \overline{\Delta q_u}, \quad \forall u \in \Omega_{k_i}, i \in \Omega_N \tag{4.1g}$$

$$(\phi^p_{i,j}): \ p_{i,j} = \left(g^{sh}_{i,j} + g^s_{i,j}\right) w_i - \left(g^s_{i,j} - b^s_{i,j}\right) w^r_{i,j} \tag{4.1h}$$

$$+ b^s_{i,j} w^i_{i,j} \ , \forall (i,j) \in \Omega_E \tag{4.1i}$$

$$(\phi^p_{j,i}): \ p_{j,i} = g^{sh}_{i,j} w_j - g_{i,j} w^r_{i,j} - b_{i,j} w^i_{i,j}, \quad \forall (i,j) \in \Omega_{E^r} \tag{4.1j}$$

$$(\phi^q_{i,j}): q_{i,j} = (b_{i,j} - b^{sh}_{i,j}/2) w_i - b_{i,j} w^r_{i,j} - g_{i,j} w^i_{i,j}, \forall (i,j) \in \Omega_E \tag{4.1k}$$

$$(\phi^q_{j,i}): q_{j,i} = (b_{i,j} - b^{sh}_{i,j}/2) w_j - b_{i,j} w^r_{i,j} + g_{i,j} w^i_{i,j}, \forall (i,j) \in \Omega_{E^r} \tag{4.1l}$$

$$(\underline{\mu^p_{i,j}}, \overline{\mu^p_{i,j}}): \ \underline{p_{i,j}} \leq p_{i,j} \leq \overline{p_{i,j}} \ , \quad \forall (i,j) \in \Omega_E \tag{4.1m}$$

$$(\underline{\mu^p_{j,i}}, \overline{\mu^p_{j,i}}): \ \underline{p_{j,i}} \leq p_{j,i} \leq \overline{p_{j,i}} \ , \quad \forall (i,j) \in \Omega_{E^r} \tag{4.1n}$$

$$(\underline{\mu^q_{i,j}}, \overline{\mu^q_{i,j}}): \ \underline{q_{i,j}} \leq q_{i,j} \leq \overline{q_{i,j}} \ , \quad \forall (i,j) \in \Omega_E \tag{4.1o}$$

$$(\underline{\mu^q_{j,i}}, \overline{\mu^q_{j,i}}): \ \underline{q_{j,i}} \leq q_{j,i} \leq \overline{q_{j,i}} \ , \quad \forall (i,j) \in \Omega_{E^r} \tag{4.1p}$$

$$(\lambda^p_i): \sum_{(i,j) \in \Omega_E} p_{i,j} + \sum_{(i,j) \in \Omega_{E^r}} p_{j,i} = \sum_{u \in \Omega_{k_i}} \left(p^0_u + \Delta p_u\right) \ , \tag{4.1q}$$

$$\forall i \in \Omega_N$$

$$(\lambda^q_i): \sum_{(i,j) \in \Omega_E} q_{i,j} + \sum_{(i,j) \in \Omega_{E^r}} q_{j,i} = \sum_{u \in \Omega_{k_i}} \left(q^0_u + \Delta q_u\right) \ , \tag{4.1r}$$

$$\forall i \in \Omega_N$$

where τ^{DER} is the fixed tariff of DER curtailment in €$/MWh$. g^{sh}_i and b^{sh}_i are the shunt conductance and admittance of bus i. Likewise, $g^s_{i,j}$ and $b^s_{i,j}$ are series conductance and admittance of the line (i,j). $\Xi^{LL} = \{\Delta p_u, \Delta q_u, p_{i,j}, p_{j,i}, q_{i,j}, q_{j,i}, w_i, w^r_{i,j}, w^i_{i,j}\}$ is the set of independent optimization variables and Γ^{LL} is the set of Lagrange dual variables. The Greek letters between parenthesis denote Lagrangian dual variable for the corresponding constraint.

The objective function (4.1a) states that the DSO seeks to minimize the cost of curtailing the production of DERs. This is a weak assumption. One could consider other objectives as long as the objective function is convex. Constraints (4.1b)-(4.1d) enforce lower and upper bounds of the square voltage and voltage products. Constraint (4.1e) reflects the SOC-relaxation of the AC power flow. Constraints (4.1f)-(4.1g) enforce the lower and upper bound of active and reactive flexibility. Constraints (4.1h)-(4.1l) define active and reactive power flow on both directions of a line. Constraints (4.1m)-(4.1p) enforce the lower and upper bound of real and reactive power flow. Equation (4.1q)-(4.1r) are the Kirchhoff's current law (KCL) which enforce real and reactive power balance.

The SOC-OFD problem can be inexact due to relaxation error. Reference [121] showed that the relaxation error can be larger when flexibility is scarce. The non-exact solution lacks physical interpretation and at best, can be treated as an approximation of the exact solution.

In the following subsection we propose a novel approach to reduce the relaxation error.

4.3.3 Bi-level model for the OFD problem

One can define the SOC relaxation error associated with (4.1e) as follows:

$$\epsilon^{soc}_{i,j} = w_i w_j - \left((w^i_{i,j})^2 + (w^r_{i,j})^2\right) \ , \forall (i,j) \in \Omega_E. \tag{4.2}$$

If $\epsilon^{soc}_{i,j} = 0$, that is if the inequality (4.1e) becomes equality, then the relaxation error is zero and the solution of the SOC-OFD coincides with of the full-AC based OFD. However, if the error is nonzero, then the results of the OFD problem are inexact and have no physical interpretation.

To minimize the SOC-relaxation error, we introduce a novel alternative approach. The idea is to consider the SOC-relaxation error minimization as a separated optimization problem that should be solved simultaneously with the SOC-OFD problem. This can be done by formulating a bi-level optimization model in which the UL problem seeks to minimize the SOC-relaxation error as defined in (4.2). The LL problem is the original SOC-OFD problem (i.e., problem (4.1a)-(4.1r)). The bi-level OFD problem takes on the following form:

$$\min_{(\Xi^{LL} \cup \Gamma^{LL})} \Psi^{UL} = \sum_{(i,j) \in \Omega_E} \epsilon^{soc}_{i,j} \tag{4.3a}$$

$$\text{subject to}$$

$$\text{(4.1a) - (4.1r)} \ ,$$

where (4.1a)-(4.1r) is the original SOC-OFD problem. The objective (4.3a) is to minimize the aggregated SOC-relaxation error. The SOC-relaxation error minimizing problem (i.e., UL problem) is constrained by the SOC-OFD problem (i.e., LL problem). The decision variables of the UL problem includes the decision variables of the LL problem (i.e., Ξ^{LL}) in addition to the dual variables associated with constraints of the LL problem (i.e., Γ^{LL}).

Since the constraining LL problem is convex, it can be replaced by its corresponding KKT conditions. This results in a single level optimization [66]. problem which is a mathematical problem with complementarity constraints (MPCC) [66]. The resulting mathematical problem with complementarity constraints (MPCC) is a non-linear and non-convex problem, and therefore is NP-hard.

There are two sources of non-linearities in the resulting MPCC. Firstly, the quadratic terms (i.e., $(w^i_{i,j})^2$, $(w^r_{i,j})^2$) and the bi-linear product (i.e., $w_i w_j$) in the objective function (4.3a) as well as in the SOC-relaxed power flow constraint in the LL problem (4.1e). Secondly, the complementarity constraints in the KKT optimality conditions of the LL problem. The

complementarity constraints are of the form $0 \leq a \perp b \geq 0$. Each complementarity constraint can be written equivalently as a set of three constraint as $0 \leq a$, $0 \leq b$, and $a \cdot b = 0$ where the last constraint is non-linear and extremely non-convex. The MPCC problem has to be simplified to become tractable.

An alternative is to relax equality $a \cdot b = 0$ with an inequality constraint as $a \cdot b \leq \delta$, where δ is a non-negative variable to be minimized as discussed in [123]. Such relaxation transforms the MPCC into an NLP problem, which can be solved using available solvers specially for small problems. For large-scale problems however, the proposed relaxation can be problematic [124].

To reduce the size and complexity of the problem, also to improve the accuracy of the results, in the following we propose a new relaxation reformulation techniques which is to first reconstruct the bi-level formulation of the problem, then transform the resulted MPCC to a NLP problem using the relaxation discussed above.

4.3.4 Reformulation of the bi-level OFD Problem to NLP-OFD

Consider a bi-level optimization problem of the form:

$$\min_{(x,y,z)\cup(l_1,l_2,l_3)} Ax \tag{4.4a}$$

subject to

$$\min_{(x,y,z)} By \tag{4.4b}$$

subject to

$$(l_1): \ Cx \leq 0 \tag{4.4c}$$
$$(l_2): \ Hy \leq 0 \tag{4.4d}$$
$$(l_3): \ Dx + Fz \leq 0 \tag{4.4e}$$
$$(l_4): \ Gy + Tz \leq 0. \tag{4.4f}$$

Now consider shifting constraints (4.4c) and (4.4e) to the UL and reformulating the problem as follows:

$$\min_{(x,y,z)\cup(l_3)} Ax \tag{4.5a}$$

subject to

$$(l_1): \ Cx \leq 0 \tag{4.5b}$$
$$(l_2): \ Dx + Fz \leq 0 \tag{4.5c}$$
$$\min_{(y,z)} By \tag{4.5d}$$

subject to

$$(l_3): \ Hy \leq 0 \tag{4.5e}$$
$$(l_4): \ Gy + Tz \leq 0 \tag{4.5f}$$

As suggested in [125], one can show that problem (4.4a)-(4.4f) is equivalent to problem (4.5a)-(4.5f), when the dual variables $l_1, l_2 = 0$.

In a similar way, we reformulate the bi-level OFD problem by shifting all constraints from the LL to the UL except for the active power flexibility limit (4.1f) and active power balance (4.1q). The proposed reformulation reduces the LL problem to a new optimization problem that seeks to minimize curtailment of DERs subject to determine the active power flexibility only. As the constraints of the UL problem are transparent to the LL problem, the UL induces a proper choice of voltages, active and reactive power flows, and reactive power flexibility in a way that the minimum relaxation error is reached.

It is apparent that if the shifted constraints are not binding (i.e., their associated Lagrange multipliers are zero) the reduced bi-level OFD problem is equivalent to the original bi-level problem. As a result, an optimal solution of the reduced problem can be matched to a feasible solution of the original bi-level problem if the constraints that are shifted from the LL to UL are not active at the optimal solution. This point is further investigated in the next section.

Once the LL problem is reduced by shifting the constraints to the UL problem, the reduced LL problem can be replaced by its corresponding KKT conditions. The resulted complementarity conditions in the reduced MPCC can be further relaxed using the technique discussed in 4.3.3, as follows:

$$\min_{\Xi^{OFD}_{red}} \Psi^{UL}_{mod} = \sum_{(i,j)\in\Omega_E} \left(\epsilon^{soc}_{i,j} + \underline{\delta_{i,j}} + \overline{\delta_{i,j}}\right) \tag{4.6a}$$

subject to

(4.1b) - (4.1p), (4.1r),

$$0 \leq \overline{\delta_{i,j}} \leq \delta^{max}, \quad \forall (i,j) \in \Omega_N \tag{4.6b}$$

$$0 \leq \underline{\delta_{i,j}} \leq \delta^{max}, \quad \forall (i,j) \in \Omega_N \tag{4.6c}$$

$$\overline{\phi^{\Delta p}_u} - \underline{\phi^{\Delta p}_u} - \lambda^p_u - \tau^{DER} = 0, \quad \forall u \in \Omega_{G_i}, i \in \Omega_N \tag{4.6d}$$

$$\overline{\phi^{\Delta p}_u} - \underline{\phi^{\Delta p}_u} - \lambda^p_u = 0, \quad \forall \left\{u | u \in \Omega_{k_i}, u \notin \Omega_{G_i}\right\}, i \in \Omega_N \tag{4.6e}$$

$$\sum_{(i,j)\in\Omega_E} p_{i,j} + \sum_{(i,j)\in\Omega_{E^r}} p_{j,i} = \sum_{u\in\Omega_{k_i}} \left(p^0_u + \Delta p_u\right) \quad \forall u \in \Omega_{k_i}, i \in \Omega_N \tag{4.6f}$$

$$(\underline{\Delta p^k_u} - \Delta p^k_u) \geq 0, \quad \forall u \in \Omega_{k_i}, i \in \Omega_N \tag{4.6g}$$

$$(\Delta p^k_u - \overline{\Delta p^k_u}) \geq 0, \quad \forall u \in \Omega_{k_i}, i \in \Omega_N \tag{4.6h}$$

$$\underline{\phi^{\Delta p}_u} \cdot (\underline{\Delta p^k_u} - \Delta p^k_u) \leq \underline{\delta_{i,j}}, \quad \forall u \in \Omega_{k_i}, i \in \Omega_N \tag{4.6i}$$

$$\overline{\phi^{\Delta p}_u} \cdot (\Delta p^k_u - \overline{\Delta p^k_u}) \leq \overline{\delta_{i,j}}, \quad \forall u \in \Omega_{k_i}, i \in \Omega_N \tag{4.6j}$$

$$\overline{\phi^{\Delta p}_u} \geq 0, \quad \forall u \in \Omega_{k_i}, i \in \Omega_N \tag{4.6k}$$

$$\underline{\phi^{\Delta p}_u} \geq 0, \quad \forall u \in \Omega_{k_i}, i \in \Omega_N \tag{4.6l}$$

where $\Xi_{red}^{OFD} = (\{\Xi_{red}^{UL}, \underline{\delta_{i,j}}, \overline{\delta_{i,j}}\} \cup \{\Delta p_u^k, \lambda_i^p, \underline{\mu_{i,j}^p}, \overline{\mu_{i,j}^p}\})$ is the set of decision variables.

Constraints (4.1b)-(4.1p), and (4.1r) include the square voltage and voltage product limits, the SOC-relaxation of AC power flows, reactive power flexibility limit, and reactive power balance, which are shifted to the UL problem. Constraints (4.6b)-(4.6c) enforce a threshold on complementarity relaxation, where parameter δ^{max} is the maximum allowed constraint relaxation. Constraints (4.6d)-(4.6l) are the KKT conditions associated with the reduced LL problem (i.e., reduced SOC-OFD). Equalities (4.6d) and (4.6e) represent the derivatives of the Lagrangian of the LL problem with respect to its decision variable Δp_u^k (i.e., $\partial \mathcal{L}^{LL}/\partial \Delta p_u^k = 0$), for DER and load units, respectively.

Problem (4.6a)-(4.6l), (4.1b)-(4.1p), (4.1r) (referred to in this paper as bilevel-OFD) is a NLP which can be solved in a feasible time by available solvers. The proposed reformulation effectively reduces the computation complexity of the problem with the lowest loss of accuracy possible.

4.3.5 Derivation of the Sensitivity Matrix in the OFD Problem

In this paper we aim to investigate the sensitivity of the optimal solution of the OFD problem to perturbations in input data. One can study the sensitivity by deriving a linear sensitivity matrix based on the perturbed KKT equation proposed in [74]. We induce a perturbation in the KKT conditions and the objective function of problem (4.1a)-(4.1r) (i.e., Ψ^{LL}), with respect to the decision variables Ξ^{LL}, the Lagrange multipliers, and the input data parameters ($\boldsymbol{a} = [\underline{w_i}, \overline{w_i}, \underline{w_{i,j}^r}, \overline{w_{i,j}^r}, \underline{w_{i,j}^i}, \overline{w_{i,j}^i}, \underline{\Delta p_u}, \overline{\Delta p_u}, \underline{\Delta q_u}, \overline{\Delta q_u}, \underline{p_{i,j}}, \overline{p_{i,j}}, \underline{p_{j,i}}, \overline{p_{j,i}}, \underline{q_{i,j}}, \overline{q_{i,j}}, \underline{q_{j,i}}, \overline{q_{j,i}}, p_u^0, q_u^0, \tau^{DER}, g_{i,j}^{sh}, g_{i,j}^s, \underline{b_{i,j}^{sh}}, b_{i,j}^s]$). Then, as proposed in [74] we obtain the sensitivity matrix $M = dX/da$, which determines the sensitivities of the optimal solution along with the Langrange multipliers to changes in data.

Suppose that inactive constraints are removed from the analysis, and that the active inequality constraints remain active after the perturbation. As the LL problem represents the (reduced) original SOC-OFD problem, one can see that an optimal solution of the reduced-bilevel problem includes the optimal solution of the SOC-OFD. Therefore, at the optimal solution, the sensitivities of the SOC-OFD problem can be evaluated at the optimal solution of the reduced bilevel-OFD problem.

4.4 Numerical Results

In this section we present the numerical results obtained using the SOC-OFD (i.e., problem (4.1a)-(4.1r)) and the bilevel-OFD (i.e., problem (4.6a)-(4.6g)) for three stylized case studies. We compare the results in terms of (i) the SOC-relaxation error (ϵ_{SOC} as defined in equation (4.2)), (ii) the DER curtailment (Ψ as defined in equation (4.1a)), and (iii) locational flexibility prices (LFPs) which are derived as dual variables of active power balance

constraint (i.e., λ_i^p). Furthermore, we numerically analyze the sensitivity of the OFD problem to perturbations in input parameters (i.e., $\underline{\Delta p_u}, \overline{\Delta p_u}, p_u^0$).

4.4.1 Case study

In the power system research it is a common practice to use synthetic electric grid models as case studies. The reason is, they provide standard benchmark that enable researchers to validate newly developed analytic methods against the existing ones, without using any confidential critical energy infrastructure information [126].

In this study to investigate the feasibility and scalability of the proposed framework, three stylised power grids from MATPOWER, with 9-bus, 30-bus, and 300-bus, are considered. The grid data and topology of the three case studies are adopted from a subset of automated tests prepared for MATPOWER [127, 128, 129]. MATPOWER is an open-source power system simulation package. It provides a set of power flow based tools that are specifically designed for research purposes [130]. The network parameters are customized to make the technical characteristics of the test networks consistent with of distribution networks. Table 4.1 provides an overview of the grid parameters, including the number of buses with DER resource, number of branches, average per unit (p.u.) values of the series resistance ($\overline{R}$), inductance ($\overline{X}$), and shunt susceptance ($\overline{B}$) for each case study.

Table 4.1: Grid parameters for the three test systems. *No. Buses*, *No. DERs* and *No. Branches* represent the total number of buses, the number of buses with DER resources, and total number of branches respectively. $\overline{R}$, $\overline{X}$, and $\overline{B}$ are average series resistance, inductance, and shunt susceptance of all branches, respectively. The values are in per unit (p.u.) with 100 MVA base.

	No. Buses	**No. DERs**	**No. Branches**	$\overline{R}$	$\overline{X}$	$\overline{B}$
Case 1	9	3	9	0.040	0.096	10.990
Case 2	30	6	41	0.076	0.200	7.498
Case 3	300	69	411	0.046	0.117	88.392

4.4.2 Assumptions

1. Each bus represents a cluster of aggregated end-users which can be either a net flexible generator or net flexible load.
2. The OFD problem is solved per single time-step. Cross-temporal linkages are neglected.
3. A fix cost for curtailing DER production is considered, and $\tau_{cur}^{DER} = 0.05$ €$/kWh$.
4. Load is curtailed at no cost.
5. Load is modeled as negative generation. That is, negative flexibility for a net flexible load bus indicates an increase in the total consumption of that bus.

Table 4.2: The maximum, minimum, and average SOC-relaxation error ϵ^{SOC} of all lines, determined by SOC-OFD and bilevel-OFD models for the three cases.

	ϵ^{SOC}					
	SOC-OFD			Bilevel OFD		
	min	max	avg	min	max	avg
Case1	0.00	0.64	0.25	0.00	0.00	0.00
Case2	0.01	0.24	0.07	0.00	0.00	0.00
Case3	0.00	0.61	0.09	0.00	0.25	0.01

4.4.3 Simulation results

The SOC-OFD problem and the bilevel-OFD problems are implemented in MATLAB 2017b, and solved by optimization toolbox YALMIP [131]. The computer used ran Windows 7 Enterprise 64-bit, with an Intel Xeon CPU E5-1650 processors running at 3.20 GHz and 24 GB memory. The bilevel-OFD problem is solved for $\delta^{max} = 1e^{-6}$.

SOC-relaxation error (ϵ_{SOC})

Table 4.2 presents the minimum, maximum, and average SOC-relaxation error (i.e., $\epsilon^{SOC} = \sum_{i,j\in\Omega_E} \epsilon_{ij}^{SOC}$) for each case study, calculated by solving the SOC-OFD and bilevel-OFD models. One can observe that for Case 1 and Case 2, ϵ^{SOC} is minimized to zero when the bilevel-OFD model is used. For Case 3, this figure is reduced by an average of 89% when compared with the results of SOC-OFD model. This shows that the bilevel-OFD model effectively eliminates the SOC-relaxation error for 9-Bus and 30-Bus networks, and reduces it considerably for the 300-Bus network. It also suggests that solving the bilevel-OFD model indeed results in solutions that have physical interpretation, as outlined in the previous section.

Now consider Figure 4.1 which depicts the distribution of bus voltages calculated by both models for each case. The horizontal red lines inside the boxes indicate the median of the voltages in the network. One can observe that, under each case the bus voltages of the majority of buses are lower when calculated by the bilevel-OFD model compared with the SOC-OFD model.

This observation can be explained via relaxation error. As outlined in [121], relaxation error can be interpreted as an artificially increased active and reactive loss over the transmission lines. Now consider the results of SOC-OFD model (in which no boundary is superimposed on increasing the relaxation error). One can observe that in the SOC-OFD model, the solver finds solutions with a higher relaxation error, and therefore higher (artificial) losses. This leads to higher voltage difference as well as a higher system voltage level, especially at the DER buses. The contrary is true for the bilevel-OFD model, in which the relaxation error is minimized, and as a result, the bus voltages get lower values.

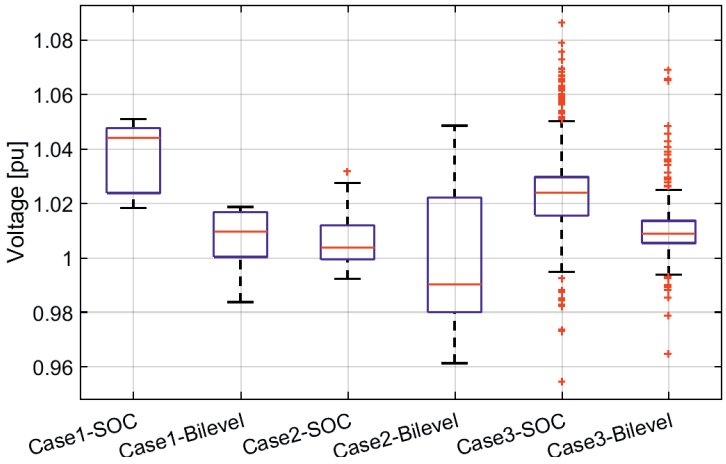

Figure 4.1: Distribution of bus voltages calculated by SOC-OFD and bilevel-OFD models, for the three case studies.

DER Curtailment (Ψ)

Figure 4.2 presents the aggregated production of DERs calculated by the SOC-OFD model (blue bar) and the bilevel-OFD model (red bar). One can see that the bilevel-OFD model yields the same aggregated DER production as of the SOC-OFD model. This implies that the bi-level model finds a solution in which, the flexible units are dispatched in a such way that the aggregated DER production (and thus DER curtailment) remains the same as is for the SOC-model, but with no SOC-relaxation error.

Locational flexibility prices (LFPs)

Figures 4.3 and 4.4 respectively present the LFPs and the flexibility dispatch from each bus, as calculated by the bilevel-OFD model for Case 1 (the top sub-plot), Case 2 (the middle sub-plot), and Case 3 (the bottom sub-plot). Variable $\Delta p_i = \sum_{u \in \Omega_{k_i}} \Delta p_u$ indicates the aggregated active power flexibility dispatched from bus i.

One can see that the LFP of every DER bus (i.e., the red dots in Figure 4.3) is a positive value which is lower than or equal to the DER curtailment tariff set by the regulators (i.e., $\tau^{DER} = 5$ €$cent/kWh$). Likewise, one can see in Figure 4.4 that for the three cases, the flexibility dispatched from the DER buses is positive. This implies that the DSO pays the DERs to increase their production (i.e., decrease curtailment).

Now consider the flexible load buses (i.e., blue dots in Figure 4.3). For Case 1 and Case 2 the LFPs at load buses are very close to zero. In Case 3, however, there are certain load buses with a negative LFP. From (4.6e),(4.6i)-(4.6j) one can observe that for load buses, λ_i^p gets

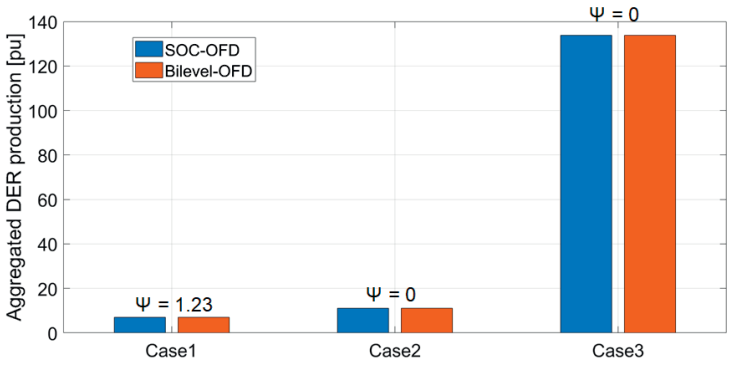

Figure 4.2: Aggregated production of DER buses, and curtailment level (Ψ), calculated by SOC-OFD model (the blue bars) and bilevel-OFD model (the red bars) for the three cases.

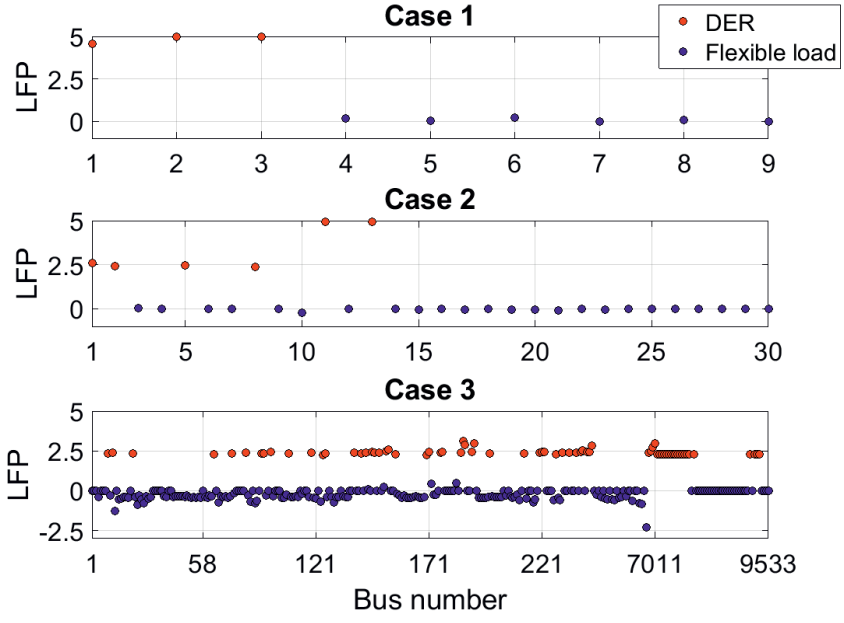

Figure 4.3: Locational Flexibility Price (LFP) (€$cent/kWh$) for Case 1 (top), Case 2 (middle), and Case 3 (bottom). The red and blue dots represent a DER or a load bus, respectively.

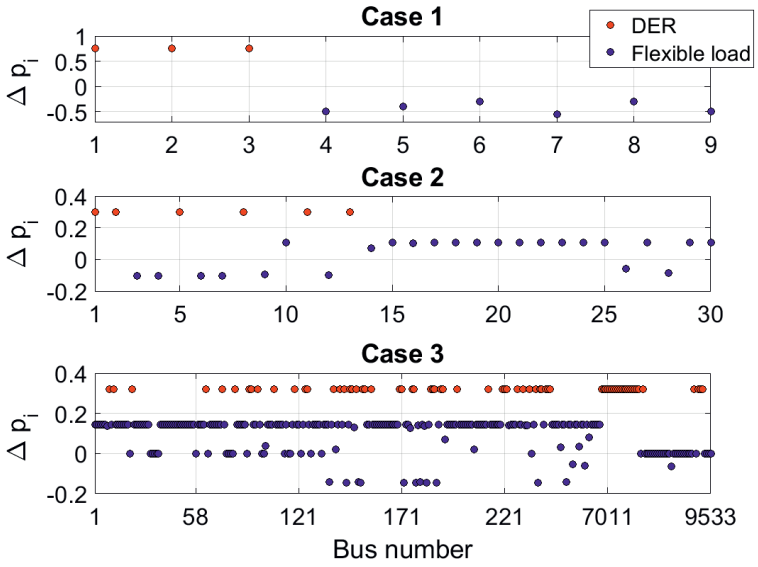

Figure 4.4: Active power flexibility (kWh) sourced from each bus (i.e., $\Delta p_i = \sum_{u \in \Omega_{k_i}} \Delta p_u$), for Case1 (top), Case2 (middle), and Case3 (bottom). The red and blue dots represent a DER or a load bus.

a non-zero value only when the boundaries of active flexibility is reached. Consequently, if flexibility is dispatched such that consumers' flexibility boundaries are not binding, the LFP of the respective bus becomes zero, and therefore, the consumers do not receive any payment from the DSO.

From Figure 4.4, one can also observe that in Case 1, the bi-level model yields negative flexibility values for load buses. This implies that the model steers the load busses to increase their load to match DER production and contain DER curtailment. This is in contrast to Case 2 and Case 3, in which some load buses get a positive flexibility value. A positive value means that the model sets the price such that it enables the DSO to steer the load buses to reduce their load. This observation can also be explained through curtailment; In Case 2 and Case 3, DERs are producing at their maximum capacity (the zero curtailment levels in Figure 4.2), therefore the model tends to set the load such that it meets the supply, by reducing the load at certain busses.

Sensitivity of LFP to data perturbation

For Case 1 and Case 2, Figures 4.5 and 4.6 respectively present the aggregated sensitivity of LFPs of all buses (j), to perturbation in the lower- or upper bound of active flexibility $\underline{\Delta p_i}$, $\overline{\Delta p_i}$, as well as the base-power program p_i^0 of a certain bus i, that is: $\sum_{j \in \Omega_E} \frac{\partial \lambda_j^p}{\partial a_i}, \forall a_i \in$

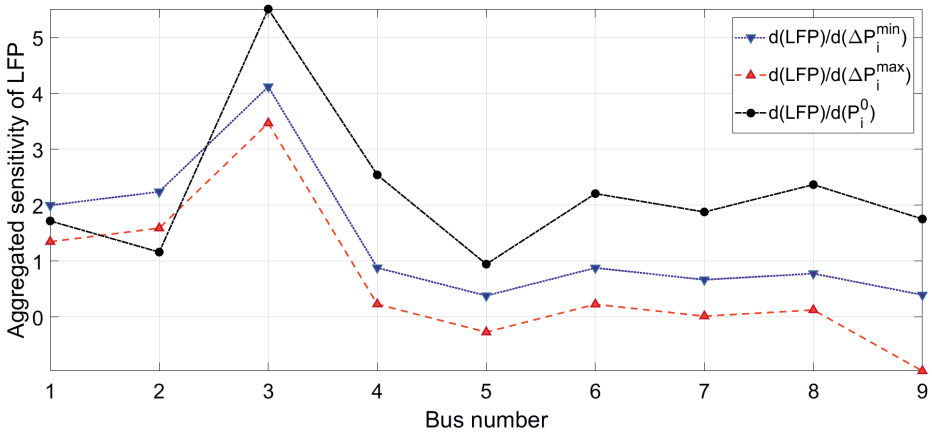

Figure 4.5: Aggregated impact of perturbations in lower and upper bound of flexibility (blue and red line, respectively), and base-power program (black line) at each bus on the LFPs of the whole network in Case 1.

$\{\underline{\Delta p_i}, \overline{\Delta p_i}, p_i^0\}, i, j \in \Omega_E$. The aggregated sensitivity indicates how an error in each of the input parameters (a_i) propagates throughout the whole network and influences all buses at the system level.

The blue line represents the sensitivity of the LFPs to perturbation in the lower bound of active power flexibility of different buses (i.e., $\frac{\partial \lambda^p}{\partial \underline{\Delta p_i}}$). Comparing the DER buses (e.g., buses 1, 2, 5, 8, 11, 13 in Figure 4.6) with the flexible load buses, one can see that, perturbation in $\underline{\Delta p_i}$ of DER buses has larger impact on the formation of LFPs of all buses in the entire network. A similar pattern can be observed from the sensitivity of the LFPs to perturbation in the upper bound of active power flexibility (i.e., $\frac{\partial \lambda^p}{\partial \overline{\Delta p_i}}$), which is represented in the red line in Figures 4.5 and 4.6. In addition, one can observe that the sensitivity of the LFPs to $\overline{\Delta p_i}$ of the flexible load buses is, in general, close to zero.

4.5 Discussion

The results of the bus voltages calculated by the SOC-OFD and bi-level-OFD show that, in general, the bus voltages are lower when calculated by the bi-level-OFD model. This observation can be explained via the relaxation error. As outlined in [121], the relaxation error can be interpreted as an artificially increased active and reactive loss over the lines. Now consider the results of the SOC-OFD model (in which no boundary is superimposed on increasing the relaxation error). One can observe that in the SOC-OFD model, the solver finds solutions with a higher relaxation error, and therefore higher (artificial) losses. This leads to higher voltage differences as well as higher network voltage levels, especially at the DER buses.

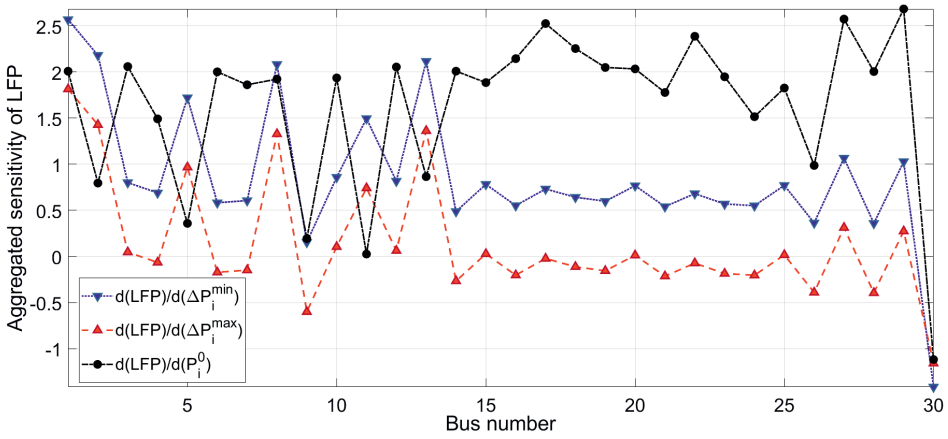

Figure 4.6: Aggregated impact of perturbations in lower and upper bound of flexibility (blue and red line, respectively), and base-power program (black line) at each bus on the LFPs of the whole network in Case 2.

The opposite is true for the bi-level-OFD model, in which the relaxation error is minimized, and as a result, the bus voltages obtain lower values.

The results of the flexibility prices show that if flexibility is dispatched such that consumers' flexibility boundaries are binding, the LFP of the respective bus equals the penalty tariff. This implies that the flexible loads have incentive to provide flexibility services such that they reach their full flexibility limits. Note that other settings could also be possible, for instance, those in which flexible loads are also remunerated when deviations remain within stated boundaries, which is beyond the scope of this work.

The local sensitivity analysis and the results provided are dependent on the specific network configuration. However, the methodology is generic. In this light, we argue that the DSO can use the local sensitivity analysis to identify the relative importance of (uncertain) input data (e.g., forecast on flexibility limits and load) on the solution of OFD problem. This includes the optimal flexibility dispatch and the formation of LFPs.

In the context of this work we assumed flexibility providers and DERs are competitive but are not able to exercise market power. However, the absence of an adequate regulatory framework, especially in the short-run, in the context of local energy and flexibility trading platforms, may encourage opportunistic participants to engage in strategic behavior. Therefore, regardless of the market setting considered, such behaviors could significantly influence the operation of the local energy market and from there, the decision making process of the DSO. Different mathematical models would be necessary for capturing strategic behavior of flexibility providers.

4.6 Conclusion

The OFD is an optimal power flow-based method that enables the DSO to determine the amount of flexibility (and associated prices) that it needs to dispatch from flexible resources to meet its operational constraints. Due to non-linearities in the power flow, the SOC relaxation of the AC power flow is typically used in the OFD problem, i.e., the SOC-OFD model. However, a solution to the SOC-OFD model can be inaccurate and thus will lack physical interpretation. When formalised, the SOC-OFD model takes certain input parameters that neither the DSO nor the flexibility providers are entirely aware of, and therefore, are highly uncertain (e.g., forecasts on available flexibility in the day-ahead).

In this work, we introduced a bi-level optimisation problem in which the UL seeks to minimise the SOC-relaxation error and the LL seeks to solve the SOC-OFD. The objective of the LL is set to minimise the curtailment of DERs subject to operational limits. Next, we derived a linear sensitivity matrix based on the perturbed KKT conditions of the SOC-OFD problem. We use the sensitivity matrix to investigate the sensitivity of the optimal flexibility dispatch solution (i.e., LFP and Δp_i) to forecast errors in input data (i.e., $\underline{\Delta p_i}, \overline{\Delta p_i}, p_i^0$) .

To solve the proposed bi-level problem, we firstly reduced the complexity by shifting certain constraints from the LL to the UL. We showed that such reformulation causes no loss of accuracy as long as the shifted constraints are not binding. Secondly, we recasted the reduced bi-level problem as a MPCC by replacing the LL with its corresponding KKT conditions. Finally, we relaxed the complementarity constraint and reformulated the problem as a NLP which is computationally tractable, even for large-scale problems. The proposed framework is general and can be applied regardless of network topology, as long as the objective of the lower-level problem is linear.

We compared the results of our bi-level-OFD model for three test networks with that of the SOC-OFD model. The analysis shows that for the same level of DER production, the bi-level-OFD model can effectively reduce the SOC-relaxation error.

Our results show that the DSO pays the DERs when they provide flexibility by increasing their production. However, flexible loads have no incentive to provide flexibility services unless they reach their operational flexibility boundaries. This is due to the way the OFD problem is formulated in this work. Therefore, one avenue for research in the future is to investigate other settings that provide an incentive by reimbursing flexible loads even before hitting the boundaries of their flexibility range.

A practical implication of our proposed sensitivity analysis framework is that, the DSO can identify the forecast error of which bus(es) has the most prominent impact on the optimal flexibility dispatch and the LFPs of the other buses in the network. This would allow the DSO to take adequate preventive actions to restrain unintentional deviations from the optimal values, and therefore, ensure the economic efficiency of the resulting flexibility dispatch in

practice.

A direct extension of the current work would be to investigate sensitivity of an optimal flexibility schedule to uncertainty associated with exercising such strategic behaviour. Additionally, along with the recent development in peer-to-peer distributed energy trading, there is a growing need for determining the hosting capacity of the distribution network for enabling such trades in advance. In this regard, one application of the proposed methodology in practice is for the DSO to estimate the hosting capacity of its network, considering the uncertainties associated with imperfect forecast and/or, the (un)intentional non-compliance of peers from the scheduled trades in the real time operation.

In conclusion, the methods and resulting insights of this paper can support the DSO in its many activities related to planning and operation of the distribution grid with increasing amounts of (intermittent) distributed resources.

Chapter 5

Impact of energy saving measures on energy consumption of residential buildings

This chapter is submitted for publication as:

E. Bozileva*, D. Azari*, H. Cappon, I. Leusbrock, K.J. Keesman, and H.H. Rijnaarts, Impact of energy saving measures on energy consumption of residential buildings

*Shared first authorship

Abstract

In this paper a framework was developed to simulate the building energy demand, considering technological energy saving measures, as well as consumers involvement in a demand response program. Technological measured are addressed by using the urban harvest approach, including demand minimization (e.g., improving building insulation), output minimization (e.g., greywater heat recovery), and using renewable energy sources (e.g., installing PV modules). Response surface methodology (RSM) was used to determine the system configuration (i.e., combination of technological modifications) which yields the minimum non-renewable primary energy consumption (NRPE) in residential buildings. The results show that, for the selected case study, NRPE consumption was most effectively reduced via measures that directly affect the electricity use (e.g., installing PV and battery). Moreover, a non-linear relationship between the installed PV and battery capacity was identified. The results of this work can be used to determine the most effective changes of energy systems in buildings.

5.1 Introduction

Global energy consumption is currently dominated by fossil sources which in 2012 comprised 81.7% of the world total primary energy supply [132]. Approximately 40% of this supply is attributed to the energy demand of buildings [133], which suggests that implementing energy efficiency measures in the built environment can significantly decrease the world's dependence on fossil energy. To transform the existing built environment into a more energy self-sufficient system, various technological and behavioral measures can be considered. These measures can be classified, as described in the Urban Harvest Approach (UHA) [134], into three categories: activities that (i) directly minimize resource demand via changes in users' behavior, as well as via efficiency and control measures; (ii) minimize (waste) output via cascading, recycling and recovery ; and (iii) orient on multi-sourcing, thus exploiting local renewable energy resources, such as solar and wind energy.

Extensive research has focused on reducing net electricity demand via efficient implementation of various building-scale technologies, such as solar photovoltaics (PV) coupled with electrical energy storage (EES) [135, 78], as well as demand-side management (DSM) strategies [79, 136, 61]. Numerous authors additionally looked into measures affecting net thermal energy demand of a building at the demand side, such as improving building insulation [81, 137], and at supply side, such introducing combined heat and power [138], collecting solar thermal energy [139], installing heat pumps.

None of these studies investigated the combined effect and interactions of these measures in order to assess the overall energy improvement in a building. In this work we specifically looked into the combined effects of technological and demand-side measures, in reducing both net electricity and heating demand of a building. The focus is on the net building demand of non-renewable primary energy (NRPE). NRPE represents the weighted sum of net gas and electricity demand, corrected for delivery and conversion losses, as well as the share of non-renewable sources in the grid electricity mix [140].

Building energy consumption after technology implementation can be accurately simulated with tools such as EnergyPlus [51] and TRNSYS [50]. These tools, however, require the knowledge of building parameters, which vary per building and are often difficult to obtain [141]. In this work already available historical demand data and available dynamic models of the components of renewable energy systems (e.g., described in [142]) were used to estimate the changes to building performance indicators [135, 78, 138].

The aim of this study is to clarify the complex relationships between NRPE consumption in a residential building and technological modifications, as well as involvement of end-users in a demand response (DR) program. Specifically, we aim to identify the optimal configuration of technological modifications and demand-side interventions which has the highest impact on reducing the NRPE consumption.

The main contributions of this paper are summarized as follows:

1. Proposal of a framework to simulate the energy demand of a residential building (including electricity and heat), considering technological modifications for improving the energy efficiency.
2. The proposed framework is used to determine the optimal configuration, including the combination of technological modifications, which improves the energy efficiency of a building. This framework includes a mixed-integer nonlinear optimization problem, which is hard to solver. To tackle this issue, the optimal solution is found via enumeration of pre-selected technological combinations, using response surface methodology (RSM).
3. To quantify the impact of the decision variables on the optimization problem, one-at-a-time sensitivity analysis is performed. The nonlinear relationship between the model output (i.e., NRPE consumption of the building) and the scalar model inputs (i.e., the capacity of the technological factors used in each configuration), as well as the interaction between different factors, were approximated using a second-order polynomial function.

5.2 Material and methods

We first define the residential building system and key performance indicator (KPI) characterizing building's non-renewable primary energy (NRPE) consumption. To elucidate the relationship between the technological or demand-side interventions and the KPI, we define several technological configurations (combination of technologies) and calculate maximal KPI values obtainable for each configuration. For selected configurations we additionally use Response Surface Methodology to investigate the impacts of various technology-characterizing factors on KPI. To do this we define a grid in factor space and simulate the system at each grid point. The resulting KPI surface is then approximated by an empirical function using regression techniques.

5.2.1 System outline

In this study the system of concern is a residential building of 625 apartments. In the baseline assessment, the energy demand of the system is covered only by NRPE. NRPE is either directly supplied to the system in the form of natural gas for space and water heating, or converted to electricity outside the system boundary and supplied to the system via the grid. A schematic presented in Figure 5.1 shows the energy flows in the system, that seeks to minimize its net NRPE demand via implementing direct demand minimizing, output minimizing and multi-sourcing measures:

1. Net energy demand is directly minimized via installing energy efficient boilers and improving building envelope insulation.

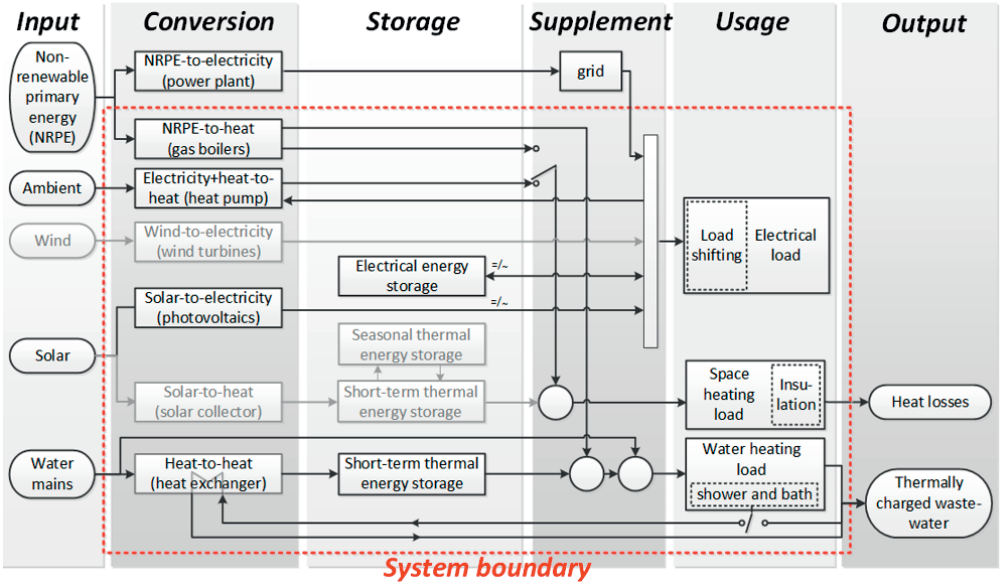

Figure 5.1: Schematic of the energy flows in the investigated system. Greyed units correspond to options ruled out during the baseline assessment phase

2. Energy output is minimized by recovering residual thermal energy from greywater (water from showers and baths) and using it for water heating.
3. Multi-sourcing measures are represented by harnessing wind energy in a form of electricity (wind turbines), solar energy in a form of thermal (solar collectors) or electrical energy (photovoltaics, PV), and ambient heat in a form of thermal energy (heat pump).
4. For both output minimizing and multi-sourcing activities, electrical storage options and Demand Side Management (DSM) strategies associated with electrical load shifting are introduced to address demand and supply mismatch.

A mathematical model was used to simulate the system over a period of one year with a global time-step of 15 min. Dynamic model inputs are the yearly heating, electricity and water demand profiles, as well as weather data on solar irradiance and outside temperature. Scalar model inputs are factors listed in Table 5.2. Dynamic model outputs are the net gas and grid electricity demand profiles adjusted to account for the effects of technological modifications (Table 5.1). These net demand profiles are used to calculate yearly gas (D_{gas}) and grid electricity (D_{ele}) consumption, which are combined to the weighted sum of yearly NRPE net demand D_E by

$$D_E = C_{nrpe2gas} D_{gas} + C_{nrpe2ele} D_{ele} \tag{5.1}$$

where coefficients $C_{nrpe2gas}$ and $C_{nrpe2ele}$ represent NRPE costs associated with "generation" of gas and electricity, and are assumed 1 and 2.24, respectively. The latter corresponds to electricity generation mix for the Netherlands for the year 2012 [132], the average electricity generation technology efficiencies for the year 2006, additionally assuming 5% transmission losses [143] and 13% supply losses for gas-fired power plants, as in [140] (see section 5.3.4).

The NRPE consumption in the building, which can be characterized by the Non-renewable Primary Energy Net Demand Minimization Index ($nDMI_E$), is then defined as

$$nDMI_E = D_E / D_{E0} \cdot 100 \tag{5.2}$$

where D_{E0} is the baseline yearly NRPE consumption and D_E is the yearly NRPE consumption after a technological modification.

5.2.2 System configurations

Five configurations (combinations of technological modifications) are selected for the analysis (Table 5.1). Configuration 0 represents the reference baseline. Configurations 1 and Configuration 2 correspond to either relatively 'simple' or passive solutions, that do not involve substantial maintenance or a change of infrastructure. Configuration 3 introduces the link between water and energy cycles of the building using heat exchangers for water heat recovery. Configuration 4 assesses the contribution of added electrical energy storage (EES). Configuration 5 illustrates an all-electric system (net heating demand is reduced via use of heat pumps) with electrical energy storage. The configuration selection ensures that each UHA activity is represented by one or two technological modifications. Additionally, non-technological modifications associated with consumer load shifting are considered when relevant.

5.2.3 System evaluation

In order to find the best combination of technologies optimization was performed via enumeration of the system configurations, and identifying the one with the optimal value of the objective function. Factor effect nonlinearities and interactions of technologies were assessed by fitting the relationship between scalar model inputs (e.g., building insulation) and output (i.e., $nDMI_E$) to a regression function of appropriate complexity. The simplest such function including interactions is the full second order polynomial given by

Table 5.1: System configurations evaluated in this study. 'Config. 0' represents the baseline with no modifications.

	Water heating	**Space heating**			**Electricity**		
Modification	Grey water heat recovery	Improving building envelop insulation	Installing energy efficient gas boiler	Installing heat pump	Installing PV system	Electrical energy storage	Load shifting
Config. 0							
Config. 1		×	×				
Config. 2		×	×		×		(×)
Config. 3	×	×	×		×		(×)
Config. 4	×	×	×		×	×	(×)
Config. 5	×	×		×	×	×	(×)

$$Y^k = \beta_0 + \sum_{i \in \Psi_F} \beta_i X_i^k + \sum_{j \in \Psi_F} \sum_{i \in \Psi_F} \beta_{ij} X_i^k X_j^k + e^k \tag{5.3}$$

where $\Psi_F = \{1, \cdots, N\}$ is the set of the number of factors. Index $k \in \Psi_k = \{1, \cdots, K\}$ is the level index according to a selected factor sampling design and K represents a total number of factor-level combinations. Y is the output $nDMI_E$. Variable X_i, is the normalized factor values. β are the regression (sensitivity) coefficients. Unknown β coefficients are estimated via polynomial regression, and characterize offset (β_0), main (β_i), nonlinear (β_{ii}) and interactive (β_{ij}) effects of factors on $nDMI_E$. Lastly, e represent the approximation error.

Fitting such function requires sampling the factor space in a way that uniformly covers various factor-level combinations. Common sampling designs include, e.g., Latin hypercube [144] and full factorial design [145]. The latter is more computationally expensive. However, it allows generation of easily visualized response surfaces that illustrate the model input-output relationships [145], thus facilitating the result interpretation.

All modifications and their corresponding factors considered in this study are given in Table 5.2. Factor ranges are characterized by "baseline", "realistic" and "explorative" limits. Each factor is sampled at 5 levels between its limits using a regular grid in order to adequately cover the design space.

The following assumptions are considered to determine the values of the values of the corresponding factors in Table 5.2:

- TES is assumed to be insulated with 8 cm thick rock-wool layer (thermal conductivity 0.04 $Wm^{-1}K^{-1}$. The "real" value of V_{TES} corresponds to daily average thermal energy demand for water heating.

Table 5.2: Characterization of technological modifications considered in this study.

Modification	Corresponding Factors	Symbol	Range			Unit
			Base	Real.	Expl.	
Water Heating						
Grey-water heat recovery	Thermal energy storage tank (TES) capacity	V_{TES}	-	29	-	m^2
	Heat transfer efficiency between warm greywater and cold water	η_{MX}	-	90	-	%
Space Heating						
Improving building envelop insulation	Overall heat transfer coefficient through the building envelop	U_{env}	1.67	1.06	0.97	$Wm^{-2}k^{-1}$
Installing energy efficient gas boiler	Boiler efficiency	η_{boiler}	75	85	95	%
Installing air source heat pump	Coefficient of performance	COP	-	$0.5COP_{Carnot}$		-
Electricity						
Electricity energy generation via PV	Area available for PV installation	A_{PV}	0	2700	15400	m^2
(positioned to maximize yearly energy generation)	PV module efficiency	η_{PV}	-	16	-	%
Electricity energy storage (EES)	EES capacity	Q_{EES}	0	1	3	days of autonomy
Load shifting	Downward flexibility	α^d	0	20	40	%
	Load time shifting window	ω_{tt}	-	-	23	h

- Baseline value for U_{env} is calculated assuming U-values of walls, windows and doors being respectively 0.3, 2.8 and 1.7 $Wm^{-2}k^{-1}$. Explorative value of U_{env} is calculated assuming the respective values being 0.1, 1.65 and 1.7 $Wm^{-2}k^{-1}$. Realistic value for U_{env} is calculated assuming that only window insulation has been improved. In all cases fraction of total area corresponding to walls, windows and doors is 0.44, 0.54 and 0.02 respectively.
- COP_{Carnot} is estimated as $T_{hot}/(T_{hot} - T_{cold})$, where $T_{hot}(K)$ is the temperature that needs to be supplied to the radiator (max 45°C) plus 4, and $T_{cold}(K)$ is the outside temperature minus 6.
- The "realistic" value of A_{PV} corresponds to the sum of the roof area of the building and the area of the nearby parking lot for the case study (see Section 5.4.1). Maximum "explorative" value corresponds to three-times the area that is needed to generate each year power equivalent of yearly average electricity demand assuming 16% PV efficiency.
- One average day of autonomy for EES corresponds to 2.51 MWh (see Figure 5.5).
- The EES is assumed to be Li-ion battery with round-trip efficiency of 95%, 6000 cycle lifetime at 80% depth of discharge and 6% self-discharge per month [146, 147].

Finally, the consumers in this study apply local electricity generation through PV panels and are able to adapt their energy consumption pattern according to their wishes. This is referred to as load shifting. To assess the effect of factors and additional load shifting (last column Table 5.1), the model based on [100] was proposed. The proposed model is an optimization problem, which aims to minimize the difference between the load and local PV generation. It does so by shifting the load to times when local PV generation exceeds baseline load assuming a "realistic" setting (see section 5.3.3 for PV output calculation). The load shifting was primary constrained by the preferences of the flexible consumers, which are characterized by two factors: (i) downward flexibility, α (%): the maximum percentage of load, that consumers allow to reduce at any time instance, and (ii) load shifting time window, ω_{tt} (h): the time window within which the consumers allow for load shifting. Load shifting is performed over one operating day (i.e., 24 hours).

To simulate the NRPE consumption under the configurations given in Table 5.1 we used a Matlab implementation of a mathematical model, describing the physical processes occurring in the unit operations depicted in Figure 5.1. The model consists of four modules (water, water heating, space heating, and electricity), and represents a set of water and energy balances, as well as auxiliary algebraic relationships that characterize each unit operation in Figure 5.1. Detailed description of the balances and model assumptions are given in section 5.3. To address the uncertainty associated with discrepancies in energy demands and meteorological data for different years, the simulation was performed for each factor-level combination using the yearly data from 2005 to 2010. The average and confidence interval of the six resulting $nDMI_E$ values were used for further analysis.

5.3 Model Description

This section presents the models used in the water heating and the electricity modules in the proposed framework.

5.3.1 Water heating module

Modeling assumptions

- Piping is neglected. Therefore, there are no losses associated with piping and pumping.
- Thermal energy is stored in a form of a warm water in an insulated tank (i.e., thermal energy storage (TES) tank). TES is characterized by storage capacity and magnitude of heat losses.
- Storage capacity of TES depends on volume of water in TES and maximal temperature difference of water in TES: a temperature of a boiling water (100 °C) and ambient temperature (inside the building, but not in the apartments) which is assumed to be constant throughout a year (T_a).
- Heat losses are determined by the overall heat transfer coefficient and proportional to the temperature difference of water currently in TES and ambient (T_a).
- Warm water charged with thermal energy is first directed to TES and, if there's a demand for heating, is further distributed to heat consuming appliances (there is no option to bypass storage if demand and supply coincide).
- TES is completely filled with water at all times, i.e., the subtraction of warm water is instantaneously compensated by the supply of equal amount of cold water.
- Temperature dependency of physical characteristics of water (density, thermal capacity) are neglected.
- TES discharge is instantaneous.
- A heat exchanger is at the steady state at all times.

Water demand profiles for different water consuming appliances (i.e., $\dot{m}_{app}(t)[kg/s]$) are generated with [148] for 625 single-person dinky apartments assuming 80% average occupancy. Baseline gas demand for water heating (i.e., $\dot{E}_{gas2wh0}$ is calculated as follows:

$$\eta_{boiler}\dot{E}^{0}_{gas2wh}(t) = \sum_{app\in\Psi_{app}} \dot{m}_{app}(t)C_p\left(T_{app}(t) - T_{cold}\right) \tag{5.4}$$

where app corresponds to water consuming appliances, such as bath, shower, washbasin, kitchen sink, dishwasher, washing machine, and toilet. c_p is the specific heat capacity of water

in $JK^{-1}kg^{-1}$. η_{boiler} is boiler efficiency, T_{cold} is the temperature of cold water (assumed 10 °C), and T_{app} is the average temperature for appliances.

Gas demand for water heating after greywater heat recovery is calculated as the difference between the energy required by the appliances and the energy currently available in TES, corrected for boiler efficiency, as given by the following expression:

$$\eta_{boiler}\dot{E}_{gas2wh}(t) = \sum_{app\in\Psi_{app}} \dot{m}_{app}(t) f_{hot,app} C_p \left(T_{hot} - T_{TES}(t)\right) \tag{5.5}$$

where T_{TES} is water temperature in TES, which can be calculated from:

$$\begin{aligned}\rho V_{TES} C_p \frac{d(T_{TES})}{dt} = &\sum_{app\in\Psi_{app}} \dot{m}_{app}(t) f_{hot,app} C_p \left[T_{HX}(t) - T_{TES}(t)\right] \\ &- U_{TES} A_{TES} (T_{TES}(t) - T_a)\end{aligned} \tag{5.6}$$

where ρ is the density of water $[kg/m^3]$, V_{TES} is TES capacity $[m^3]$, A_{TES} is the surface area of TES tank $[m^2]$, U_{TES} is the overall heat transfer coefficient through TES walls $[Wm^{-2}K^{-1}$, T_a is temperature of the non-living space in the building (assumed to be 15 °C throughout the year), T_{HX} is water temperature after heat exchange with thermally charged greywater, coming from bath and shower.

To calculate T_{HX}, we assume that the heat exchange between greywater and drinking water is a steady-state process, and the thermal energy taken up by the drinking water is a constant fraction (η_{HX}) of the maximal amount of thermal energy, that can be released by the greywater:

$$\begin{aligned}&\sum_{app\in\Psi_{app}} \dot{m}_{app}(t) f_{hot,app} C_p \left[T_{HX}(t) - T_{TES}(t)\right] = \\ &\eta_{HX} \min\left(\sum_{app\in\{sh,ba\}} \dot{m}_{app}(t) C_p, \sum_{app\in\Psi_{app}} \dot{m}_{app}(t) f_{hot,app} C_p \right) \left[T_{GW}(t) - T_{cold}\right]\end{aligned} \tag{5.7}$$

where sh and ba represent shower and bath, respectively. T_{GW} is the average temperature of the greywater, given as follows:

$$T_{GW}(t) = \frac{\sum_{app\in\{sh,ba\}} \dot{m}_{app}(t) C_p T_{app}}{\sum_{app\in\{sh,ba\}} \dot{m}_{app}(t) C_p} \tag{5.8}$$

5.3.2 Space heating module

Assumptions

- The building is assumed to be a single compartment black-box, characterized by an overall heat transfer coefficient (weighted sum of overall heat transfer coefficients for walls, roof and windows connected in parallel), total surface area (sum of area of walls, roof and windows), and the homogeneous temperature inside the building.
- Central heating is assumed.
- Consumers' behavior is unaffected by the technological modifications implemented in the system.
- Temperature inside the building (i.e.,T_{inside}) during the heating season is 20°C from 7am to 10am and from 3pm to 10pm, and 18°C during the rest of the day.
- Fraction of demand associated with heat losses due to leakages and heat gains from the residents and appliances is unaffected by any technological modifications, implemented in the system, and is lumped into a single term.
- The year is divided into a "heating period" (baseline gas demand is above the threshold value) and "non-heating period" (baseline gas demand is below a threshold value). During the non-heating period thermal energy is only required to cover the demand for water heating. During the heating period thermal energy is required to cover the demands for both space and water heating.
- Radiators for the baseline configuration are sized for 75/65°C temperature drop and 20°C room temperature. Radiators for a configuration with a heat pump are sized for 45/35°C temperature drop and 20°C room temperature.

Baseline

Baseline gas demand for space heating $\dot{E}^0_{gas2sh}(t)$ in $[W]$ is extracted from historical data on total gas use $\dot{E}_{gas}(t)$. For the non-heating period $\dot{E}^0_{gas2sh}(t)$ is assumed to be zero. For the heating period $\dot{E}^0_{gas2sh}(t)$ is determined by subtracting the mean gas use during the non-heating period $\overline{E}_{gas0,nonheatin}$ from the total gas use.

Gas use for space heating is required to compensate for the heat losses due to convection $\dot{E}_{loss,convection}(t)$, heat losses associated with air leakages $\dot{E}_{loss,air}(t)$, as well as heat gains from the residents $\dot{E}_{gain,res}(t)$ and appliances $\dot{E}_{gain,app}(t)$. The latter three can be assumed unaffected by technological modifications. It is lumped into a single net loss term $\dot{E}_{netloss}(t)$. Consequently, gas demand $\dot{E}_{(gas2sh}(t)$ after implementing the passive measures, such as installing more energy efficient gas boiler and improving the building envelop insulation (characterized by U_{env}, in $[Wm^{-2}K^{-1}]$), can be estimated from:

$$\eta_{boiler}\dot{E}_{gas2wh}(t) = \dot{E}_{netloss}(t) + \dot{E}_{loss,convection}(t) \tag{5.9}$$

where $\dot{E}_{loss,convection}(t) = U_{env}A_{env}\left(T_{inside}(t) - T_{outside}(t)\right)$. A_{env} is total surface area of the building envelop, T_{inside} is the temperature inside the building, and $T_{outside}$ is the outside temperature.

The remaining space heating demand can be covered via a heat pump. Introduction of heat pump necessitates the resizing of radiators. Consequently, conventional radiators, operating in 75/65/20°C regime, are replaced by the low temperature radiators, operating, e.g., in 45/35/20°C regime. Operating temperatures of the radiators affect the electricity demand for the heat pump. These temperatures, namely, supply temperature of the radiator $T_{rad,s}$, return temperature of the radiator $T_{rad,r}$, and mean radiator temperature $\overline{T}_{rad}$, can be estimated from the following system of equations:

$$\frac{\overline{T}_{rad}(t) - T_{inside}(t)}{\Delta T_{rad,rated}} = \left(\frac{\dot{E}_{gas2wh}(t)}{\dot{E}_{rad,rated}}\right)^{1/n} \tag{5.10}$$

$$\overline{T}_{rad}(t) = 1/2\Big(T_{rad,s}(t) + T_{rad,r}(t)\Big) \tag{5.11}$$

$$\dot{E}_{gas2wh}(t) = \dot{m}_{rad}(t)C_p\left[T_{rad,s}(t) - T_{rad,r}(t)\right] \tag{5.12}$$

Where $\dot{E}_{rad,rated}$ is heat emission from the radiator. Additionally, water mass flowr ate in the radiator $\dot{m}_{rad}(t)$ during the heating season are estimated from:

$$\dot{m}_{rad} = \left(\frac{\dot{E}_{rad,rated}}{C_p\left[T_{rad,s}(t) - T_{rad,r}\right]}\right) \tag{5.13}$$

5.3.3 Electricity module

Assumptions

- Total electricity load is a sum of baseline electricity demand and electricity demand for air source heat pump.
- Power generated by a PV module is used to cover the load and any excess power is stored in the battery (EES).
- EES is characterized by the nominal capacity (i.e., Q_{EES} in $[J]$, storage efficiency η_{EES}, self-discharge rate σ, and depth of discharge. The charging and discharging of EES is instantaneous.

Balances

Base electricity demand from the grid $\dot{E}^0_{grid2ele}$ is derived from the historical data. Implementing a heat pump increases the base electricity demand. The amount of increase is determined by $\dot{E}_{elec2sh}(t) = \frac{\dot{E}_{gas2sh}(t)}{CoP_{HP}(t)}$, where CoP_{HP} is the coefficient of performance of a heat pump, which is assumed to be half of the Carnot coefficient of performance. The Carnot coefficient can be found from:

$$CoP_{HP,Carnot)} = \frac{T_{HP,cond}(t) + 273}{T_{HP,cond}(t) - T_{HP,evap}(t)} \tag{5.14}$$

Where $T_{HP,cond}$ is the condensation temperature of the refrigerant circulating in a heat pump (in °C) and $T_{HP,evap}$ is the evaporation temperature of the refrigerant circulating in a heat pump. Condensation temperature is roughly assumed to be $T_{HP,cond}(t) = T_{rad,s}(t) + 4$, whereas evaporation temperature is assumed to be $T_{HP,evap}(t) = T_{outside}(t) - 6$.

Combined net electricity demand is partially covered by electricity generated by PV modules $\dot{E}_{PV} = \eta_{PV}(t)I(t)A_{PV}$. η_{PV} is the efficiency of the PV module, $I(t)$ is the irradiance received by a PV module, A_{PV} is the area covered by PV modules.

Electricity demand that is directly covered by PV-generated power $\dot{E}_{PV2ele}$ depends on both PV supply, corrected by DC/AC inverter efficiency (i.e., η_{Inv}, and net demand. Excess power generated by PV is stored in the battery, as long as it does not exceed maximal state of charge $E_{EES,max}$, which depends on nominal storage capacity and the depth of discharge. Therefore, power supplied to the battery is determined as:

$$\dot{E}_{PV2EES}(t) = \min\left(\left(\dot{E}_{PV}(t) - \dot{E}_{PV2ele}(t)/\eta_{Inv}\right), \left(E_{EES,max} - E_{EES}(t)\right)/dt\right) \tag{5.15}$$

where E_{EES} is the state of charge of the battery. Power supply from the battery, that can be used to cover the remaining electricity demand, is calculated from:

$$\dot{E}_{EES2ele}(t) = \min\left(\left(E_{EES}(t) - E_{EES,min}(t)\right)/dt + \dot{E}^0_{grid2ele}(t) + \dot{E}_{grid2sh}(t) + \dot{E}_{PV2ele}(t)\right) \tag{5.16}$$

Where $E_{EES,min}$ is the minimal state of charge. Any remaining power generated by PV is fed to grid and can be found from:

$$\dot{E}_{PV2grid}(t) = \dot{E}_{PV}(t) - \dot{E}_{PV2ele}(t)/\eta_{Inv} - \dot{E}_{PV2EES}(t) \tag{5.17}$$

State of charge of the battery can be found from :

$$E_{EES}(t+dt) = E_{EES}(t)(1-\sigma) + \eta_{EES}\big[\dot{E}_{PV2EES}(t) - 1/\eta_{Inv}\dot{E}_{EES2ele}(t)\big]dt \tag{5.18}$$

Where η_{EES} is the efficiency of battery storage, and σ is the self-discharge rate. Finally, the net electricity demand from the grid can be calculated as:

$$\dot{E}_{grid2ele}(t) = \dot{E}^{0}_{grid2ele}(t) + \dot{E}_{ele2sh}(t) - \dot{E}_{PV2ele}(t) - \eta_{EES}\dot{E}_{EES2ele}(t) \tag{5.19}$$

5.3.4 Non-renewable primary energy factor

Non-renewable primary energy factor for electricity generation is calculated using the following expression:

$$C_{NRPE} = (1 + loss_{tr}) \sum_{f \in \Psi_{fuel}} \theta_f/\gamma_f(1 + loss_{leak,f}) \tag{5.20}$$

Where θ_f corresponds to the share of fuel f in the electricity mix, γ_f is the average electricity generation efficiency corresponding to fuel f, $loss_{tr}$ is transmission losses, and $loss_{leak,f}$ is gas losses due to leaks.

5.3.5 Knee-point identification

To identify the "knee" points of the asymptotic surfaces, such as that of $nDMI_E$ for configuration 4 (see Figure 5.2), we use the procedure, similar to that described by [149].

According to the previously described procedure, the original surface is first smoothened while taking care of preserving the shape. To do that we use regression to fit $nDMI_E$ surface to a rational function, given by the following expression:

$$Y_s(k) = \frac{\beta_0 + \sum_{i \in \Psi_{fact}} \beta_i X_i(k) + \sum_{i \in \Psi_{fact}} \sum_{j \in \Psi_{fact}} \beta_{ij} X_i X_j(k)}{\sum_{i \in \Psi_{fact}} \alpha_i X_i(k)} \tag{5.21}$$

where Y_s is smoothened $nDMI_E$, X_i represents the design factors (e.g., A_{PV} and Q_{EES}), α_i, β_0, β_i and β_{ij} are the regression coefficients, $\Psi_{fact} = \{1, \cdots N\}$ is the set of factors, and k is the factor level index according to a selected factor sampling design. The $nDMI_E$ fit to this rational function is shown on Figure 5.3.

The values of smoothed Y_s and X_i are normalized to a unit square as follows:

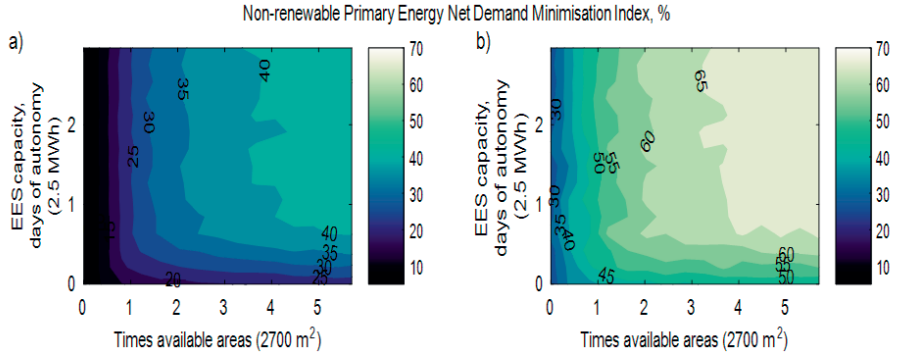

Figure 5.2: $nDMI_E$ for configuration 4 as a function of area available for PV installation and EES capacity for 'baseline' (a) and 'explorative' (b) values of U_{env} and η_{boiler} and greywater heat recovery.

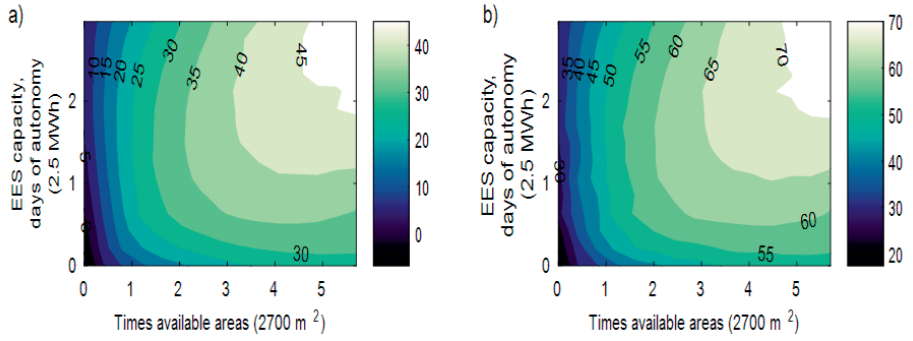

Figure 5.3: Approximation of $nDMI_E$ by a rational function (configuration 4).

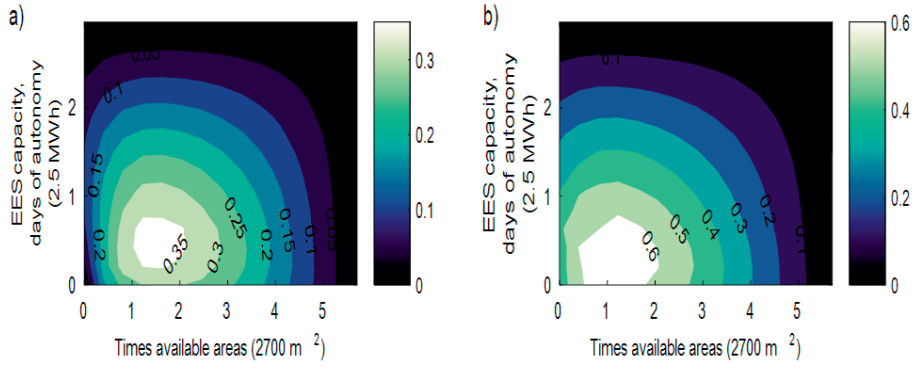

Figure 5.4: The curvature surface of $nDMI_E$ (configuration 4).

$$Y_{sn}(k) = \frac{Y_s(k) - \min Y_s}{\max Y_s - \min Y_s} \tag{5.22}$$

$$X_{sn,i}(k) = \frac{X_i(k) - \min X_i}{\max X_i - \min X_i} \tag{5.23}$$

Afterward, the curvature of the smoothened normalized surface is found as an element-wise product of the original surface and "inverted" factor values $(1 - X_{sn,i})$. The general expression used in this study to find the aforementioned curvature is given by:

$$Y_c(k) = Y_{sn}(k) \prod (1 - X_{sn}(k) \tag{5.24}$$

The maximum of the resulting surface is used to identify the "knee" points of the original surface, as shown in Figure 5.4

5.4 Results

5.4.1 Case study

To illustrate the method, a case study of a residential multi-story building was implemented. The dataset is from a a student house with 625 single-person apartments located in the city of Wageningen[1], the Netherlands. Year-round, daily demand profiles for hot water appliances (shower and bath) were obtained from simulations using SIMDEUM® software [148], assuming that all apartments could be modeled as one-person one-income apartments. Electricity (five-minute measurements) and gas demands (hourly measurements) during a period from 2005 to 2010 were provided by a local energy distribution network operator (Alliander, Personal Communication). Heating demands (required as model inputs) were derived from gas demands assuming 75% baseline boiler efficiency. Outside temperature, wind speed and solar irradiance (hourly measurements) for the same period were provided by a local weather station. All raw input data were adjusted to match the global time step of the model (15 min) using the zero-order hold method.

5.4.2 Baseline assessment

The baseline assessment for the case study was conducted to provide an inventory of current energy demands and supply potentials (Figure 5.5). Supplies are estimated for "realistic" area values indicated in Table 5.2.

[1]The city of Wageningen is located in a temperate climate zone (51.97°N, 5.66°E), with mild winters and summers (average temperatures in January and July are 3.3°C and 18.1°C, respectively [143]. Average local wind speed is 3.6 m/s (at 10 meter height), and average local annual solar irradiance is about 1000 kWh/m^2.

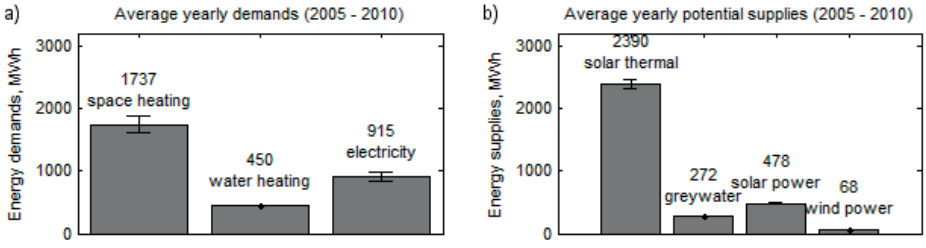

Figure 5.5: Baseline yearly energy demands and potential local energy supplies from renewable sources.

Yearly demand adds up to 3102 MWh and supplies to 3208 MWh. Additionally, solar thermal energy supply was estimated assuming 80% solar collector optical efficiency; wind power supply was estimated assuming 10 rooftop wind turbines with 1.5 m rotor diameter; greywater thermal energy supply was estimated assuming 40°C water temperature for shower and bath . The inventory was used to make a preliminary selection of technologies, one scenario of which was to be analyzed in more detail.

Figure 5.5 shows the baseline of yearly energy consumption, and potential of local energy supply from renewable energy sources. It can be seen that local PV electricity generation (478 MWh) can potentially cover up to 15% of total energy demand (corresponding to 25% of total NRPE net demand), whereas local solar thermal energy generation (2390 MWh) can potentially cover up to 77% of total energy demand (corresponding to 56% of total NRPE net demand) This might suggest that it is more attractive to use the available area to generate heat rather than electricity. Nevertheless, little advantage can be taken from the former due to seasonal demand-supply mismatch, as shown in Figure 5.6, unless seasonal thermal energy storage is addressed. Net electrical energy demand reduction relies chiefly on solar power generation, as wind power generation potential is negligible compared to electricity demand for the case study ($\leq 8\%$, Figure 5.5).

Consequently, in this study we focused on configurations that involve solar energy collection via PV rather than solar collectors. Furthermore, wind power generation is discarded, whereas thermal energy demand reduction is evaluated based on improving building envelope insulation, installing a more energy efficient gas boiler, recovering thermal energy of greywater with a heat exchanger, and installing a heat pump.

5.4.3 Configuration comparison

The maximal $nDMI_E$ values that can be achieved for the five studied configurations (Table 5.1) under "realistic" and "explorative" scenarios are shown in Figure 5.7. In the "realistic" scenario implementing passive measures only (Config. 1) reduced NRPE consumption by 19% and addition of PV added another 13% (Config. 2). The remaining solar production cannot be

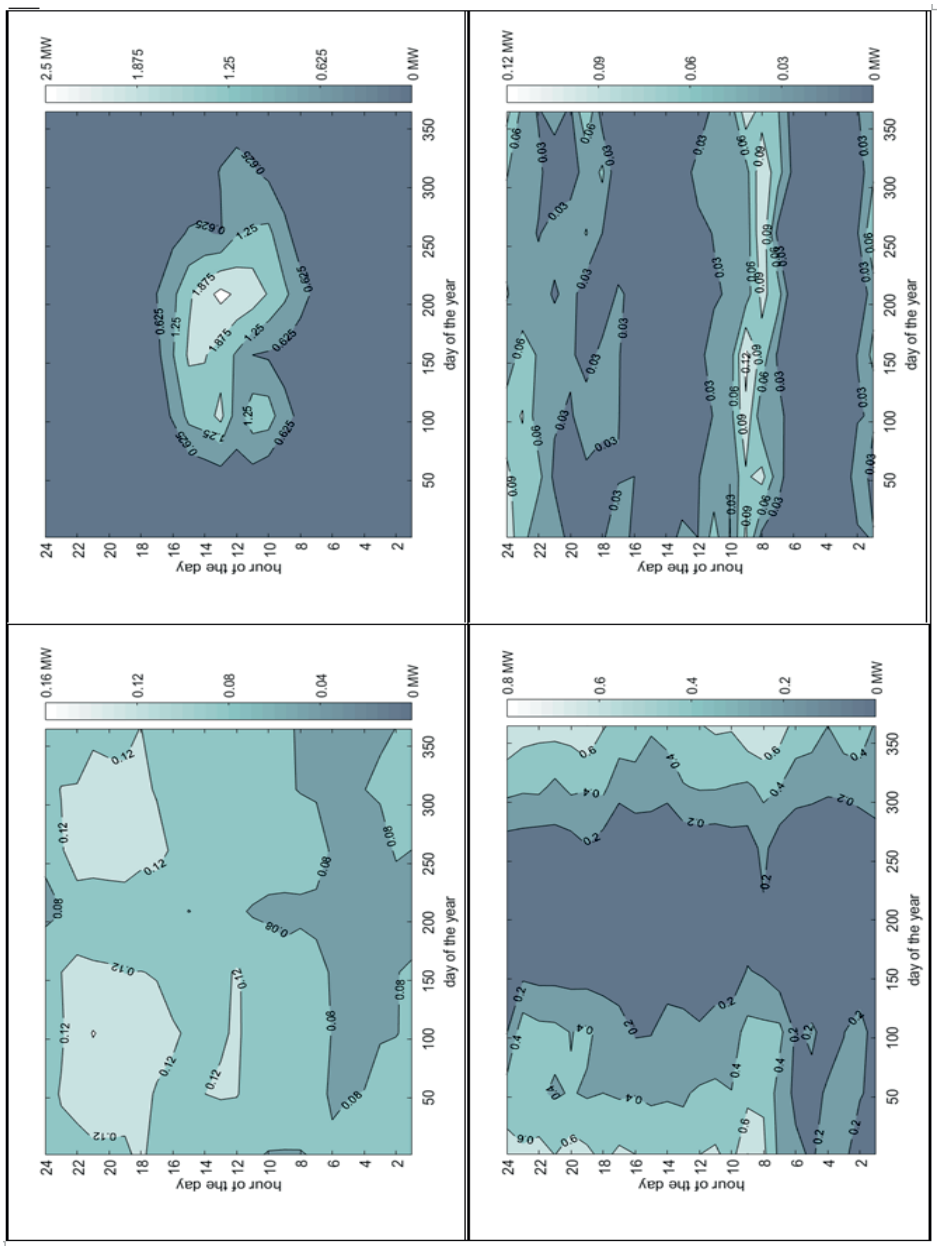

Figure 5.6: Baseline demand contours, left: (a) for electrical energy and (c) for thermal energy. And baseline supply contours, right: (b) for solar energy and (d) for thermal energy of greywater.

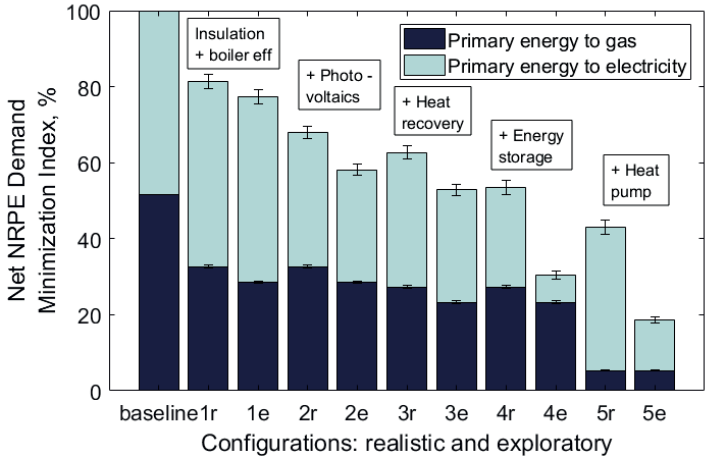

Figure 5.7: Maximum $nDMI_E$ values for five studied configurations under "realistic" (r) and "explorative" (e) scenarios (1-5) for the years 2005 - 2010.

consumed directly due to demand-supply mismatch (Figure 5.6). Heat recovery from hot water appliances added another 5% (Config. 3), whereas electrical energy storage added 9% of reduction (Config. 4). Finally, the heat pump reduced NRPE by 10% (Config. 5), which brings the total reduction to 57% in the "realistic" scenario.

Substantial reduction in NRPE consumption caused by the introduction of an EES and an ASHP (especially prominent for the "explorative" scenario) makes it of interest to further analyse configuration 5 in more detail.

5.4.4 Configuration 5 in detail

In configuration 5 net heating demand is initially reduced by improving the building envelope insulation, and the remaining demand is covered by a heat pump. Net electricity demand is reduced via PV-generated solar power coupled with EES. These technologies are characterized, respectively, by U_{env}, COP, A_{PV}, and Q_{EES} (Table 5.2). The COP of the heat pump is not a varied parameter, but dependent on the outside temperature.

The relationship between $nDMI_E$ and the aforementioned normalized technological factors is approximated by a full second-order polynomial (equation (5.3)) and reads as:

$$\begin{aligned} nDMI_E = {} & 17.9A_{PV} - 14.0A_{PV}^2 + 0.6U_{env}A_{PV} + \\ & 5.3Q_{EES} - 7.3Q_{EES}^2 + 4.2A_{PV}Q_{EES} - \\ & 5.6U_{env} - 0.5U_{env}^2 + 0.1U_{env}Q_{EES}. \end{aligned} \tag{5.25}$$

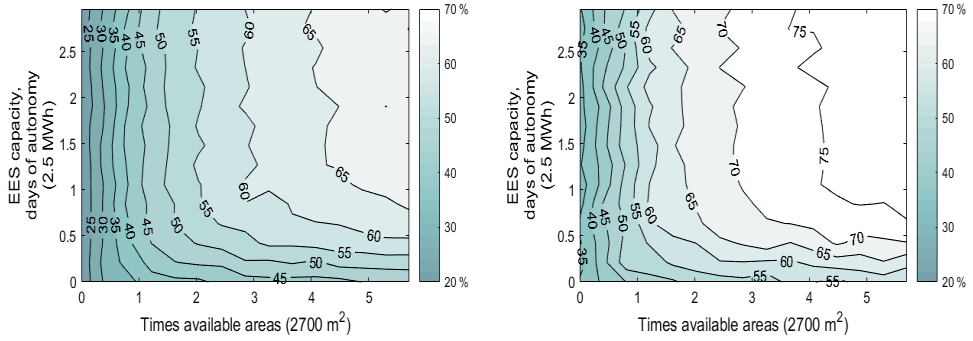

Figure 5.8: Response surface of $nDMI_E$ illustrating its dependence on A_{PV} and Q_{EES} for $U_{env} = 1.67 W m^{-2} K^{-1}$ (left), and $U_{env} = 0.97 W m^{-2} K^{-1}$(right)

The polynomial suggests that the response is rather linear with respect to U_{env}. The quadratic, non-linear behavior with respect to A_{PV} suggests that increasing the number of installed PV arrays only results in sensible reduction in NRPE consumption up to a certain limit. Furthermore, strong interaction between area available for PV installation and EES capacity ($\beta_{(A_{PV}-Q_{EES})} = 4.2$) suggests that the value of this limit depends on the available storage capacity. Moreover, the effect of Q_{EES} is also characterized by strong nonlinearity.

To better understand the relationship between A_{PV}, Q_{EES} and $nDMI_E$ we studied the respective cross-section of the response surface of $nDMI_E$ shown in Figure 5.8. One can see that as long as the area available for PV installation is below $1 \times 2700 m^2$ (i.e., approximately half of what is needed to generate the yearly electricity demand for our case study), EES installation has virtually no effect on net NRPE demand reduction. For larger areas the effect of Q_{EES} on $nDMI_E$ appears to be asymptotic. Asymptotic surfaces, as cross-sections of $nDMI_E$ with respect to A_{PV} and Q_{EES}, can be characterized by the points of maximal curvature (the so-called "knee"). Evidently, investing in increase of A_{PV} and Q_{EES} above the "knee" values is wasteful, due to rapid diminishing returns of additional benefit, discussed by various authors [79, 138]. Consequently, identifying the "knee" becomes an important task. Accomplishing this task is greatly facilitated by the use of the response surface methodology. The method for identifying the "knee" points of $nDMI_E$ is given in section 5.3.5.

When applying $A_{PV} = 1.5\times$ available-area, and $Q_{EES} = 0.5$ days and NRPE reduction of 60% can be achieved (Figure 5.8). These NRPE savings appear despite the evident increase in electricity consumption above the baseline during the cold months (Figure 5.9), which makes both seasonal and daily electricity demand-supply mismatch during the cold months even more pronounced.

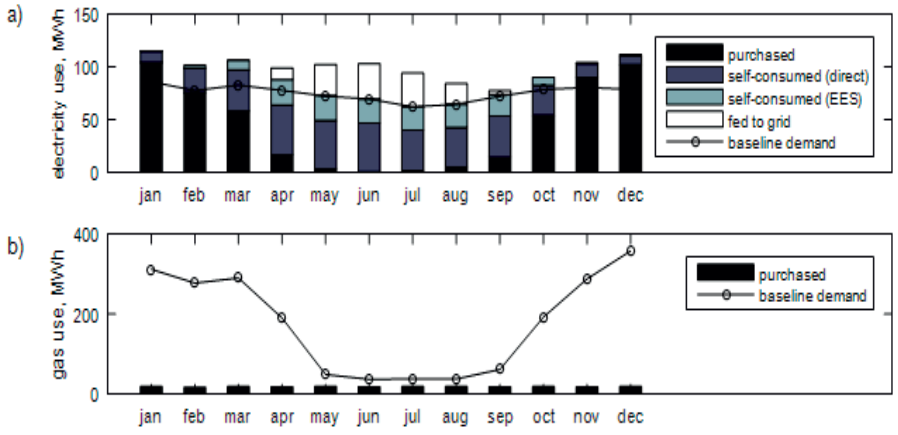

Figure 5.9: Monthly breakdown of a) electricity and b) gas consumption after introducing a heat pump for the year 2008 for $A_{PV} = 1.5\times$ available area, $Q_{EES} = 0.5\times$ days of autonomy, $U_{env} = 0.97 W m^{-2} K^{-1}$.

This increase in demand-supply mismatch makes it of interest to examine how demand-side flexibility affects "knee" PV and EES capacity requirements after introducing a heat pump. Figure 5.10 shows how load-shifting allows to achieve the same reduction in NRPE consumption at lower battery capacity, compared to a situation, when load-shifting is not implemented. Specifically, if the residents can be persuaded to shift up to 20-40% of the load to different time slots during the day, the "knee" reduction in NRPE consumption (about 60%) can be achieved with battery capacity corresponding to 0.4 days of autonomy. In other words, flexibility to shift 20-40% of the load reduces battery capacity requirements by 20% for configuration 5.

5.5 Discussion

In this study we used Response Surface Methodology to investigate how technological and demand-side measures affect the reduction of non-renewable primary energy (NRPE) consumption in a residential building. Results indicate that for the Dutch case study NRPE consumption appears to be most sensitive to factors characterizing measures associated with net electricity demand reduction, namely, installation of PV and EES. The effects of corresponding factors, specifically, area available for PV installation and EES capacity, have pronounced though nonlinear effect on reducing yearly NRPE consumption.

Particularly, installing PV capacity, that is needed to generate the equivalent of 75% of yearly electricity demand, and EES capacity, that corresponds to 0.5 average days of autonomy, alone can reduce NRPE consumption by 20-25% for a case study. The respective PV and EES

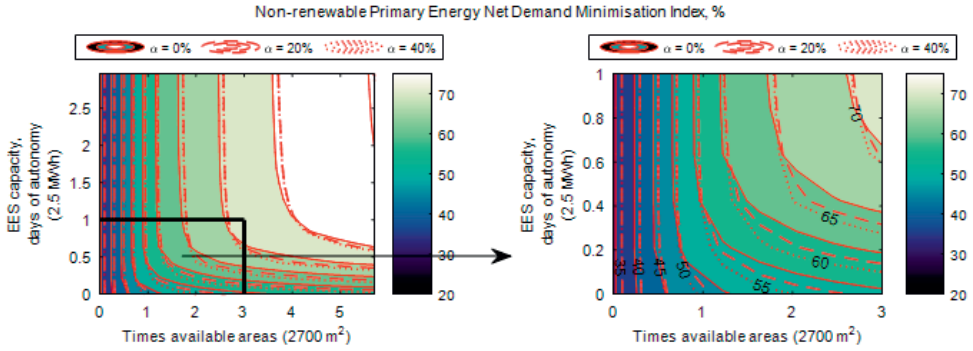

Figure 5.10: Response surface of $nDMI_E$ (in a vicinity of the "knee" point) illustrating its dependence on A_{PV}, Q_{EES} and α^d for $U_{env} = 0.97 Wm^{-2}K^{-1}$.

capacity values represent the thresholds or "knees", such that further capacity increase above these values corresponds to plateauing of the yearly NRPE consumption. This is in contrast with linear effects of the passive measures associated with net heating demand reduction, namely, installing energy efficient boilers and improving building envelope insulation. Consequently, the increase in NRPE savings, associated with the latter factors, is not subject to diminishing returns and is not affected by other measures. Accordingly, increasing boiler efficiency from 70% to 95% and improving building envelope insulation from 1.67 $Wm^{-2}K^{-1}$ to $0.97 Wm^{-2}K^{-1}$ reduces net NRPE demand by an additional 24%. Introducing a heat pump brings about additional 10% NRPE savings and greywater heat recovery – additional 5% NRPE savings.

In fact, the high impact of the evaluated measures, associated with net electricity demand reduction, is partially due to the fact, that the electricity mix in the Netherlands is dominated by non-renewable energy sources, which accounted for 87.5% of gross electricity generation in 2015. Therefore, each unit of power not consumed from the grid translates into 2.24 units of NRPE savings. This gives high weight to the measures that reduce net electricity demand when calculating the reduction in NRPE consumption. For the same reason installing a heat pump only results in reducing NRPE consumption by about 10% on top of savings achieved by other measures (Figure 5.8). Clearly, for countries with larger renewable energy shares in the electricity mix or colder winters, the benefits associated with the measures, that directly reduce net heating demand, should be more substantial. Authors in [150] showed that for a multi-family house in Sweden, where the renewable energy share in the electricity mix accounts for 55%, installing an exhaust air heat pump alone would reduce non-renewable energy consumption by 23%. Whereas with additional net-heating-demand-reducing measures (improving facade, roof and window insulation from 0.60, 0.60 and 2.58-2.72 to 0.26, 0.15 and 1.22-1.38 $Wm^{-2}K^{-1}$, respectively, as well as reducing hot water use from 53 to 39 $Lpers^{-1}day^{-1}$ non-renewable energy consumption could be reduced by up to 56%.

The predictions based on simulation results are prone to uncertainty, largely associated with the uncertainty in energy consumer behavior after implementing the energy saving modification. Behavioral changes, associated with technological modifications of the energy systems, can decrease or even counteract the effects of energy-saving technologies, and eventually lead to overall increase in energy consumption. Such phenomenon has been pointed out by a number of authors [151, 152, 153] and is known as the rebound effect. The magnitude of these effects is highly uncertain and depends on, e.g., financial gains from savings, elasticity of energy demand, satiation or physical as well as time limitations associated with energy use [152]. On the other hand, flexibility in energy consumer behavior can also amplify the effect of energy-saving technologies, if the energy consumers can be persuaded to time their activities such as to reduce the mismatch between the demand and renewable supply. Again, the extent of this flexibility is highly uncertain. It is, however, possible to assess the sensitivity of the NRPE savings with respect to this flexibility. In this work we observed that if residents can be persuaded to shift maximum of 20-40% of electricity load to different time slots during the day, the "knee" NRPE savings can be achieved with 20% lower battery capacity, compared to a situation without load-shifting. This is a noteworthy improvement, considering high costs of battery storage both in terms of money [78] and embodied energy [154].

Whereas demand-side measures can help to reduce battery capacity requirements via reducing the daily demand-supply mismatch, they do not address the seasonal demand-supply mismatch. The latter can be addressed by providing more storage capacity or by introducing additional renewable energy sources, that are characterized by less pronounced seasonal supply intermittency compared to solar.

Thermal energy is commonly stored in the underground aquifers or boreholes coupled with a ground source heat pump as seasonal thermal energy storage [155, 156]. Electrical energy can be stored over the seasons in the form of either potential energy, as in pumped hydro installations or the energy of the chemical bonds, as in hydrogen or biogas storage [157]. Pumped hydro installations require adequate elevation and water supply, and, therefore, their use is often restricted. On the other hand, chemical electricity storage is characterized by low round-trip efficiency (around 30% for hydrogen storage and substantial capital investments (around 2000 $\$/kW$ capital and replacement costs for electrolyzer, 3000 $\$/kW$ capital and replacement costs for hydrogen fuel cell, 1500 $\$/kg$ of hydrogen gas for hydrogen storage tank, and 1000 $\$/kW$ capital and replacement costs for converter [158]). Seasonal storage capacity requirements can be reduced by increasing the share of wind energy in the electricity mix, as, unlike solar, wind power generation peaks at winter. Nevertheless, local installation of roof-top wind turbines in the area of the case-study, characterized by average wind speeds of 3.6 m/s (at 10m height), was ruled out during the early stages of this study as an option with low potential (see section 5.4.2). Efficient implementation of wind power can, nevertheless, be possible at a larger scale. Larger scale technology evaluation falls out of scope of the present study, but evidently represents a vast interest for future research.

5.6 Conclusions

In this study we used response surface methodology to compare combinations of building-scale technological and behavioral measures in terms of non-renewable primary energy (NRPE) consumption, and to study the effects of individual measure, by characterizing factors on NRPE consumption in Dutch residential building.

This study showed that non-renewable primary energy (NRPE) consumption in a Dutch residential building is most effectively reduced by implementing measures that affect electricity consumption, namely, installation of PV and electrical energy storage. The effect of these measures, however, is nonlinear, meaning that substantial reduction in NRPE consumption is not evident above certain limits for PV and battery capacity. Specifically, in our case-study, a PV capacity corresponding to the area, needed to generate 75% of the yearly electricity demand (150% of the practically available area), and battery capacity, corresponding to 0.5 days of autonomy, were identified as viable limits. Installing specified PV and battery capacities alone reduces NRPE consumption in this case study by up to 20-25%. Greywater heat recovery reduces NRPE consumption by an additional 5%. Additional improvement of insulation (from 1.67 $Wm^{-2}K^{-1}$ to 0.97 $Wm^{-2}K^{-1}$), gas boiler efficiency (from 70% to 95%), further reduces NRPE consumption up to 50-55%. Additional installation of a heat pump further reduces NRPE consumption up to 60% for the same PV and battery storage capacity values.

We also showed that flexibility in electricity demand allows to achieve the same NRPE savings at lower battery storage capacities, thus contributing to reducing the embedded primary energy and capital costs of the system. Specifically we showed that, if the residents can be persuaded to shift maximum of 20-40% of the electricity load to a different time slot during the day, the same 60% reduction in NRPE consumption can be achieved with battery capacity corresponding to 0.4 days of autonomy, resulting in 20% required battery capacity reduction. Considering high costs of battery storage in terms of price and embodied energy, these results highlight the importance of non-technological changes for the transition towards fossil-free energy systems.

In our case study, the high contribution of measures associated with the electricity use rather than measures associated with thermal energy use is partially due to the fact, that the electricity mix in the Netherlands is currently dominated by non-renewable energy sources (87.5% of gross electricity generation in 2015 [37]). Therefore, each unit of power not consumed from the grid translates into 2.24 units of NRPE savings.

Chapter 6

Discussion, Conclusions and Future Research

In this closing chapter a summary of the main contributions of this thesis, and the answers to the research questions is provided (Section 6.1). Next, a synthetic discussion is given on the main findings and conclusions of this research (Section 6.2), followed by a reflection on limitations of this work (Section 6.3). Finally, some recommendations for future research are presented (Section 6.4).

6.1 Contributions

Along with large scale integration of renewable energy resources with variable power production and unpredictable nature, it is becoming increasingly important to harness the flexibility that is embedded in the demand side of the energy value chain. A key issue in assessing the potential value of flexibility as such, is data uncertainty. Consequently, there is a need for defining a flexibility assessment framework to investigate the impact of data uncertainty on the performance and operation of different stakeholders in future energy systems with flexible resources. Data uncertainty mainly results from absence of historical data, and/or inaccurate forecasts. In the context of this thesis, we specifically looked into the impact of data uncertainty on the performance of an aggregator (as the main operator of DR programs in the future) and the DSO (as the main operator of distribution grids). Subsequently, the main contributions of this thesis are as follows:

6.1.1 Sensitivity Analysis Framework

A comprehensive framework is devised to assess the sensitivity of a hypothetical energy system with flexible sources to uncertain and inaccurate data. The sensitivity analysis framework consists of three modules: a simulation module, a local sensitivity analysis (LSA), and a global sensitivity analysis (GSA). The sensitivity analysis framework is used to identify the relative importance of the uncertain parameters and input data.

Several mathematical models are used in this thesis to simulate a hypothetical energy system that harnesses the flexibility available from the demand side of the distribution grid. Such models are formulated as optimization problems, and reflect physical characteristics of the energy system under study, as well as the requirements of the actors in that system. The simulation module is designed to run simulations on the mathematical models given a subset of the historical input data.

When historical data is not available, or the model parameters vary extensively, scenarios are developed and evaluated. The GSA module provides a framework to define scenarios on the given range of the uncertain parameter, and systematically evaluate and compare the variation in the results of the optimization problem. The results of GSA are used to identify the dependency of the simulation model output to each of the uncertain parameters.

On the other hand, when there is limited uncertainty in the input data, LSA is used. The LSA module provides an analytical framework by taking partial derivatives of the objective function

and the Karush–Kuhn–Tucker (KKT) equations of the optimization problem with respect to the uncertain inputs. One should note that, consequently, the LSA framework requires continuity and differentiability of the optimization problem formulated in the simulation module.

6.1.2 Flexibility Assessment Framework for a Demand Response (DR) Program

A continuous optimization problem is formulated to simulate load shifting of residential consumers for an aggregator, as future DR operator. The optimization problem aims to minimize daily load variation, without enforcing excessive cost to the flexibility providers. The proposed framework reflects the preferences of the flexible consumers using two variables: the amount of load that the flexible consumers are willing to reduce (downward flexibility α^d), and the time interval within which flexible consumers are willing to shift their load (load shifting time window ω^{tt}). One important feature of the proposed optimization problem is that, under certain assumptions, it ensures that the objective of the system operator can be reached without modelling the distribution grid.

The proposed optimization framework enables aggregators to evaluate the performance of a hypothetical DR program under data uncertainty. Two sources of data uncertainty were considered: load and price forecast errors, and flexibility preferences of the consumers. The LSA module in the Flexibility Assessment Framework was used to investigate the sensitivity of the performance of the proposed DR program in reducing load variability to load and price forecast error. An analytical expression was derived for the sensitivities, and from there, computed the local sensitivities. In addition, using the GSA module, first, various scenarios on the preferences of the flexibility providers were defined. Then, we compared the optimal value of the variance of daily load, and identified the dependency of the DR model to the preferences of flexibility providers (α^d and ω^{tt}).

6.1.3 Error-free optimal flexibility dispatch (OFD) framework

A novel bi-level optimization framework was devised to solve the optimal flexibility dispatch (OFD) problem (Chapter 4). The proposed OFD framework determines the amount of flexibility system operator needs to procure from the flexible resources available on the demand side, and its associate price. The OFD problem is formulated as an optimal power flow based optimization problem that seeks to minimize the cost of the curtailing the RES, while keeping the distribution gird congestion free. To account for non-linearities of AC power flow, second-order cone (SOC) relaxation of the AC power flow is used that was used in the OFD problem (SOC-OFD). The novelty of the proposed optimization problem is in the bi-level structure which seeks to minimize the SOC relaxation error in the upper level (UL), while solving the SOC-OFD problem in the lower level (LL) problem. One complexity in solving bi-level optimization problems is dealing with non-linear complementarity constraints. To reduce this complexity, and make the problem tractable for large networks, I reduced the number of complementarity constraints by shifting the non-binding constraints from the lower level (LL) to the upper level

(UL) problem. Furthermore, a practical relaxation technique is used to relax the rest of the complementarity constraints. As a result of such relaxation, the final problem is a non-linear optimization problem that can be solved by available solvers.

The inputs to the OFD problem include forecasts on active power demand and flexibility ranges of the flexible buses. To investigate how sensitive the decision of the system operator is to the forecast errors of each bus, the analytical sensitivity matrix by perturbing the objective function and the KKT conditions of the reduced LL problem was derived.

6.1.4 Building's Energy Efficiency Assessment

In Chapter 5 a comprehensive framework is proposed to simulate the energy consumption of a residential building. The proposed framework consists of four modules: water, water heating, space heating, and electricity. Each module accounts for water and energy balances, as well as auxiliary algebraic relations that characterize each unit. Such formulation allows us to investigate the combined effects of, and the interactions between, the technological and demand side management measures affecting electrical and thermal energy demand of a building.

Global sensitivity analysis was performed to investigate the impact of uncertain parameters on the total energy demand of the building. Feasible combinations of technological modifications are defined in various scenarios (referred to as configurations). One of the main contributions of this framework is in using second-order polynomial regression to determine the sensitivity of building's energy consumption to uncertain parameters in each configuration. Such analysis is then used to identify the most dominant factor in improving building's energy efficiency.

6.2 Main Findings: Insights on Future Energy Systems with Flexibility Resources

The proposed sensitivity analysis framework was used to gain insight into the future distribution grid with flexible resources at the demand side. Special attention was paid to how the results of the models, used to simulate future energy systems, change under data uncertainty. Figure 6.1 presents an overview of the present and future energy systems, as well as the point of view of the actor considered in this thesis. In this regard, the following findings are of importance:

6.2.1 Performance of a DR program in reducing daily load variability has a non-linear relationship with the available flexibility.

Using 20 different scenarios on different preferences of flexibility providers, the results of Chapter 2 and 3 show that the performance of a DR program in reducing load variability has a strong, and non-linear relationship with the amount of flexibility that flexible consumers are willing to offer. One can conclude that when the flexible load is scarce, offering wider load shifting time window (ω^{tt}) has low impact on reducing the variations of the daily load profile.

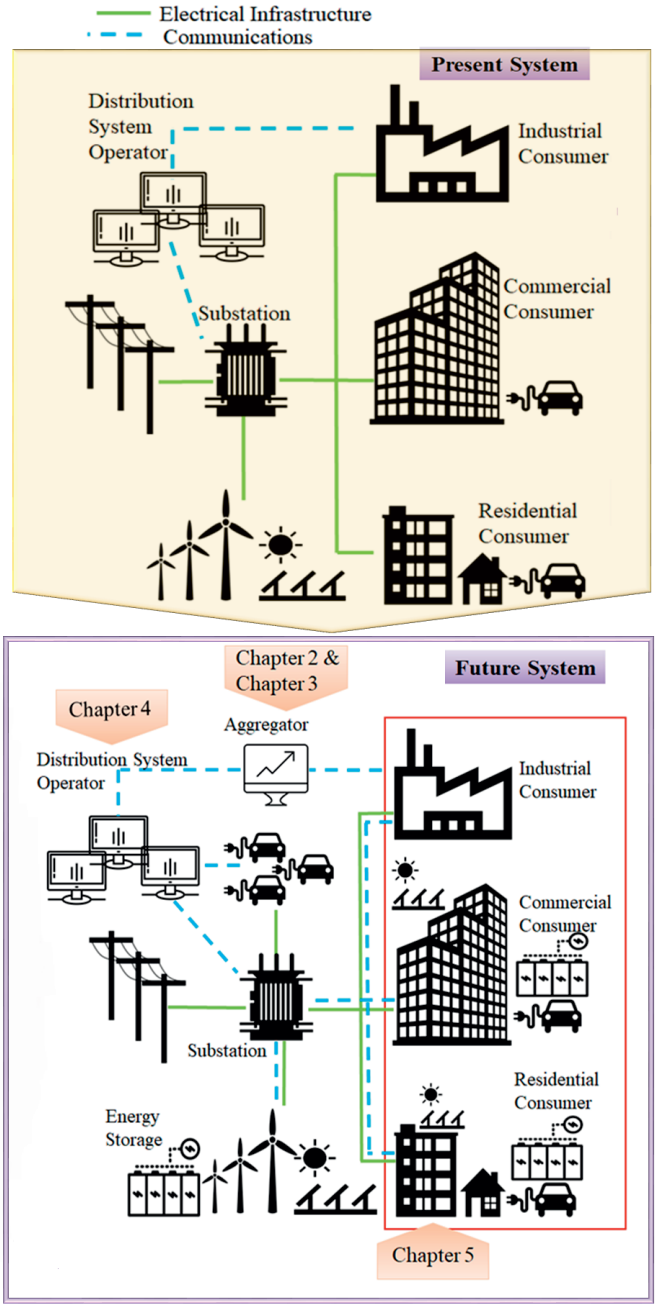

Figure 6.1: Overview of the present and future energy system (upper and lower part), and the perspective of Chapters 2, 3, 4, and 5 in this thesis.

In a similar way, when flexible consumers allow limited time window to shift their flexible load, offering larger amount of flexible load (α^d) does not necessarily lead to a lower variance of daily load, and subsequently, does not result in a flatter load profile. This observation can help the DR operators in their financial agreements with the DR providers, to engage in contracts with the flexibility providers based on their effective contribution in a DR program, although they might be offering very large amount flexibility. Moreover, DR operators can consider combinations of load reduction (α^d) and load shifting time window (ω^{tt}) in their contracts with the DR providers such that the same performance of the DR program is reached.

6.2.2 Performance of a DR program is significantly sensitive to inaccurate forecast.

Chapter 3 shows that small errors in load and price forecast can cause significant perturbations in the output of a DR program. Such perturbations depend on the load profile, and are larger during peak hours. In addition, when there is no limit on the load shifting time window (ω^{tt}), the DR operator need higher accuracy in load forecast of the evening peak hours when the available shiftable load (α^d) is scarce. In a similar way, DR operators can benefit from higher accuracy in price forecast of evening peak hours when DR providers offer large amount of flexible load. Such analysis can help the DR operators, to identify the preferences of the flexibility providers that result in large deviations from the optimal performance of a DR program when there is data uncertainty.

6.2.3 Locational flexibility prices are sensitive to forecast errors in active power demand and flexibility limit of the DR providers.

The comparison between the results of the proposed bi-level optimal flexibility dispatch framework, with the results of the SOC-OFD model, shows that the bi-level-OFD model can effectively reduce the SOC-relaxation error, and therefore, yield solutions which have physical interpretation.

In addition, the results of Chapter 4 show that, in general, locational flexibility prices (LFP) are sensitive to errors in active power demand forecast, and upper and lower bound of flexibility of the flexible buses. Particularly, errors in active power forecast of the load buses (i.e., buses with no flexible unit) has larger impact on the formation of LFPs. Similarly, upper and lower flexibility bounds of the flexible buses (i.e., buses with flexible units) has a larger impact on the formation of the LFPs.

The results provided from the local sensitivity analysis depend on the configuration of the network under study. However, the DSO can use the local sensitivity analysis technique to determine which buses has the most prominent impact on deviations from optimal flexibility dispatch and the optimal LFPs of the other buses in the network. Such analysis enables the DSO to take necessary actions to prevent unintentional deviations from the optimal values, and therefore, ensure the economic efficiency of the resulted flexibility dispatch in practice.

6.2.4 Net building's energy consumption has a non-linear relationship with the installed PV capacity and electrical energy storage.

Chapter 5 shows that non-renewable primary energy (NRPE) consumption in a Dutch residential building is most effectively reduced by implementing measures that affect electricity consumption, namely, installation of PV and electrical energy storage. The effect of these measures, however, is nonlinear, meaning that substantial reduction in NRPE consumption is not evident above certain limits for PV and battery capacity. Moreover, flexibility in electricity demand allows to achieve the same NRPE savings at lower battery storage capacities, thus contributing to reducing the embedded primary energy and capital costs of the system. Considering high costs of battery storage in terms of price and embodied energy, these results highlight the importance of non-technological changes for the transition towards fossil-free energy systems. In other words, proactive consumers aware and willing to contribute to load shifting, i.e. contributing to the systems flexibility, can have a major contribution in transition towards sustainable urban energy systems.

6.3 Reflection on Assumptions, Potentials and Limitations

The analysis presented in this thesis are based on simplifying assumptions and selection of input data. In this section, the potential implications and limitations of the results of this thesis are elaborated. Specifically, a reflection on how the assumptions used in the model design might have affected the conclusions is provided.

6.3.1 Objective Function of the DR Program

The objective function of the load-shifting problem (presented in Chapters 2 and 3) is minimizing the variations of daily load profile. The selected objective function helps the system operator to manage network congestion by reducing peak load, without enforcing excessive cost on flexible consumers. The assumed objective function allows for derivation of a variety of useful results that shed light on the value of a potential DR in solving network problems, as well as its limitations associated with preferences of flexibility providers. However, using the same framework, one can consider an alternative objective for the DR program, including but not limited to, maximizing the utility of the consumers during the specified time horizon [159], maximizing the profit of the DR aggregators [160].

6.3.2 Preferences of Flexibility Providers

Preferences of flexibility providers on the amount of load they allow the system operator to reduce and the time window within which they allow the load to be shifted (i.e., α^d and ω^{tt}, respectively), are assumed to be constant at all time units during one simulation period.

While such assumption reduces the size of the variable space, and therefore, allows for a comprehensive global sensitivity analysis, it ignores the dependency of α^d and ω^{tt} on the time of the day. In an extensive analysis, based on surveys gathered through choice experiment, authors in [161] show that in addition to the type of service, consumers willingness to provide flexibility varies over the time of the day. In case of considering time dependency of consumers' preferences, which includes assigning a daily profile to the two parameters α^d and ω^{tt}, the same methodology can be used to solve the optimization problem and perform the local sensitivity analysis. However, global sensitivity analysis would become challenging as the number of input parameters increases. The results presented in this thesis can be used as the first step to identify the most sensitive hours, and then perform in depth analysis per hour.

In addition to time dependency, flexibility preferences can vary over different consumer type. The results provided in Chapters 2 and 3 correspond to a special case of a load profile, which includes only the residential consumers as DR providers. However, the proposed framework is generic and can be employed for analyzing other consumer types (i.e., commercial and industrial). In that case, different ranges of flexibility should be used for various consumer types.

6.3.3 Sensitivity Analysis Framework

The local sensitivity analysis framework used in this thesis is based on the assumption that all perturbations are in the feasible perturbations set, such that active inequality constraints remain active such that the framework has the same active constraints as the initial problem after the perturbation. However, one can consider moving within the feasible region by allowing the active inequality constraints to be allowed to become inactive after perturbation. In that case, further analysis is required to determine the cone representation of feasible perturbations [162], and from there, determine the existence of directional derivatives.

The local sensitivity analysis framework used in this thesis is based on deriving the KKT conditions of the optimization problem, and therefore, requires that the optimization problem is differentiable. For that reason, the factors which would make the problem mixed-integer were neglected.

6.3.4 Optimal Flexibility Dispatch Framework

The objective of the optimal flexibility dispatch problem is to minimize the cost of curtailing the distributed energy sources. The selected objective function supports the DSO to promote integration of renewable energy sources in the distribution grid. As a result, the DER buses are paid accordingly when providing flexibility services (see Chapter 4). On the other hand, the flexible load buses are reimbursed only when they provide flexibility at their maximum flexibility bound. Such situation is due to the underlying assumption of allowing load curtailment at no cost. Note that, although the results presented in this work correspond to the specific objective function and the underlying assumptions, the proposed model and the

analytical discussion is entirely generic. As a result, the framework can be applied when considering other objectives of the DSO.

The reformulation of the bi-level-OFD problem, used to reduce the number of complementarity constraints in the lower level problem, requires that the dual variable of the constraint to be shifted equals zero. In this regard, I assumed that the shifted constraints were not binding, and therefore, their associated dual variables are zero, which was then confirmed by the simulation results. However, in cases that the results show that the shifted constraints are binding, one needs to keep the binding constraint in the lower level and solve the newly formed reduced problem again.

6.4 Recommendations for Future Work

The work presented in this thesis provides theoretical background for analyzing the need for flexibility, in the operation of urban energy system that is organized in a competitive setting. The analytical part of the proposed methodologies lays the basis for investigating the economic impact of data uncertainty, on DR providers, the DSO and pro-active energy consumers and thereof, the operational decision they make. The result of this work provides projections on the financial potentials that deemed necessary when engaging in contractual agreement with other parties. The recommendations for future work listed below involves possible applications and improvements of this work.

6.4.1 Emergence of Opportunistic Participants

The emergence of different setting of competitive energy trading frameworks at the local (retail) market level (e.g., centralized market [86, 163] vs. distributed [164]) is changing the face of energy systems. From the participants view, it leads to higher exposure of various stakeholders (i.e., market participants) such as pro-active energy consumers and DR providers to risks associated with short- and long-term uncertainties. For instance, the absence of an adequate regulatory framework especially in the short-run can encourage opportunistic participants to exercise strategic behavior. Regardless of the market setting considered, such behaviors can significantly influence the operation of the local energy market and from there, the decision making process of both strategic and competitive participants. In this view, a direct extension of the current work could be to investigate sensitivity of a flexibility program determined by a DR provider, or the DSO, to exercising such strategic behavior by e.g., a set of flexibility providers and/or aggregators, under various market settings.

6.4.2 Non-compliance of Flexibility Providers

A key assumption that is made in the context of this research is that once the flexibility program is determined (by DR operator or the DSO) the flexibility providers will be fully compliant with the program. This implies that the flexibility program will be implemented

exactly as is determined by DR operator or the DSO. However, due to forecast inaccuracies and the occurrence of unprecedented events, there is always a risk of uncertainty associated with intended and unintended deviations in the execution of the accepted flexibility programs. Such deviations could also be known after the closure of the DR program (or the OFD). However, their impact could be studied and accounted for when assessing the robustness of the optimal flexibility program, well in advance. Consequently, another extension of this work is to investigate the impact of uncertainty of (un)intentional deviations resulted from the consumers' non-compliance to their flexibility schedule, on the optimal flexibility program and formation of flexibility prices.

6.4.3 Stochastic Analysis of Uncertainty

Data uncertainty corresponds to lack of knowledge regarding the value of input variables that play a predominant role in decision making process i.e., determining the functional state of the power system in the future. Uncertainty in some input data can be describable through probability distribution functions (PDFs). Such data are not considered in the scope of this research. However, they include a wide range of input data in the real-world applications. Therefore, another avenue for research will be to make use of rigorous analytical techniques to analyze the existing historical load and price data to obtain the PDFs describing the stochastic characteristics of the data [33]. As outlined before, such PDFs can later be used to carry out uncertainty analysis i.e., to quantify the variability of the performance of DR program in the future by producing a plausible sets of scenarios such that the stochastic nature of the unknown input variables are properly represented in the analysis. The outcome of such analysis can be complementary to the analysis presented in this thesis.

6.4.4 Sector Integration on the Demand-side

It is anticipated that two third of the world's population will be living in cities by the year 2050 [165]. In parallel with the rapid urbanization, various sectors including, water, energy are becoming increasingly interconnected [166]. This is generally referred to water-energy-nexus [167, 168]. This shift has called for more complex models that accounts for the dynamics of one sector, when studying the other one. In this thesis the limited interaction between water and energy system at building level is briefly touched upon in 5. It would be interesting to revise the proposed sensitivity analysis framework and include various urban resources including energy and water systems at the distribution level. Such framework can then be sued to study the sensitivity of e.g., consumers preferences on the operation of an integrated energy and water market, especially in a distributed market setting (i.e., peer-to-peer markets).

References

[1] J. Powell, "Scientists reach 100% consensus on anthropogenic global warming," *Bulletin of Science, Technology & Society*, vol. 37, no. 4, pp. 183–184, 2017.

[2] A. Arneth, H. Barbosa, T. Benton, K. Calvin, E. Calvo, S. Connors, A. Cowie, E. Davin, F. Denton, and R. van Diemen, "Ipcc special report on climate change, desertification, land degradation, sustainable land management, food security, and greenhouse gas fluxes in terrestrial ecosystems," *Technical report, Intergovernmental Panel on Climate Change*, 2019.

[3] A. Herold, V. Cook, Y. Baron, M. Cames, S. Gores, J. Graichen, P. Kasten, G. Mehlhart, A. Simons, C. Urrutia, *et al.*, "Eu environment and climate change policies," *Policy Department for Economic, Scientific and Quality of Life Policies, European Parliament, Luxembourg*, 2019.

[4] G. Boyle, *Renewable energy*. Open University., 2004.

[5] H. Scorah, A. Sopinka, and G. C. van Kooten, "The economics of storage, transmission and drought: integrating variable wind power into spatially separated electricity grids," *Energy Economics*, vol. 34, no. 2, pp. 536 – 541, 2012.

[6] D. Azari, S. S. Torbaghan, M. Gibescu, and M. A. van der Meijden, "The impact of energy storage on long term transmission planning in the north sea region," in *North American Power Symposium (NAPS), 2014*, pp. 1–6, IEEE, 2014.

[7] M. G. Molina, "Distributed energy storage systems for applications in future smart grids," in *2012 Sixth IEEE/PES Transmission and Distribution: Latin America Conference and Exposition (T D-LA)*, pp. 1–7, Sep. 2012.

[8] I. Atzeni, L. G. Ordóñez, G. Scutari, D. P. Palomar, and J. R. Fonollosa, "Demand-side management via distributed energy generation and storage optimization," *IEEE Transactions on Smart Grid*, vol. 4, no. 2, pp. 866–876, 2012.

[9] M. Alam, K. Muttaqi, and D. Sutanto, "Mitigation of rooftop solar pv impacts and evening peak support by managing available capacity of distributed energy storage systems," *IEEE transactions on power systems*, vol. 28, no. 4, pp. 3874–3884, 2013.

[10] G. Brusco, A. Burgio, D. Menniti, A. Pinnarelli, and N. Sorrentino, "Energy management

system for an energy district with demand response availability," *IEEE Transactions on Smart Grid*, vol. 5, no. 5, pp. 2385–2393, 2014.

[11] J. M. Morales, A. J. Conejo, H. Madsen, P. Pinson, and M. Zugno, "Managing uncertainty with flexibility," in *Integrating Renewables in Electricity Markets*, pp. 137–171, Springer, 2014.

[12] P. D. Lund, J. Lindgren, J. Mikkola, and J. Salpakari, "Review of energy system flexibility measures to enable high levels of variable renewable electricity," *Renewable and Sustainable Energy Reviews*, vol. 45, pp. 785–807, 2015.

[13] P. Palensky and D. Dietrich, "Demand side management: Demand response, intelligent energy systems, and smart loads," *IEEE transactions on industrial informatics*, vol. 7, no. 3, pp. 381–388, 2011.

[14] P. Pinson, H. Madsen, *et al.*, "Benefits and challenges of electrical demand response: A critical review," *Renewable and Sustainable Energy Reviews*, vol. 39, pp. 686–699, 2014.

[15] J. Naus, B. J. van Vliet, and A. Hendriksen, "Households as change agents in a dutch smart energy transition: On power, privacy and participation," *Energy Research & Social Science*, vol. 9, pp. 125–136, 2015.

[16] D. P. Kaundinya, P. Balachandra, and N. H. Ravindranath, "Grid-connected versus stand-alone energy systems for decentralized power—a review of literature," *Renewable and Sustainable Energy Reviews*, vol. 13, no. 8, pp. 2041–2050, 2009.

[17] F. Gangale, A. Mengolini, and I. Onyeji, "Consumer engagement: An insight from smart grid projects in europe," *Energy Policy*, vol. 60, pp. 621–628, 2013.

[18] S. E. Collective, "An introduction to the universal smart energy framework," *Arnhem, The Netherlands*, vol. 1, 2014.

[19] S. Pfenninger, A. Hawkes, and J. Keirstead, "Energy systems modeling for twenty-first century energy challenges," *Renewable and Sustainable Energy Reviews*, vol. 33, pp. 74–86, 2014.

[20] R. Banos, F. Manzano-Agugliaro, F. Montoya, C. Gil, A. Alcayde, and J. Gómez, "Optimization methods applied to renewable and sustainable energy: A review," *Renewable and sustainable energy reviews*, vol. 15, no. 4, pp. 1753–1766, 2011.

[21] J. Keirstead, M. Jennings, and A. Sivakumar, "A review of urban energy system models: Approaches, challenges and opportunities," *Renewable and Sustainable Energy Reviews*, vol. 16, no. 6, pp. 3847–3866, 2012.

[22] H.-G. Beyer and B. Sendhoff, "Robust optimization–a comprehensive survey," *Computer methods in applied mechanics and engineering*, vol. 196, no. 33-34, pp. 3190–3218, 2007.

[23] D. E. Majewski, M. Wirtz, M. Lampe, and A. Bardow, "Robust multi-objective

optimization for sustainable design of distributed energy supply systems," *Computers & Chemical Engineering*, vol. 102, pp. 26–39, 2017.

[24] F. Pourahmadi, J. Kazempour, C. Ordoudis, P. Pinson, and S. H. Hosseini, "Distributionally robust chance-constrained generation expansion planning," *IEEE Transactions on Power Systems*, 2019.

[25] C. Wang, B. Jiao, L. Guo, Z. Tian, J. Niu, and S. Li, "Robust scheduling of building energy system under uncertainty," *Applied energy*, vol. 167, pp. 366–376, 2016.

[26] G. Liu, Y. Xu, and K. Tomsovic, "Bidding strategy for microgrid in day-ahead market based on hybrid stochastic/robust optimization," *IEEE Transactions on Smart Grid*, vol. 7, no. 1, pp. 227–237, 2015.

[27] M. Mazidi, H. Monsef, and P. Siano, "Robust day-ahead scheduling of smart distribution networks considering demand response programs," *Applied Energy*, vol. 178, pp. 929–942, 2016.

[28] G. Mavromatidis, K. Orehounig, and J. Carmeliet, "Uncertainty and global sensitivity analysis for the optimal design of distributed energy systems," *Applied Energy*, vol. 214, pp. 219–238, 2018.

[29] C. J. Hopfe, "Uncertainty and sensitivity analysis in building performance simulation for decision support and design optimization," *PhD diss., Eindhoven University*, 2009.

[30] E. Borgonovo and E. Plischke, "Sensitivity analysis: a review of recent advances," *European Journal of Operational Research*, vol. 248, no. 3, pp. 869–887, 2016.

[31] F. Ni, M. Nijhuis, P. H. Nguyen, and J. F. Cobben, "Variance-based global sensitivity analysis for power systems," *IEEE Transactions on Power Systems*, vol. 33, no. 2, pp. 1670–1682, 2017.

[32] A. Soroudi and T. Amraee, "Decision making under uncertainty in energy systems: State of the art," *Renewable and Sustainable Energy Reviews*, vol. 28, pp. 376–384, 2013.

[33] A. J. Conejo, M. Carrión, J. M. Morales, *et al.*, *Decision making under uncertainty in electricity markets*, vol. 1. Springer, 2010.

[34] G. Kariniotakis, *Renewable Energy Forecasting: From Models to Applications*. Woodhead Publishing, 2017.

[35] H. Madsen, H. A. Nielsen, P. Pinson, P. Bacher, and L. Allé, "Forecasting wind and solar power production," *Research Thesis, Technical University of Denmark*, 2011.

[36] H. Chitsaz, H. Shaker, H. Zareipour, D. Wood, and N. Amjady, "Short-term electricity load forecasting of buildings in microgrids," *Energy and Buildings*, vol. 99, pp. 50–60, 2015.

[37] H.-x. Zhao and F. Magoulès, "A review on the prediction of building energy consumption," *Renewable and Sustainable Energy Reviews*, vol. 16, no. 6,

pp. 3586–3592, 2012.

[38] P. G. Da Silva, D. Ilic, and S. Karnouskos, "The impact of smart grid prosumer grouping on forecasting accuracy and its benefits for local electricity market trading," *IEEE Transactions on Smart Grid*, vol. 5, no. 1, pp. 402–410, 2014.

[39] M. Beaudin and H. Zareipour, "Home energy management systems: A review of modelling and complexity," *Renewable and Sustainable Energy Reviews*, vol. 45, pp. 318–335, 2015.

[40] C. J. Bennett, R. A. Stewart, and J. W. Lu, "Forecasting low voltage distribution network demand profiles using a pattern recognition based expert system," *Energy*, vol. 67, pp. 200–212, 2014.

[41] K. Pan, A. Teixeira, M. Cvetkovic, and P. Palensky, "Cyber risk analysis of combined data attacks against power system state estimation," *IEEE Transactions on Smart Grid*, vol. 10, no. 3, pp. 3044–3056, 2018.

[42] S. C. Müller, H. Georg, J. J. Nutaro, E. Widl, Y. Deng, P. Palensky, M. U. Awais, M. Chenine, M. Küch, M. Stifter, *et al.*, "Interfacing power system and ict simulators: Challenges, state-of-the-art, and case studies," *IEEE Transactions on Smart Grid*, vol. 9, no. 1, pp. 14–24, 2016.

[43] D.-H. Choi and L. Xie, "A framework for sensitivity analysis of data errors on home energy management system," *Energy*, vol. 117, pp. 166–175, 2016.

[44] G. Liang, J. Zhao, F. Luo, S. R. Weller, and Z. Y. Dong, "A review of false data injection attacks against modern power systems," *IEEE Transactions on Smart Grid*, vol. 8, no. 4, pp. 1630–1638, 2017.

[45] X. Chen and A. N. Kleit, "Money for nothing? why ferc order 745 should have died.," *Energy Journal*, vol. 37, no. 2, 2016.

[46] A. Albert and R. Rajagopal, "Smart meter driven segmentation: What your consumption says about you," *IEEE Transactions on Power Systems*, vol. 28, no. 4, pp. 4019–4030, 2013.

[47] M. Pipattanasomporn, M. Kuzlu, S. Rahman, and Y. Teklu, "Load profiles of selected major household appliances and their demand response opportunities," *IEEE Transactions on Smart Grid*, vol. 5, no. 2, pp. 742–750, 2014.

[48] J. L. Mathieu, D. S. Callaway, and S. Kiliccote, "Examining uncertainty in demand response baseline models and variability in automated responses to dynamic pricing," in *Decision and Control and European Control Conference (CDC-ECC), 2011 50th IEEE Conference on*, pp. 4332–4339, IEEE, 2011.

[49] W. Wei, F. Liu, and S. Mei, "Energy pricing and dispatch for smart grid retailers under demand response and market price uncertainty," *IEEE transactions on smart grid*, vol. 6, no. 3, pp. 1364–1374, 2015.

[50] S. Klein, W. Beckman, J. Mitchell, J. Duffie, N. Duffie, T. Freeman, J. Mitchell, J. Braun, B. Evans, J. Kummer, *et al.*, "Trnsys 16–a transient system simulation program, user manual," *Solar Energy Laboratory. Madison: University of Wisconsin-Madison*, 2004.

[51] D. B. Crawley, L. K. Lawrie, F. C. Winkelmann, W. F. Buhl, Y. J. Huang, C. O. Pedersen, R. K. Strand, R. J. Liesen, D. E. Fisher, M. J. Witte, *et al.*, "Energyplus: creating a new-generation building energy simulation program," *Energy and buildings*, vol. 33, no. 4, pp. 319–331, 2001.

[52] S. W. Wallace, "Decision making under uncertainty: Is sensitivity analysis of any use?," *Operations Research*, vol. 48, no. 1, pp. 20–25, 2000.

[53] R. Yin, E. C. Kara, Y. Li, N. DeForest, K. Wang, T. Yong, and M. Stadler, "Quantifying flexibility of commercial and residential loads for demand response using setpoint changes," *Applied Energy*, vol. 177, pp. 149–164, 2016.

[54] N. Good, L. Zhang, A. Navarro-Espinosa, and P. Mancarella, "High resolution modelling of multi-energy domestic demand profiles," *Applied Energy*, vol. 137, pp. 193–210, 2015.

[55] I. Richardson, M. Thomson, and D. Infield, "A high-resolution domestic building occupancy model for energy demand simulations," *Energy and buildings*, vol. 40, no. 8, pp. 1560–1566, 2008.

[56] E. C. Kara, M. D. Tabone, J. S. MacDonald, D. S. Callaway, and S. Kiliccote, "Quantifying flexibility of residential thermostatically controlled loads for demand response: a data-driven approach," in *Proceedings of the 1st ACM Conference on Embedded Systems for Energy-Efficient Buildings*, pp. 140–147, ACM, 2014.

[57] G. W. Hart, "Nonintrusive appliance load monitoring," *Proceedings of the IEEE*, vol. 80, no. 12, pp. 1870–1891, 1992.

[58] E. Mocanu, P. H. Nguyen, and M. Gibescu, "Energy disaggregation for real-time building flexibility detection," in *Power and Energy Society General Meeting (PESGM), 2016*, pp. 1–5, IEEE, 2016.

[59] D. He, W. Lin, N. Liu, R. G. Harley, and T. G. Habetler, "Incorporating non-intrusive load monitoring into building level demand response," *IEEE Transactions on Smart Grid*, vol. 4, no. 4, pp. 1870–1877, 2013.

[60] Z. Erkin, J. R. Troncoso-Pastoriza, R. L. Lagendijk, and F. Pérez-González, "Privacy-preserving data aggregation in smart metering systems: An overview," *IEEE Signal Processing Magazine*, vol. 30, no. 2, pp. 75–86, 2013.

[61] C. Zhao, J. Wang, J.-P. Watson, and Y. Guan, "Multi-stage robust unit commitment considering wind and demand response uncertainties," *IEEE Transactions on Power Systems*, vol. 28, no. 3, pp. 2708–2717, 2013.

[62] D. T. Nguyen and L. B. Le, "Risk-constrained profit maximization for microgrid aggregators with demand response," *IEEE Transactions on smart grid*, vol. 6, no. 1,

pp. 135–146, 2015.

[63] K. Akbari, M. M. Nasiri, F. Jolai, and S. F. Ghaderi, "Optimal investment and unit sizing of distributed energy systems under uncertainty: A robust optimization approach," *Energy and Buildings*, vol. 85, pp. 275–286, 2014.

[64] A. Ashouri, F. Petrini, R. Bornatico, and M. J. Benz, "Sensitivity analysis for robust design of building energy systems," *Energy*, vol. 76, pp. 264–275, 2014.

[65] S. Boyd, S. P. Boyd, and L. Vandenberghe, *Convex optimization*. Cambridge university press, 2004.

[66] S. A. Gabriel, A. J. Conejo, J. D. Fuller, B. F. Hobbs, and C. Ruiz, *Complementarity modeling in energy markets*, vol. 180. Springer Science & Business Media, 2012.

[67] B. Eldridge, R. O'Neill, and B. Hobbs, "Pricing in day-ahead electricity markets with near-optimal unit commitment," 2018.

[68] B. Colson, P. Marcotte, and G. Savard, "An overview of bilevel optimization," *Annals of operations research*, vol. 153, no. 1, pp. 235–256, 2007.

[69] H. v. Stackelberg *et al.*, "Theory of the market economy," 1952.

[70] H. D. Sherali, A. L. Soyster, and F. H. Murphy, "Stackelberg-nash-cournot equilibria: characterizations and computations," *Operations Research*, vol. 31, no. 2, pp. 253–276, 1983.

[71] A. Migdalas, P. M. Pardalos, and P. Värbrand, *Multilevel optimization: algorithms and applications*, vol. 20. Springer Science & Business Media, 2013.

[72] S. Dempe, "Foundations of bilevel programming, ser," *Nonconvex Optimization and Its Applications. Dordrecht, The Netherlands: Kluwer Academic Publishers*, vol. 61, 2002.

[73] I. I. Cplex, "V12. 1: User's manual for cplex," *International Business Machines Corporation*, vol. 46, no. 53, p. 157, 2009.

[74] A. J. Conejo, E. Castillo, R. Minguez, and R. Garcia-Bertrand, *Decomposition techniques in mathematical programming: engineering and science applications*. Springer Science & Business Media, 2006.

[75] S. S. Torghaban, H. Zareipour, *et al.*, "Medium-term electricity market price forecasting: a data-driven approach," in *North American Power Symposium (NAPS), 2010*, pp. 1–7, IEEE, 2010.

[76] N. Amjady, F. Keynia, and H. Zareipour, "Short-term load forecast of microgrids by a new bilevel prediction strategy," *IEEE Transactions on smart grid*, vol. 1, no. 3, pp. 286–294, 2010.

[77] S. Pazouki, M.-R. Haghifam, and A. Moser, "Uncertainty modeling in optimal operation of energy hub in presence of wind, storage and demand response," *International Journal of Electrical Power & Energy Systems*, vol. 61, pp. 335–345, 2014.

[78] G. Merei, J. Moshövel, D. Magnor, and D. U. Sauer, "Optimization of self-consumption and techno-economic analysis of pv-battery systems in commercial applications," *Applied Energy*, vol. 168, pp. 171–178, 2016.

[79] M. Castillo-Cagigal, E. Caamano-Martín, E. Matallanas, D. Masa-Bote, A. Gutiérrez, F. Monasterio-Huelin, and J. Jiménez-Leube, "Pv self-consumption optimization with storage and active dsm for the residential sector," *Solar Energy*, vol. 85, no. 9, pp. 2338–2348, 2011.

[80] J. Zhao, S. Kucuksari, E. Mazhari, and Y.-J. Son, "Integrated analysis of high-penetration pv and phev with energy storage and demand response," *Applied energy*, vol. 112, pp. 35–51, 2013.

[81] N. Good, E. A. M. Cesena, L. Zhang, and P. Mancarella, "Techno-economic and business case assessment of low carbon technologies in distributed multi-energy systems," *Applied energy*, vol. 167, pp. 158–172, 2016.

[82] S. S. Torbaghan, M. Gibescu, B. G. Rawn, H. Müller, M. Roggenkamp, and M. van der Meijden, "Investigating the impact of unanticipated market and construction delays on the development of a meshed hvdc grid using dynamic transmission planning," *IET Generation, Transmission & Distribution*, vol. 9, no. 15, pp. 2224–2233, 2015.

[83] S. S. Torbaghan, H. K. Müller, M. Gibescu, M. van der Meijden, and M. Roggenkamp, "The legal and economic impacts of implementing a joint feed-in premium support scheme on the development of an offshore grid," *Renewable and Sustainable Energy Reviews*, vol. 45, pp. 263–277, 2015.

[84] H. Müller, S. S. Torbaghan, M. Gibescu, M. Roggenkamp, and M. van der Meijden, "The need for a common standard for voltage levels of hvdc vsc technology," *Energy Policy*, vol. 63, pp. 244–251, 2013.

[85] S. de la Torre, A. Conejo, and J. Contreras, "Transmission expansion planning in electricity markets," *Power Systems, IEEE Transactions on*, vol. 23, no. 1, pp. 238–248, 2008.

[86] S. S. Torbaghan, N. Blaauwbroek, P. Nguyen, and M. Gibescu, "Local market framework for exploiting flexibility from the end users," in *European Energy Market (EEM), 2016 13th International Conference on the*, pp. 1–6, IEEE, 2016.

[87] R. Morales González, S. Shariat Torbaghan, M. Gibescu, and S. Cobben, "Harnessing the flexibility of thermostatic loads in microgrids with solar power generation," *Energies*, vol. 9, no. 7, p. 547, 2016.

[88] K. C. Armel, A. Gupta, G. Shrimali, and A. Albert, "Is disaggregation the holy grail of energy efficiency? the case of electricity," *Energy Policy*, vol. 52, pp. 213–234, 2013.

[89] V. Kalkhambkar, R. Kumar, and R. Bhakar, "Energy loss minimization through peak shaving using energy storage," *Perspectives in Science*, vol. 8, pp. 162–165, 2016.

[90] K. Devabalaji, A. M. Imran, T. Yuvaraj, and K. Ravi, "Power loss minimization in radial distribution system," *Energy Procedia*, vol. 79, pp. 917 – 923, 2015.

[91] "Nord pool spot price," http://www.nordpoolspot.com/historical-market-data/ [Accessed 20-12-2016].

[92] A. Ramos, C. De Jonghe, V. Gómez, and R. Belmans, "Realizing the smart grid's potential: Defining local markets for flexibility," *Utilities Policy*, vol. 40, pp. 26–35, 2016.

[93] T. A. Deetjen, J. S. Vitter, A. S. Reimers, and M. E. Webber, "Optimal dispatch and equipment sizing of a residential central utility plant for improving rooftop solar integration," *Energy*, vol. 147, pp. 1044–1059, 2018.

[94] S. S. Torbaghan, N. Blaauwbroek, D. Kuiken, M. Gibescu, M. Hajighasemi, P. Nguyen, G. J. Smit, M. Roggenkamp, and J. Hurink, "A market-based framework for demand side flexibility scheduling and dispatching," *Sustainable Energy, Grids and Networks*, 2018.

[95] M. Milligan and B. Kirby, "Utilizing load response for wind and solar integration and power system reliability," tech. rep., National Renewable Energy Laboratory (NREL), Golden, CO., 2010.

[96] J. M. Morales, A. J. Conejo, H. Madsen, P. Pinson, and M. Zugno, "Facilitating renewable integration by demand response demand response," in *Integrating Renewables in Electricity Markets*, pp. 289–329, Springer, 2014.

[97] G. Strbac, "Demand side management: Benefits and challenges," *Energy policy*, vol. 36, no. 12, pp. 4419–4426, 2008.

[98] R. Shaw, M. Attree, T. Jackson, and M. Kay, "The value of reducing distribution losses by domestic load-shifting: a network perspective," *Energy Policy*, vol. 37, no. 8, pp. 3159–3167, 2009.

[99] J. Kays, A. Seack, T. Smirek, F. Westkamp, and C. Rehtanz, "The generation of distribution grid models on the basis of public available data," *IEEE Transactions on Power Systems*, vol. 32, no. 3, pp. 2346–2353, 2017.

[100] D. Azari, S. S. Torbaghan, H. Cappon, M. Gibescu, K. Keesman, and H. Rijnaarts, "Assessing the flexibility potential of the residential load in smart electricity grids—a data-driven approach," in *2017 14th International Conference on the European Energy Market (EEM)*, pp. 1–6, IEEE, 2017.

[101] K. J. Keesman, *System identification: an introduction*. Springer Science & Business Media, 2011.

[102] G. Suryanarayana, J. Lago, D. Geysen, P. Aleksiejuk, and C. Johansson, "Thermal load forecasting in district heating networks using deep learning and advanced feature selection methods," *Energy*, vol. 157, pp. 141–149, 2018.

[103] J. Lago, F. De Ridder, and B. De Schutter, "Forecasting spot electricity prices: Deep learning approaches and empirical comparison of traditional algorithms," *Applied Energy*, vol. 221, pp. 386–405, 2018.

[104] J. A. Jardini, C. M. V. Tahan, M. R. Gouvea, S. U. Ahn, and F. M. Figueiredo, "Daily load profiles for residential, commercial and industrial low voltage consumers," *IEEE Transactions on Power Delivery*, vol. 15, pp. 375–380, Jan 2000.

[105] C. D. Korkas, S. Baldi, I. Michailidis, and E. B. Kosmatopoulos, "Occupancy-based demand response and thermal comfort optimization in microgrids with renewable energy sources and energy storage," *Applied Energy*, vol. 163, pp. 93–104, 2016.

[106] X. Ayón, J. Gruber, B. Hayes, J. Usaola, and M. Prodanović, "An optimal day-ahead load scheduling approach based on the flexibility of aggregate demands," *Applied energy*, vol. 198, pp. 1–11, 2017.

[107] E. Dall'Anese, H. Zhu, and G. B. Giannakis, "Distributed optimal power flow for smart microgrids," *IEEE Transactions on Smart Grid*, vol. 4, no. 3, pp. 1464–1475, 2013.

[108] D. Forner, T. Erseghe, S. Tomasin, and P. Tenti, "On efficient use of local sources in smart grids with power quality constraints," in *2010 First IEEE International Conference on Smart Grid Communications*, pp. 555–560, IEEE, 2010.

[109] B. P. Bhattarai, K. Kouzelis, I. D. D. C. Mendaza, B. Bak-Jensen, J. R. Pillai, and K. S. Myers, "Smart grid constraint violation management for balancing and regulating purposes," *IEEE Transactions on Industrial Informatics*, vol. 13, no. 6, pp. 2864–2875, 2017.

[110] F. Capitanescu, I. Bilibin, and E. R. Ramos, "A comprehensive centralized approach for voltage constraints management in active distribution grid," *IEEE Transactions on Power Systems*, vol. 29, no. 2, pp. 933–942, 2013.

[111] C. J. Dent, L. F. Ochoa, and G. P. Harrison, "Network distributed generation capacity analysis using opf with voltage step constraints," *IEEE Transactions on Power systems*, vol. 25, no. 1, pp. 296–304, 2010.

[112] J. G. Robertson, G. P. Harrison, and A. R. Wallace, "Opf techniques for real-time active management of distribution networks," *IEEE Transactions on Power Systems*, vol. 32, no. 5, pp. 3529–3537, 2016.

[113] T. Sansawatt, L. F. Ochoa, and G. P. Harrison, "Smart decentralized control of dg for voltage and thermal constraint management," *IEEE transactions on power systems*, vol. 27, no. 3, pp. 1637–1645, 2012.

[114] M. Caramanis, E. Ntakou, W. W. Hogan, A. Chakrabortty, and J. Schoene, "Co-optimization of power and reserves in dynamic t&d power markets with nondispatchable renewable generation and distributed energy resources," *Proceedings of the IEEE*, vol. 104, no. 4, pp. 807–836, 2016.

[115] R. Li, Q. Wu, and S. S. Oren, "Distribution locational marginal pricing for optimal electric vehicle charging management," *IEEE Transactions on Power Systems*, vol. 29, no. 1, pp. 203–211, 2013.

[116] H. Yuan, F. Li, Y. Wei, and J. Zhu, "Novel linearized power flow and linearized opf models for active distribution networks with application in distribution lmp," *IEEE Transactions on Smart Grid*, vol. 9, no. 1, pp. 438–448, 2016.

[117] A. Papavasiliou, "Analysis of distribution locational marginal prices," *IEEE Transactions on Smart Grid*, vol. 9, no. 5, pp. 4872–4882, 2017.

[118] P. Mandatova and O. Mikhailova, "Flexibility and aggregation: Requirements for their interaction in the market," *Eurelectric: Brussels, Belgium*, 2014.

[119] S. Minniti, N. Haque, P. Nguyen, and G. Pemen, "Local markets for flexibility trading: key stages and enablers," *Energies*, vol. 11, no. 11, p. 3074, 2018.

[120] P. Olivella-Rosell, P. Lloret-Gallego, Í. Munné-Collado, R. Villafafila-Robles, A. Sumper, S. Ottessen, J. Rajasekharan, and B. Bremdal, "Local flexibility market design for aggregators providing multiple flexibility services at distribution network level," *Energies*, vol. 11, no. 4, p. 822, 2018.

[121] S. S. Torbaghan, G. Suryanarayana, H. Hoschle, R. D'hulst, F. Geth, C. Chris, and D. Van Hertem, "Optimal flexibility dispatch problem using second-order cone relaxation of ac power flow," *IEEE Transactions on Power Systems*, 2019.

[122] S. H. Low, "Convex relaxation of optimal power flow—part ii: Exactness," *IEEE Transactions on Control of Network Systems*, vol. 1, no. 2, pp. 177–189, 2014.

[123] S. A. Gabriel, A. J. Conejo, C. Ruiz, and S. Siddiqui, "Solving discretely constrained, mixed linear complementarity problems with applications in energy," *Computers & Operations Research*, vol. 40, no. 5, pp. 1339–1350, 2013.

[124] C. Ruiz, A. J. Conejo, and S. A. Gabriel, "Pricing non-convexities in an electricity pool," *IEEE Transactions on Power Systems*, vol. 27, no. 3, pp. 1334–1342, 2012.

[125] L. Brotcorne, M. Labbé, P. Marcotte, and G. Savard, "Joint design and pricing on a network," *Operations research*, vol. 56, no. 5, pp. 1104–1115, 2008.

[126] K. P. Schneider and J. C. Fuller, "Voltage control devices on the ieee 8500 node test feeder," in *IEEE PES T&D 2010*, pp. 1–6, IEEE, 2010.

[127] W3Techs. Last accessed 25 August 2019.

[128] R. D. Zimmerman and C. E. Murillo-Sánchez, "Matpower 4.1 user's manual," *Power Systems Engineering Research Center, Cornell University, Ithaca, NY*, 2011.

[129] R. D. Zimmerman, C. E. Murillo-Sánchez, and R. J. Thomas, "Matpower: Steady-state operations, planning, and analysis tools for power systems research and education," *IEEE Transactions on power systems*, vol. 26, no. 1, pp. 12–19, 2010.

[130] R. D. Zimmerman and C. E. Murillo-Sanchez, "MATPOWER User's Manual," tech. rep., Power Systems Engineering Research Center (PSerc), 06 2019.

[131] J. Löfberg, "Yalmip : A toolbox for modeling and optimization in matlab," in *In Proceedings of the CACSD Conference*, (Taipei, Taiwan), 2004.

[132] IEA, "Energy policies of the iea countries: The netherlands 2014 review," 2014.

[133] WBCSD, "Energy efficiency in buildings facts & trends," *Summary Report*, 2008.

[134] C. M. Agudelo-Vera, A. Mels, K. Keesman, and H. Rijnaarts, "The urban harvest approach as an aid for sustainable urban resource planning," *Journal of Industrial Ecology*, vol. 16, no. 6, pp. 839–850, 2012.

[135] M. Bortolini, M. Gamberi, and A. Graziani, "Technical and economic design of photovoltaic and battery energy storage system," *Energy Conversion and Management*, vol. 86, pp. 81–92, 2014.

[136] C. W. Tan, T. C. Green, and C. A. Hernandez-Aramburo, "A stochastic method for battery sizing with uninterruptible-power and demand shift capabilities in pv (photovoltaic) systems," *Energy*, vol. 35, no. 12, pp. 5082–5092, 2010.

[137] M. Salvador and S. Grieu, "Methodology for the design of energy production and storage systems in buildings: Minimization of the energy impact on the electricity grid," *Energy and Buildings*, vol. 47, pp. 659–673, 2012.

[138] P. Balcombe, D. Rigby, and A. Azapagic, "Energy self-sufficiency, grid demand variability and consumer costs: Integrating solar pv, stirling engine chp and battery storage," *Applied Energy*, vol. 155, pp. 393–408, 2015.

[139] S. Sanaye and A. Sarrafi, "Optimization of combined cooling, heating and power generation by a solar system," *Renewable Energy*, vol. 80, pp. 699–712, 2015.

[140] V. Dorer and A. Weber, "Energy and co2 emissions performance assessment of residential micro-cogeneration systems with dynamic whole-building simulation programs," *Energy Conversion and Management*, vol. 50, no. 3, pp. 648–657, 2009.

[141] X. Li and J. Wen, "Review of building energy modeling for control and operation," *Renewable and Sustainable Energy Reviews*, vol. 37, pp. 517–537, 2014.

[142] M. Deshmukh and S. Deshmukh, "Modeling of hybrid renewable energy systems," *Renewable and sustainable energy reviews*, vol. 12, no. 1, pp. 235–249, 2008.

[143] W. Bank, "Electric power transmission and distribution losses (% of output)," 2014.

[144] J. C. Helton and F. J. Davis, "Latin hypercube sampling and the propagation of uncertainty in analyses of complex systems," *Reliability Engineering & System Safety*, vol. 81, no. 1, pp. 23–69, 2003.

[145] G. E. Box, W. G. Hunter, J. S. Hunter, *et al.*, *Statistics for experimenters*, vol. 664. John Wiley and sons New York, 1978.

[146] M. Naumann, R. C. Karl, C. N. Truong, A. Jossen, and H. C. Hesse, "Lithium-ion battery cost analysis in pv-household application," *Energy Procedia*, vol. 73, no. C, pp. 37–47, 2015.

[147] G. Fuchs, B. Lunz, M. Leuthold, and D. U. Sauer, "Technology overview on electricity storage," *ISEA, Aachen, Juni*, p. 26, 2012.

[148] E. Blokker, J. Vreeburg, and J. Van Dijk, "Simulating residential water demand with a stochastic end-use model," *Journal of Water Resources Planning and Management*, vol. 136, no. 1, pp. 19–26, 2010.

[149] V. Satopaa, J. Albrecht, D. Irwin, and B. Raghavan, "Finding a" kneedle" in a haystack: Detecting knee points in system behavior," in *2011 31st international conference on distributed computing systems workshops*, pp. 166–171, IEEE, 2011.

[150] M. Gustafsson, M. S. Gustafsson, J. A. Myhren, C. Bales, and S. Holmberg, "Techno-economic analysis of energy renovation measures for a district heated multi-family house," *Applied energy*, vol. 177, pp. 108–116, 2016.

[151] I. M. Azevedo, "Consumer end-use energy efficiency and rebound effects," *Annual Review of Environment and Resources*, vol. 39, pp. 393–418, 2014.

[152] L. A. Greening, D. L. Greene, and C. Difiglio, "Energy efficiency and consumption—the rebound effect—a survey," *Energy policy*, vol. 28, no. 6-7, pp. 389–401, 2000.

[153] S. Sorrell, "Jevons' paradox revisited: The evidence for backfire from improved energy efficiency," *Energy policy*, vol. 37, no. 4, pp. 1456–1469, 2009.

[154] C. J. Barnhart and S. M. Benson, "On the importance of reducing the energetic and material demands of electrical energy storage," *Energy & Environmental Science*, vol. 6, no. 4, pp. 1083–1092, 2013.

[155] L. Gao, J. Zhao, and Z. Tang, "A review on borehole seasonal solar thermal energy storage," *Energy procedia*, vol. 70, pp. 209–218, 2015.

[156] N. Zhu, P. Hu, L. Xu, Z. Jiang, and F. Lei, "Recent research and applications of ground source heat pump integrated with thermal energy storage systems: A review," *Applied thermal engineering*, vol. 71, no. 1, pp. 142–151, 2014.

[157] M. Aneke and M. Wang, "Energy storage technologies and real life applications–a state of the art review," *Applied Energy*, vol. 179, pp. 350–377, 2016.

[158] A. Al-Sharafi, A. Z. Sahin, T. Ayar, and B. S. Yilbas, "Techno-economic analysis and optimization of solar and wind energy systems for power generation and hydrogen production in saudi arabia," *Renewable and Sustainable Energy Reviews*, vol. 69, pp. 33–49, 2017.

[159] A. J. Conejo, J. M. Morales, and L. Baringo, "Real-time demand response model," *IEEE Transactions on Smart Grid*, vol. 1, no. 3, pp. 236–242, 2010.

[160] N. Mahmoudi, E. Heydarian-Forushani, M. Shafie-khah, T. K. Saha, M. Golshan, and P. Siano, "A bottom-up approach for demand response aggregators' participation in electricity markets," *Electric Power Systems Research*, vol. 143, pp. 121–129, 2017.

[161] T. Broberg and L. Persson, "Is our everyday comfort for sale? preferences for demand management on the electricity market," *Energy Economics*, vol. 54, pp. 24–32, 2016.

[162] E. Castillo and F. Jubete, "The γ-algorithm and some applications," *International Journal of Mathematical Education in Science and Technology*, vol. 35, no. 3, pp. 369–389, 2004.

[163] S. S. Torbaghan, N. Blaauwbroek, D. Kuiken, M. Gibescu, M. Hajighasemi, P. Nguyen, G. J. Smit, M. Roggenkamp, and J. Hurink, "A market-based framework for demand side flexibility scheduling and dispatching," *Sustainable Energy, Grids and Networks*, 2018.

[164] C. Zhang, J. Wu, C. Long, and M. Cheng, "Review of existing peer-to-peer energy trading projects," *Energy Procedia*, vol. 105, pp. 2563–2568, 2017.

[165] U. N. P. Division, "World urbanization prospects: The 2018 revision," 2018.

[166] R. V. Walker, M. B. Beck, J. W. Hall, R. J. Dawson, and O. Heidrich, "The energy-water-food nexus: Strategic analysis of technologies for transforming the urban metabolism," *Journal of environmental management*, vol. 141, pp. 104–115, 2014.

[167] S. Chen and B. Chen, "Urban energy–water nexus: a network perspective," *Applied Energy*, vol. 184, pp. 905–914, 2016.

[168] J. Wang, H. Zhong, Z. Ma, Q. Xia, and C. Kang, "Review and prospect of integrated demand response in the multi-energy system," *Applied Energy*, vol. 202, pp. 772–782, 2017.

Summary

There is a significant interest in harnessing the available flexibility that exists on the demand side of the distribution energy systems by implementing energy storage or demand response programs. Appropriate choices regarding technical design parameters, involvement of flexibility providers in the demand response program, and economic preferences of different actors are necessary for proper planning and operation of future energy systems. However, such choices require data and information which are either not available to the decision makers, or if available, are prone to uncertainty. Proper accounting of such uncertainties is key to understanding of the performance of energy system of the future. The quest to understand the performance of future energy system with flexible resources, demands an adequate framework that accounts for uncertainties in the data.

This thesis looks into the impact of data uncertainty on the techno-economic decisions of the actors in a future energy system, with flexibility resources. It considers three actors, namely the distribution system operator, aggregators (as potential operators of a demand response program), and end-users, like building energy managers and residential consumers. A comprehensive framework is developed to quantify the sensitivity of a hypothetical energy system with flexible sources, which might be put in place in the future, to unknown and inaccurate data. The proposed framework consists of three modules: a simulation module, a local sensitivity analysis (LSA), and a global sensitivity analysis (GSA). Hypothetical energy systems that harness the available flexibility from the demand side are simulated as optimization problems. Such models reflect the requirement of existing, or emerging actors in the system.

After an introduction in Chapter 1, in **Chapter 2** a data-driven framework is proposed to assess the performance of a hypothetical demand response (DR) program in the absence of historical data on flexibility potential of flexible consumers (i.e., DR providers) and grid parameters. A continuous optimization problem is formulated to simulate load shifting of residential consumers for an aggregator, as future DR operator. The optimization problem minimizes the daily load variation, while limiting the total energy cost not to increase. One important aspect of the proposed framework is that it reflects the preferences of the flexible consumers. Such characteristics allows for investigating the sensitivity of the results to different flexibility levels. In addition, the proposed optimization problem ensures that the objective of

the system operator can be reached without modeling the distribution grid.

In **Chapter 3** the impact of uncertainties in load and price data (i.e., input uncertainty) on the performance of a potential DR program was investigated. The main contribution of this chapter was in developing a sensitivity analysis framework to perform local and global sensitivity analysis on the DR optimization model, introduced in Chapter 2. Two sources of data uncertainty were considered: load and price forecast errors, and flexibility preferences of the consumers. The local sensitivity was used to investigate the sensitivity of the performance of the proposed DR program in reducing load variability to load and price forecast error. An analytical expression was derived for the sensitivities, and from there, the local sensitivities were computed. In addition, by performing global sensitivity analysis, first, various scenarios on the preferences of the flexibility providers were defined. Then, the optimal value of the variance of daily load under different flexibility preferences of the consumers were compared, and the dependency of the DR model to such preferences were identified.

The optimal flexibility dispatch (OFD) is a recently-introduced, power flow based method that a distribution system operator (DSO) can use to effectively determine the amount of flexibility it needs to procure from the flexible resources available on the demand side. However, the drawback of this method is that the optimal flexibility dispatch is inexact due to its relaxation error. In **Chapter 4** a novel error-free OFD framework is introduced, as a bi-level optimization problem where the upper level problem seeks to minimize the relaxation error and the lower level solves the second-order cone convex optimal flexibility dispatch problem. Furthermore, the sensitivity of the optimal flexibility schedules and the locational flexibility prices to uncertainty in load forecast and flexibility ranges of the flexible resources, which are input to the problem, are investigated using local sensitivity analysis. The sensitivity analysis is performed based on the perturbed KKT conditions of the lower level optimization problem. The proposed problem considered a local flexibility market framework and accounted for distribution network constraints.

In **Chapter 5** a simulation framework is used to capture the impact of modifications in energy consumption of a residential building to improve the energy efficiency. The proposed simulation tool enables investigating the combined effects of, and the interactions between, the technological measure, as well as consumers' involvement in a DR program. To investigate the impact of uncertain parameters on the total energy demand of the building, and identify the most impactful modification, a global sensitivity analysis was performed. Feasible combinations of technological modifications were investigated in various scenarios (referred to as configurations).

This thesis ends with **Chapter 6**, in which a synthesis of the results on future energy system with flexibility resources at the demand side is presented. This chapter places the results obtained in this thesis in a broader perspective of urban energy systems. The synthesis reflects the importance of investigating the impact of data uncertainty, on the operational decisions of the system operator, the aggregator, and pro-active energy consumers and thereof. The results

provide projections on the potential factors different actors need to consider when engaging in contractual agreements with the others. This research shows that the demand side flexibility can contribute to an efficient network management, as well as, efficient utilization of the local energy sources in a building energy system. However, there is an uncertainty associated with the compliance of the flexible consumers in the execution of the accepted flexibility program, which requires further research for practical implications.

Acknowledgments

Although my name is standing alone on the cover of this dissertation, there are a number of people who supported me and helped me during my PhD journey.

First and foremost I would like to thank my promotor, Professor Huub Rijnaarts for giving me the opportunity to do my PhD at the Department of Environmental Technology (ETE). Huub, you always trusted me, supported me, gave me the flexibility in planning my work, and provided me with necessary resources to develop and make this PhD a success. I would also like thank my co-promotors, Professor Karel Keesman and Dr. Hans Cappon, for their supervision and valuable feedback on my work. Thank you for giving me the freedom to build my own path. Karel, thank you for your help specially with my mathematical questions. Hans, thank you for always offering help and being supportive. I would like to acknowledge the role of Dr. Ingo Leusbrock for introducing me to this project. Ingo, thank you for getting me started at ETE.

I would like to specially thank Professor Madeleine Gibescu and Dr. Shahab Shariat Torbaghan for accepting to supervise me in my PhD, although not officially being (co-)promotors. Madeleine, thank you for the invaluable guidance you provided me with throughout the past years. Your support, encouragement, together with critical reasoning and experience in the field were a major contribution to shaping many ideas in this thesis. I am grateful that I had this opportunity of having you as my mentor. Shahab, you took my hand when I was lost in my PhD. Your vision and brilliant ideas helped me move forward and step by step form a concrete PhD research. You motivated me when I was doubting myself, and encouraged me to step into the unknown without being afraid to fail. Making this PhD journey a success would be impossible without your help.

I would like to thank Elvira Bozileva for initiating our collaboration within the Urban System Engineering group at ETE. Elvira, thank you for sharing your ideas, and taking the lead to join forces in the group.

I would like to thank the unique ETE community. Liesbeth, thank you for your patience towards all the issues I came to you with, for which you would always find a solution. Gea, thank you for all the effort you put to strengthen the community feeling in the department. Joes, Marjolein, Wies, and other supporting staff, thank you for always being available to help. Kasia and Tim,

thank you for guiding and advising me in the educational tasks. Miriam, thank you for your positive and caring attitude. Darja, thank you for checking in, and for the pleasant conversations we had. Grietje, Alette, Annemiek, and Nora, thank you for inspiring me by your passion for your work, your dedication, and your success. Momo, thank you for advising me and sharing your experiences with me.

Thank all those at ETE who made some gray and long PhD days at the department colorful, made me smile during a coffee chat or over beers, made the China trip unforgettable, and made memorable moments during togetherness and knitting nights: Yvone, Lucia, Rosanne, Justine, Sophie, Arnoud, Sanne, Sam, Dandan, Koen, Livio, Nora, Yujie, Silvi, Andrea, Joeri, Emilius, Kasper, Kamonashish, Thomas, Dainis, Carlos, Ivonne, Sanne, Adrian, Jess, Tania, Vincent, Jouke, Koen, Annemerel, Pradip, Merijn, Selin, Jiyao, Dilan, Abiodon, Margo, Shiyang, Pim, Yu, Bingnan, Elackiya, Suzanne, and Hani.

I would like to specially thank my office mates of old times: Indra, you were always positive, friendly and spreading the good vibe around. Ilse, you brought color to the office, not only with your plants and colorful posters, but also with your enthusiasm and energy. Hang, thank you for your kindness and generosity. Thank you all for making a friendly office atmosphere.

I would also like to thank my roommates in Wageningen. Leire, living with you in this nice apartment was a turning point for me during my stay in Wageningen. Thank you for that. Martina and Raed, thank you for putting up with me during the last phase of my PhD, and for making the whole quarantine time not only tolerable but fun.

I was lucky that I had good friends who made the challenges easier and the joys more pleasant. To my friends in Wageningen: Shokouh, thank you for hosting me during the very first days I arrived at Wageningen, and for making the rest of the days pleasant with your positive energy and optimism. Farzaneh and Mohamadreza, thank you for being an ear during the difficult moments of the PhD. Behzad and Vivi, thank you for all the fun kebab nights after work. Lucille, thank you for arranging a memorable trip to your hometown and hosting me there.

I have been blessed with meeting incredible people during my masters in Delft which turned into lasting friendships during my PhD. Daniel, your presence and company made living in Wageningen a totally different experience for me. Thank you for supporting me, challenging me, and encouraging me to be my better self. Dena, the days you were working in Wageningen were my special days. Thank you for being there for me all these years, for laughing and crying with me, and for our deep conversations. Samaneh, thank you for your friendship, your kindness, and always encouraging me to 'just get it done'. Ario, thank you for always being there, and for all the exciting discussions we had. Behzad, thank you for all the fun weekend plans. Pejman and Pantea, you were the living example of 'how being practical can make the life easier' for me. Thank you for being so welcoming, and always in for sharing a sweet. Ava and Hooman, thank you for the pleasant catch-ups in Eindhoven. Saba and Nami, thank you for hosting me in all the fun (and drunk) nights in Den Haag. Siamak, and Siavash thank you

for the after work meet-ups in Utrecht and short weekend trips. Soudi, Ali, Nadjla, Mahtab, Ghazaleh, Leila, Anton, Bernat, Nikoo, Armin Tavakkol, thank you for the occasional, but pleasant conversations we had. Pradeep, thank you for checking in, encouraging me to play the piano, and cheering me up with your jokes.

I would also like to thank my friends outside the Netherlands, with whom I had unforgettable reunions during my PhD. Setareh, and Somlaz, thank you for hosting me in New York. You made that trip a great experience for me. Mahsa, Negin, Ghazal, Saba, our short trips around Europe were unforgettable. Bahar, Ronak, Armin Parnia, Rojin, Saeed and Shaghayegh, Nojan and Negin, Arvind, Hamed, Saghar and Payam, thank you for hosting me in Toronto and making my stay there fantastic. Elnaz and Sepehr, thank you for the fun days we had in the Netherlands and in Iran. Malahat, Adeleh, Paria, Nafiseh, Shahrzad, Arezoo, Behzad Mazhari, Saba Aghazadeh, thank you for making my trips to Iran fun and memorable.

Last but not least, I want to thank my family, for their endless love and continuous support during my PhD. Thanks to my cousins, Mozhan, Mojdeh, Helia, Shima, Hoori, Haleh, Alireza, Niki, Diba, and Shirin who are the brother and sisters I never had. Atoosa, Aida, Alaleh, Vanooshe, Roja, Vandad, Nazanin, Kamran, Kianoosh, thank you for your care and hospitality. Special thanks to all my aunts and uncles, who were always there for me and for my parents in difficult times. I am deeply thankful and blessed for that.

Maman va Baba, if it was not for your encouragement, support, and patience, I would not be where I am now. Maman, you always encouraged me to aim for the sky, dream for the best I could think of, and not let anything limit my imagination. You taught me to be happy, and find joy even in the smallest things in life. Baba, I learned principles and ethics from you, not by your words, but by the way you lived. You always supported me in the decisions I made, and taught me to fight for what I want. Our phone conversations after long PhD days brought a big smile to my face. My love and respect for both of you is beyond words.

About the author

Delaram Azari was born on August 31, 1988, in Tehran, Iran. After graduating with a high school diploma in physics and mathematics, she attended Sharif University of Technology where she received her bachelor's degree in Chemical Engineering in February 2011.

In September 2011 she moved to the Netherlands to pursue her master's degree in Sustainable Energy Technology at Delft University of Technology. Her master's thesis focused on developing a market-based optimization framework to analyze the techno-economic development of an offshore wind farm and energy storage system. She obtained her master's degree from the Intelligent Electrical Power Grids group at the Faculty of Electrical Engineering, Mathematics, and Computer Science in November 2013.

In July 2014 Delaram started as a PhD candidate in the Urban Systems Engineering group of Environmental Technology department at Wageningen University & Research. Her research aimed to achieve a systematic understanding of the impact of data uncertainty on the techno-economic decisions of the actors in a future energy system with flexible resources. In the second year of her PhD she started a collaboration with Copernicus Institute of Sustainable Development at Utrecht University and the Flemish Institute for Technological Research (VITO), which resulted in peer-reviewed papers that are included as a part of this dissertation.

During her PhD, Delaram supervised several master and bachelor students for their thesis project. Her enthusiasm in teaching and education led her to take part in lecturing and organizing master's courses in Wageningen Univeristy, as well as in Amsterdam Institute for Advanced Metropolitan Solutions (AMS Institute).

Delaram is interested is in the application of mathematical optimization and statistics in data-driven decision making. Currently she is working as a data science trainee at ABN AMRO Bank, where next to developing predictive models, she is participating in specialized trainings on machine learning, statistics, and big data technology.

Netherlands Research School for the
Socio-Economic and Natural Sciences of the Environment

D I P L O M A

for specialised PhD training

The Netherlands research school for the
Socio-Economic and Natural Sciences of the Environment
(SENSE) declares that

Delaram Azari

born on 31 August 1988 in Tehran, Iran

has successfully fulfilled all requirements of the
educational PhD programme of SENSE.

Wageningen, 3 July 2020

Chair of the SENSE board

Prof. dr. Martin Wassen

The SENSE Director

Prof. Philipp Pattberg

The SENSE Research School has been accredited by the Royal Netherlands Academy of Arts and Sciences (KNAW)

KONINKLIJKE NEDERLANDSE
AKADEMIE VAN WETENSCHAPPEN

The SENSE Research School declares that **Delaram Azari** has successfully fulfilled all requirements of the educational PhD programme of SENSE with a work load of 44.6 EC, including the following activities:

SENSE PhD Courses

- Environmental research in context (2014)
- Research in context activity: 'Organized a 2-day workshop on system level modelling in Python' (2018)

Other PhD and Advanced MSc Courses

- Modelling dynamic systems, Wageningen University (2014)
- Parameter estimation, Wageningen University (2015)
- Scientific writing, Wageningen Graduate Schools (2015)
- Techniques for writing and presenting a scientific paper, Wageningen Graduate Schools (2015)
- Uncertainty in electricity markets and system operation, Denmark Technical University (2016)
- Teaching outside of academia. Wageningen Graduate Schools (2018)

Management and Didactic Skills Training

- Supervising three MSc students with thesis (2014-2018)
- Organizing PhD workshop 'Urban metabolism´ at AMS Institute (2015)

Oral Presentations

- *Characterization of urban energy demand profile.* Environmental Technology for Impact Conference, 29-30 April 2015, Wageningen. The Netherlands
- *Assessing the impact of uncertainty of input data on the executed flexibility of the residential load in smart electricity grids*. International workshop Energy-Open,18-19 May 2017, Enschede, The Netherlands
- *Assessing the flexibility potential of the residential load in smart electricity grids*. 14th International Conference on the European Energy Market, 6-9 July 2017, Dresden, Germany

SENSE coordinator PhD education

Dr. ir. Peter Vermeulen

The research described in this thesis was financially supported by the Department of Environmental Technology, Wageningen University & Research.

Financial support from Wageningen University & Research for printing this thesis is gratefully acknowledged.

Cover design by Helia Rajabpour and Maryam Rajabpour

Printed by Proefschriftmaken on FSC-certified paper